Landslide risk assessment and Cost Benefit Analysis on Mitigation Measures in Bili/bili Watershed, South Sulawesi - Indonesia

プトゥリ, パチマ, ヌルディン

https://doi.org/10.15017/4060223

出版情報：九州大学, 2019, 博士（農学）, 課程博士
バージョン：

Landslide risk assessment and Cost Benefit Analysis on Mitigation Measures in Bili-bili Watershed, South Sulawesi - Indonesia

PUTRI FATIMAH NURDIN

2019

Landslide risk assessment and Cost Benefit Analysis on Mitigation Measures in Bili-bili Watershed, South Sulawesi - Indonesia

A dissertation submitted
by
Putri Fatimah Nurdin

In partial fulfillment of the requirements for the degree of Doctor of Agriculture at Department of Forest Product Science, Graduates School of Bioresources and Bio-environment Sciences

九州大学
KYUSHU UNIVERSITY

Fukuoka, Japan

2019

署名

主查

副查

副查

Table of Contents

List of Figure

List of Tables

Chapter 1 Introduction

1.1 Background

Indonesia among countries have a relatively high mortality risks from multiple hazards. Indonesia is situated in one of the most active disaster hot spots where several types of disaster such as earthquake, tsunami, volcanic eruption, flood, landslide, drought and forest fires frequently occur. According to a global risk analysis by the World Bank, Indonesia is among the top 35 countries that have high mortality risks from multiple hazards with about 40 percent population living in areas at risk. For a country that has more than 230 million population, this percentage gives a very large nominal number of more than 90 million population potentially at risk creating a major humanitarian catastrophe in case large disasters occur.

Increasing frequency of disaster impacting public expenditures. According to the Government's disaster data (DIPI), between 2001 and 2009 alone there have been more than 2,830 occurrences of disasters including floods (750), droughts (129), landslides (515), and windstorm (829). As the disasters damage public infrastructure and people homes, mostly uninsured, they created an enormous burden on public expenditure to restore those facilities.

Disaster historical data have shown that Indonesia has experienced a substantial number of disasters, with significant number of people killed. In the period of 1980-2008, according to the UN-ISDR, Indonesia has experienced 293 disaster events that have killed 189,615 people, with an average number of people killed per year of 6,538. The number of people affected by those disasters is even bigger, i.e. 18,195,948 people, with an average number of people affected per year of 627,446. Besides human losses, economic damage effect by disasters during the period is also huge. The country suffers an annual economic damage of US $ 731,705,000 caused by disaster, with a total of US $ 21,219,450,000 for the period of 1980-2008.

Rain-induced landslide are one of the most common types of natural disaster and frequently occur in Indonesia. Landslide have a potential to cause a great damage and loss. The study of landslides, their causes and how to protect people from it is therefore of great value. Landslides are defined as "the movement of a mass of rock, debris, or earth down a slope" (Cornforth, 2005: 4). This covers all slope movements that occur from natural or manmade causes except ground subsidence (Ilyas, 2016).

Landslides are typically set in motion by natural causes such as heavy rainfall, floods, earthquakes and erosion and by manmade causes. Frequently, landslides occur in connection with other phenomena. For example, an earthquake can set off a landslide, which leads to a river blockage or natural dam that is vulnerable to collapse which can cause a flood downstream (Marui and Nadim, 2009: 435). Every year, major landslides occur and get reported in the news due to the damage or loss of life they incur. Most of the human casualties due to landslides occur in developing countries (Lacasse and Nadim, 2009: 31). When landslides occur near human settlements, and where the failure of the slope is rapid and there is a high risk of damage or injury, then it is better to prevent the landslide from occurring than to take remedial action. This means that we need to have good strategies for predicting the likelihood of landslides and this information needs to be available for decision making when undertaking engineering projects.

Landslide economic studies have been focused on direct and indirect costs associated with consequences as defined in the geological literature on landslide risk management (e.g., Schuster, 1978; Fleming and Taylor, 1980; Schuster, 1996; and Roberds, 2005). Despite the recognition of the need for mitigation approaches to landslide risk in developing countries, the delivery of 'on-the-ground' measures is rarely undertaken.

The consequences depend on the exposure and the vulnerability characteristics of the elements at risk (humans, landscape and ecosystems, buildings and constructions, the social structure, and other values in the area at risk). Both the probability and the consequences of floods and landslides are expected to increase in the coming decades, as a result of climate change and increased vulnerabilities, especially in urban areas (Poussin et al. 2012; IPCC 2013). The consequences may be damages caused directly or indirectly by a flood or landslide. An example of an indirect consequence is delays due to road or railroad damages (Holcombe and Anderson 2010; Suh et al. 2011). Strategies can be developed to reduce either the probability of an event or the consequences, or both (Dai et al. 2002; Brooks 2003).

1.2 Disaster management in Indonesia

The devastating 2004 tsunami which swept through Aceh Province leaving behind a wake of destruction accelerated the transformation of disaster management in Indonesia. The legal framework prior to the disaster consisted of Presidential decrees from 1979 which established the National Disaster Management Coordinating Board, BAKORNAS and the provincial and district counterparts. The Indonesia Government accounted for the disparities in the legal system and wrote the first comprehensive disaster management law for the country in 2007. The new Law heralded the beginning of the paradigm shift from a disaster response approach to a disaster management methodology which encompassed all phases (before, during, post). The Government adopted regulations to implement the new Law and established a new National Disaster Management Agency (BNPB).

Disaster management agencies have been created in the 34 provinces since 2010-2013. Presently, local disaster management agencies (BPBDs) exist in more than 90 percent of the districts and cities in the country. BNBP continues to encourage BPBDs and the local DRR platforms to promote DRR at the village level. Training and simulation exercises conducted at the district/city and village levels builds capacities for response, risk assessment, and community based DRR. Response capacity for climate-related risks is not as significantly matured at the local level. The systematic approach in disaster risk reduction contains three phases of the disaster management cycle, pre disaster planning, emergency response and post disaster management.

These are following mitigation strategies for reducing the number of fatalities and the socio-economic impact caused by landslides.

a. Landslide Susceptibility Mapping

This map identifies areas that are highly susceptible to landslide and the factors controlling susceptibility.

b. Early Warning System.

The main function of early warning system is to provide a potential landslide map prepared by overlaying landslide susceptibility maps and monthly rainfall forecasts. These maps are sent out monthly to local governments located in landslide hazard areas and they can be uploaded at http://www.vsi.esdm.go.id every month.

c. Monitoring landslides.

Landslide are monitored in order to understand landslide behaviour in terms of direction, intensity, and velocity of land movement. The landslide monitoring facility uses GPS, extensiometers and piezometers.

d. Socialization

Basic disaster management concepts and knowledge of landslide phenomena were introduced in Indonesia to improve the understanding and awareness of citizens. Also to empower them to develop effective disaster management measures and public education programs. The development of a mitigation system is therefore a crucial step towards the marshalling of human resources to guarantee the sustainability of life and the environment in areas susceptible to landslides.

e. Quick Response Team

Quick response team will visit hazardous areas and provide technical recommendation aimed at preventing landslide and reducing their impact.

Landslide hazard maps for geological disaster management have already been published and issued to public and mitigation efforts are underway. Unfortunately, disaster are still occurring in many areas in Indonesia and casualties remain high. This is because:

1. The number of settlements and public activity in medium and high susceptibility areas are still growing.
2. Landslide Susceptibility Maps and Early Warning System are not optimally use as a database for land use planning and regional development based on geohazard threats
3. Geohazard management is not formally a part of the early education curriculum in schools.

1.3 Landslide susceptibility analysis in developing country: lack of data availability.

Landslide risk analysis involves several steps, i.e. scope definition, landslide hazard identification and risk estimation. Scope definition addressed several issues including delineating the study area, elements at risk identification, and methodology selection. Landslide hazard identification addresses several issues on understanding physical characteristic of study area regarding to landslide processes such as understanding geology, geomorphology, hydrogeology and climate. It also includes collecting landslide data, such as landslide classification, area, volume, travel distance, data occurrence, and element at risk. Hazard identification activities are mostly related to landslide inventory. Risk estimation deals with consequence analysis and frequency analysis.

Landslide inventory is very important in the landslide risk analysis because it gives information related to frequency of occurrences, landslide typology, landslide extents and damage of elements at risk. Estimation of spatial probability, temporal probability and magnitude probability is not possible without landslide inventory containing sufficient data of past landslide events. In Indonesia, especially where this research was undertaken, adequate landslide inventory is not available. It is a central problem of quantitative landslide risk analysis in Indonesia. Thus, producing landslide inventory maps and developing approaches of using those maps for landslide risk zoning in Indonesia are challenging task that these researches focuses on.

1.4 Research Scope and Objectives.

This dissertation proposes a new approach where the whole framework is organized to identify the optimal response following a sediment-related disaster, which includes an economic analysis. We begin by evaluating the factors that contribute most to landslides. We then generate an optimal landslide susceptibility map and prioritize the areas most in need of recovery. Ultimately, we propose an optimized (economically) plan to reduce the consequences of natural disasters.

Thus, the objectives of this research are:

1. To evaluate the importance of each causative factors in landslide susceptibility assessments in Bili-bili watershed, Indonesia. For this, the occurrence of landslide was detected in the study area by field surveys and satellite imagery derived from Google Earth.
2. To comparatively evaluate the usage of certainty factor and weight of evidence to optimize causative factors in landslide susceptibility assessment in Bili-b watershed, Indonesia.
3. To develop an improved landslide susceptibility in purpose of vegetation recovery to reduce the sediment rate in Bili bili Dam
4. To proposed optimization procedure in economic point of view by compare all the mitigation plan for Bili bili Dam using cost benefit analysis and employ "damage avoided" as a benefit whereas in a conventional CBA it is not counted.

1.5 Thesis Organization

The thesis comprises of the following chapters:

Chapter 1 Introduction

- Background
- Description about disaster management and shifting of disaster mitigation policy in Indonesia

- Problem in landslide risk zoning in Indonesia
- Research scope and objective of this study
- Organization of the thesis

Chapter 2 Introduces condition of the study area, i.e., geology and geomorphology condition, precipitation, landcover and socio-economic condition.

Chapter 3 This chapter demonstrates the usefulness of the certainty factor and weight of evidence in identifying the better-fitted conditioning factors to generate an effective landslide susceptibility map. Sixteen conditioning factors have been evaluated. Based on the certainty factor (CF), eleven conditional factors (profile curvature, curvature, slope, Topography Position index, rainfall, elevation, distance to fault, land use, distance to a river, drainage density, and plan curvature) have a high correlation to landslide occurrence. Meanwhile, the weight of evidence (WoE) applied the conditional independent test to assess the independence of each factor and produce a combination of elevation, plan curvature, lithology, distance to a river, soil, Stream power index, and TPI as a combination with a significant correlation to trigger a landslide. Both models have a high accuracy, but the CF model has a slightly higher ROC result (AUC = 90.3%, prediction = 90.2%) than WoE (AUC = 90.1%, prediction =89.9%).

Chapter 4 This chapter shows an effort to improve the function of the landslide susceptibility map not only to detect landslide-prone areas but also as supporting maps for zoning the most priority area for rehabilitation, thereby reducing the erosion rate and susceptibility of landslides. The new map is generated by integrating an optimized landslide susceptibility map and the critical land map to zoning the area for revegetation recovery. The critical land map employed in this study has been verified and validated by the Ministry of Public Work and Pompengan

Jeneberang Watershed Agency. Coding for the revegetation recovery map using the matrix relationship method, the zoning area is divided into three classes; first, second, and third priorities. The first and second priority is the targeted area that needs immediate treatment for a revegetation recovery plan, and the third priority area is classified as an area that can be treated later after the first and second priority areas have been addressed.

Chapter 5 This chapter shows the impact of a reduction of Bili Bili Dam effectivity as flood control. On January 22, 2019, ten regencies in the province of South Sulawesi experienced an extreme flood. The Jeneberang River is one of the major rivers and has the most extensive impact on flooding. Bili-Bili Dam is a multipurpose dam located on Jeneberang River, Gowa regency. The heavy rainfall that occurred on January 22 was marked by heavy rainfall from January 21 to January 23. The peak rainfall recorded at three measuring stations including 329 mm at Lengkese station, 308 mm at Bawakaraeng station, and 328 mm at Limbungan station. The flood downstream was a result of the river basin not being able to accommodate the water discharge from the spillway dam, which was related to a decreasing of dam capacity caused by siltation. Landslides in some area also occurred and caused a flash flood in the sub-watershed of Kampala and destroyed a bridge further downstream. Landslides with extensive impacts occurred in the settlement area and buried half of the village in Pattalikang. The total cost of the damages by flooding and landslide for three regencies (directly impacted by Bili Bili Dam) was estimated as 611 billion rupiahs.

Chapter 6 This chapter shows an optimization in economic terms associated with sediment related disaster risk. It starts with the calculation of the lifetime of the reservoir using the dead storage volume approach, then the cost-benefit analysis (CBA) was utilized to compare the costs and benefits of proposed three scenarios. Unlike in conventional CBAs, here we use "risk reduction" as the value of benefits. There are three scenarios being considered to reduce the sediment level in Bili Bili dam;

1. Scenario 1 (Dredging work volume 82,000 m^3/year – existing condition)
2. Scenario 2 (Dredging work volume 246,000 m^3/year)
3. Scenario 3 (Dredging work volume 82,000 m^3/year and aerial bomb seeding)

All benefits and costs should be expressed in discounted present values. Costs and benefits must be compared to be able to derive at a decision (BCR). A scenario with a benefit-cost ratio greater than 1 has greater benefits than costs. Hence, they have positive net benefits. The higher the ratio, the greater the benefits relative to the costs. The result of the calculation of service time and effectivity, scenario 3 (existing dredging + revegetation) shows an increase in dam effectiveness and reduced sedimentation rates in the dam. Based on economic calculations using the CBA formula, all scenarios would be profitable (BCR > 1). If the expected rate of return is 4-5%, scenario 3 achieves a greater profit compared to scenarios 1 and 2. But if the expected rate of return is higher than 5%, the maximum profit is generated by scenario 1.

Chapter 7 Summarizes and conclusion of results and achievements of the study. Problems are also highlighted for future studies.

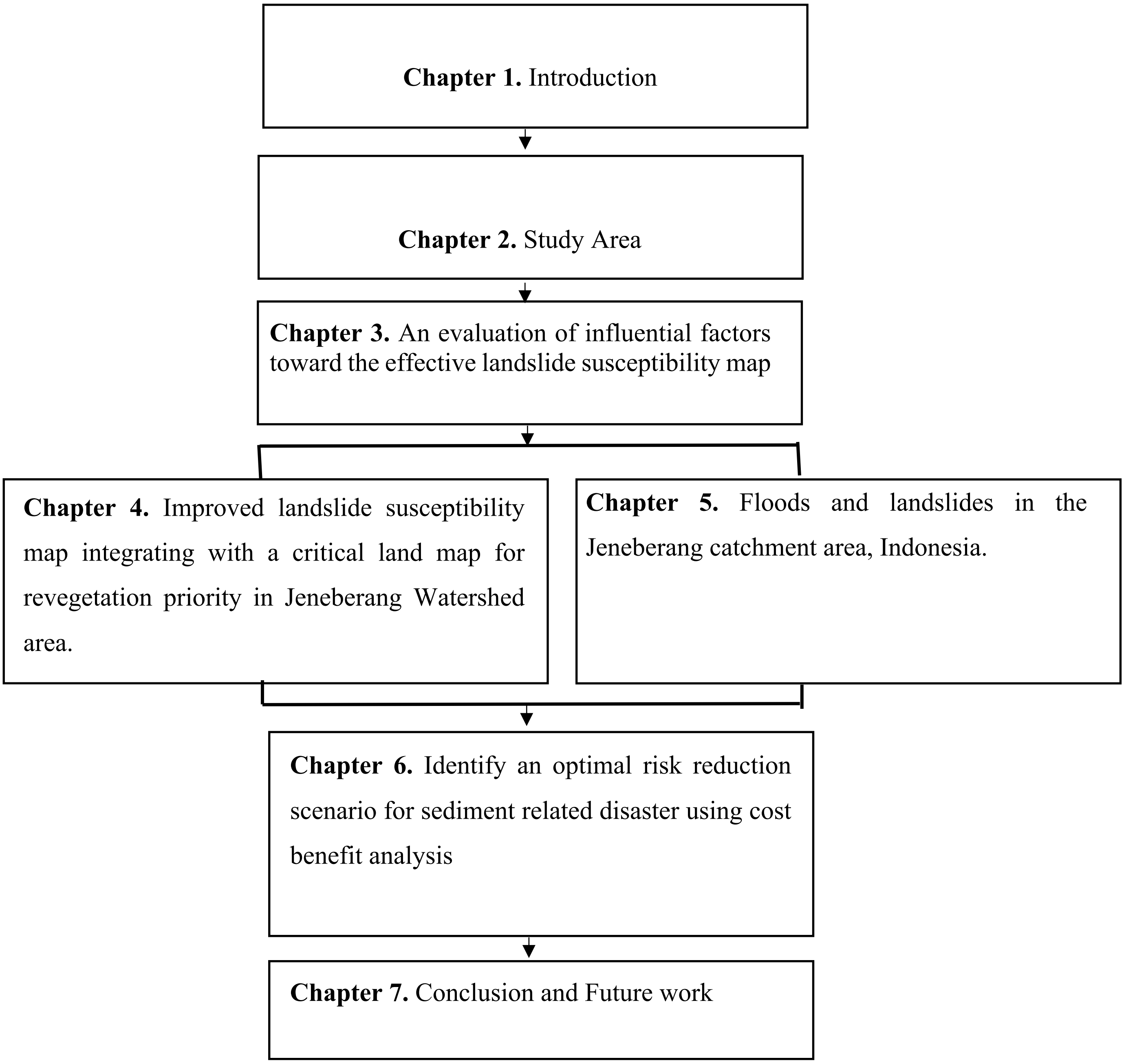

Figure 1 Research Framework

1.6 References

Brooks, N. 2003. Vulnerability, risk and adaptation: A conceptual framework. Working paper 38. Norwich, UK: Tyndall Centre for Climate Change Research and Centre for Social and Economic Research on the Global Environment (CSERGE).

Cornforth, Derek H. 2005. Landslides in Practice: Investigation, Analysis, and Remedial/Preventative Options in Soils. Hoboken, NJ: John Wiley & Sons.

Dai, F.C., C.F. Lee, and Y.Y. Ngai. 2002. Landslide risk assessment and management: An overview. Engineering Geology 64(1): 65–87.

FLEMING, R.W., & TAYLOR, F.A. 1980. Estimating the costs of landslide damage in the United States. U.S. Geological Survey Circular 832, 21

Holcombe, E., and M. Anderson. 2010. Tackling landslide risk: Helping land use policy to reflect unplanned housing realities in the Eastern Caribbean. Land Use Policy 27(3): 798–800.

Ilyas, Tommy. 2016. Landslide Anticipation and Prevention in Indonesia. Research Gate

IPCC (Intergovernmental Panel on Climate Change). 2013. The physical science basis. Cambridge: Cambridge University Press

Lacasse, Suzanne, and Nadim, Farrokh. 2009. Landslide Risk Assessment and Mitigation Strategy. In Landslides - Disaster Risk Reduction. eds. KyojiSassa and Paolo Canute, 31-62. Berlin: Springer.

Landslides: Anticipation and Prevention in Indonesia. Available from: https://www.researchgate.net/publication/292137699_Landslides_Anticipation_and_Prevention_in_Indonesia [accessed Aug 02 2019].

Marui, Hideaki, and Nadim, Farrokh. 2009. Landslides and Multi-Hazards. In Landslides - Disaster Risk Reduction. eds. KyojiSassa and Paolo Canute, 435-450. Berlin: Springer.

Poussin, J.K., P. Bubeck, J.C.-H. Aerts, and P.J. Ward. 2012. Potential of semi-structural and non-structural adaptation strategies to reduce future flood risk: case study for the Meuse. Natural Hazards and Earth System Sciences 12: 3455–3471

ROBERDS, W. 2005. Estimating temporal and spatial variability and vulnerability. In: Hungr, Oldrich., Fell, Robin., Couture, Rejean., & Eberhardt, Erik. (editors), Landslide Risk Management: Proceedings of the International Conference on Landslide Risk Management, Vancouver, Canada, May 31-June 3, 129-157.

SCHUSTER, R.L. 1978. Introduction. In Schuster, Robert L. & Krizek, Raymond .J. (editors) Landslides, Analysis and Control Transportation Research Board Special Report 176, National Academy of Sciences, Washington, DC, 1-10.

SCHUSTER, R.L. 1996. Socioeconomic significance of landslides. In Turner, A. Keith & Schuster, Robert L. (editors), Landslides Investigation and Mitigation: Transportation Research Board Special Report 247, National Academy of Sciences, Washington, DC, 1- 11.

Suh, J., Y. Choi, T.D. Roh, H.J. Lee, and H.D. Park. 2011. Nationalscale assessment of landslide susceptibility to rank the vulnerability to failure of rock-cut slopes along expressways in Korea. Environmental Earth Sciences 63(3): 619–632.

Chapter 2. Study Area

2.1. Introduction

Bili-bili watershed is located in Southern part of South Sulawesi island, Indonesia. This area was chosen because of its frequent landslide history over the past view years. In March 2004, this area experienced the gigantic collapsed of Bawakaraeng Kaldera with a volume about 235 million m^3 (width about 1600 m and length about 750 m). Fajar Local Newspaper (April 2004) informed that Gowa government of the Regency valued the loss material as a result of the landslides in the Bawakaraeng Mountain to 22 billion Rupiah or $US 2.200.000

The value of losses have covered 270 hectares of people's plantation, equivalent to 10.08 billion Rupiah or $US 1.008.000. The Regency leader assessed, the disaster losses such as 800 livestock, 12 house units, one primary school, 160 hectares rice cultivations and crop, 270 hectares of the plantations, 300.000 tree seeds, the village road along 3.000 meter, and a Mosque (Kompas, 2004). Sediment and debris from the landslide covered the Jeneberang river and causing many unstable slopes along the river. The climate of South Sulawesi island is tropical with two seasons within a year. Rainy season between November and May and a dry season from June to October.

The implications of the landslides have been influenced on the river basin by forming several small tributaries across new formation of land. Additional to that, the existing of water level is changed by landslides and it will be influence to the formation of land. The intensity of rain will be influenced to the quality of water in the river basin. Water crisis awareness is expanding, but most interest remains focused on water quantity issues (Lundvist, 1998).

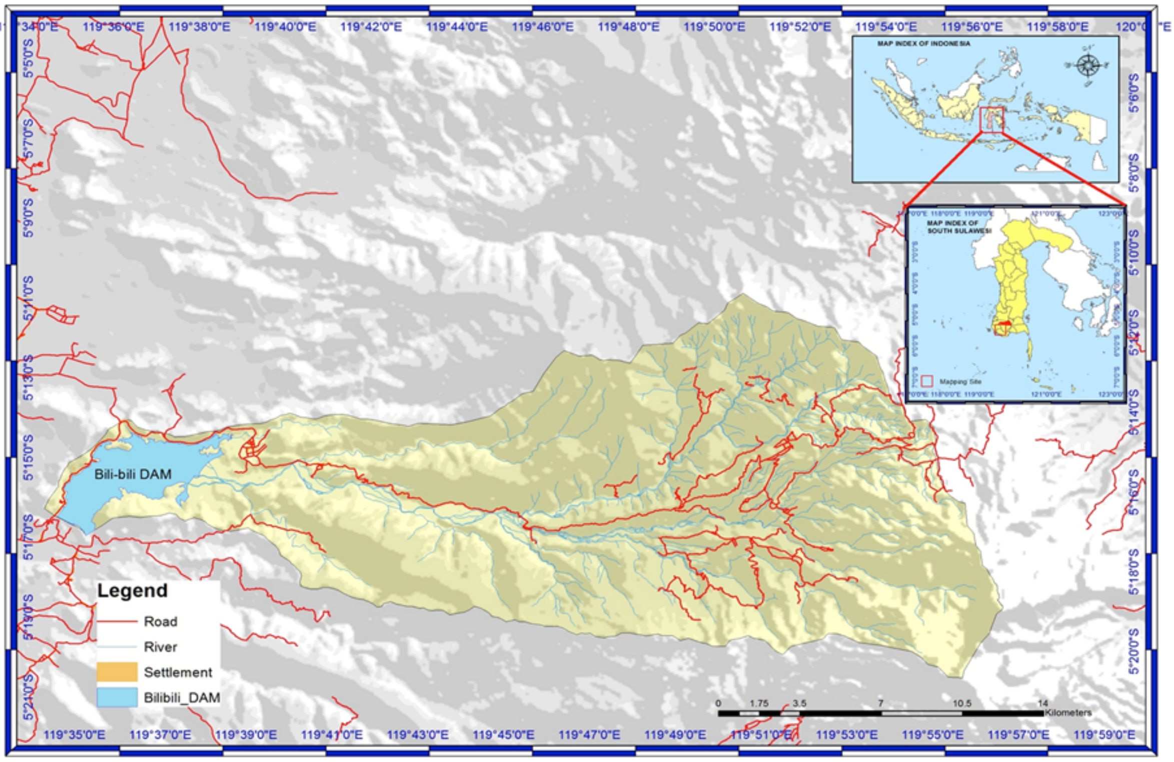

Figure 2 Study Area

The temperature in the study area can reach 34°C, and average annual precipitation is from 2864 mm to 3039 mm. The landslide occurred quite often in this area, during two rainy seasons, the number of landslide occurrences is larger than dry seasons. It indicates that rainfalls play an essential role in landslide occurrences. Floods are normally caused by rainstorms in the wet season, and often flash floods are experienced. The population living in the catchment was 747.753 in 2011. Most of the people in this area work as farmers, it causes the agriculture land dominates the land use cover in this area. The geology is dominated by Tertiary Miocene Camba (marine sediment rocks vary with volcanic rocks).

2.2. Geology and Geomorphology condition

The morphology of Mt. Bawakaraeng is characterized by high relief, extreme slope, high degree of weathering and erosion activities like as soil movement and landslide. Mt Bawakaraeng was developed as a result of volcanic activities during the Pleistocene period. It is composed of andesite rocks such as breccia, pyroclastic, tuff and interstratified lavas. As most of these rocks have not been compacted especially pyroclastic, they can be easily decomposed, eroded and slided.

The lithological units shown in the surface geologic maps were reclassified according to geology and development center. The result was a generalized geologic map. Finally, the map describes the distribution of six types of lithology:

- TMC - Tertiary Miocene Camba (40.6 %)

  Marine sediment rocks vary with volcanic rocks, tuff sand varies with sandy tuff and claystone; and have insertion marl, limestone, conglomerate, volcanic breccias, and coal.
- QLVP (7.19%), QLV(14.88%), and QLVB(14.03%) - Quarter Lompobatang Volcanic

  Agglomerates, lava, breccias, lahar deposition and tuff.
- TPBV (10.45%) and TPBL (5.48%) - Tertiary Pliocene Baturape Cindako Volcanic

  Lava and breccias, with insertion tuff and conglomerate.
- QAC (5.61) - Quarte Aluvium

  gravel, sand, clay, mud and coral limestone.

Slope instability is generally one of the most important causes of landslides. In this study, slopes divided into 5 classes, which dominated with 10-20 degrees slope (36.95%), followed with <10 degrees slope (33.17). Slope greater than 30 degrees has 29.88%.

2.3. Precipitation

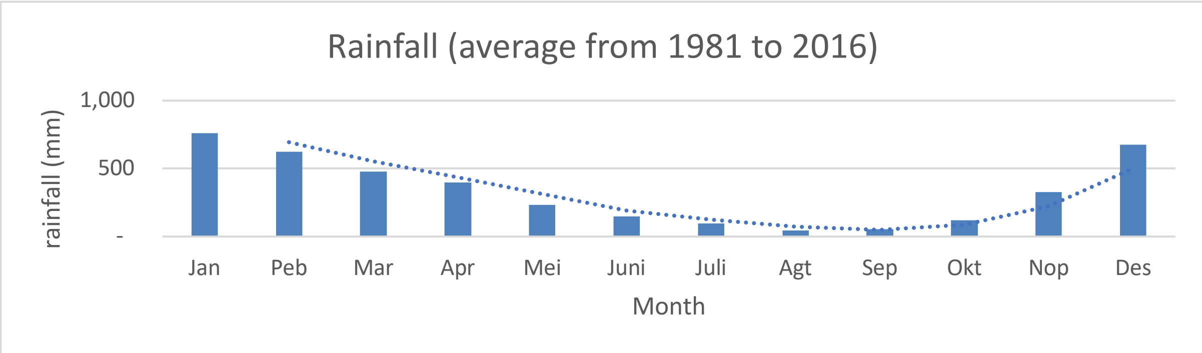

Figure 3 Monthly precipitation

Rainfall is the principal climatic variable that influences landslide distribution. It is affected by topography, elevation, and vegetation—factors that are all interrelated. Mountainous areas especially in the high elevation area, cause the air currents to rise and cool resulting in increased precipitation. Bili bili watershed area is subject to a tropical monsoon climate, which exhibits as high and rather constant air temperature throughout the year, but

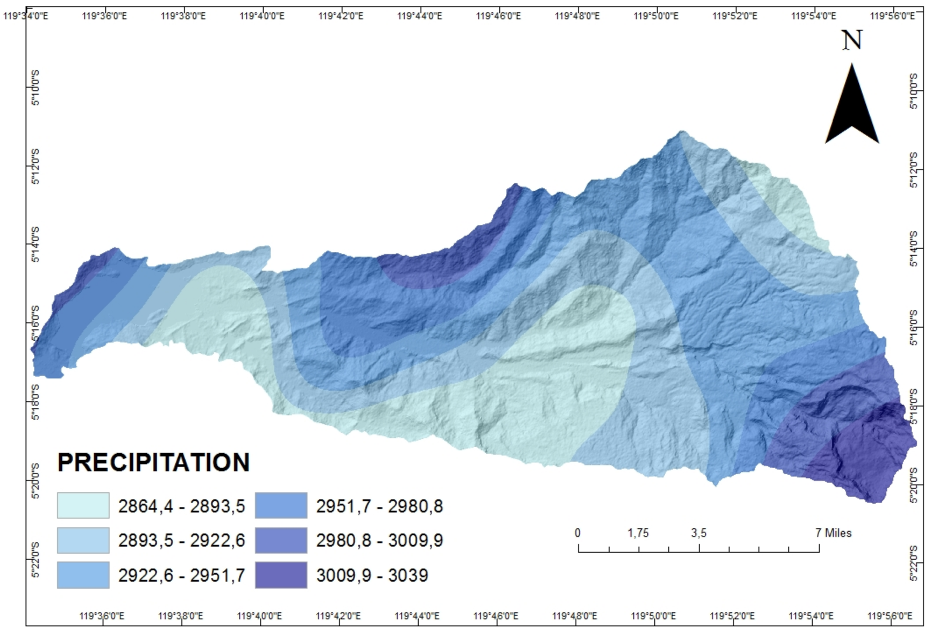

Figure 4 Precipitation map of study area

with a distinct variation in rainfall creating rainy and dry seasons. The rainy season from November to May. The annual precipitation for the catchment varies along the main stream due to the local topographic effects. The average annual precipitation for the upper basin is about 3,000 and is about 2,160 mm (2,166 mm at the Bontosunggu station) in the lower stream. The CHIRPS v.2 dataset, a satellite-based monthly rainfall product (available online at http://chg.geog.ucsb.edu/data/chirps/), was used. About 35 years (1981-2016) of rainfall data have been collected and analyzed for rainfall variation.

2.4 Social Aspect

Most of the people lived in the upstream area of the Bili-bili watershed rely on the agricultural sector as one of their livelihoods in addition to other sectors such as civil servants, military / police and others. The farming procedures adopted by the people in this area are inseparable from the procedures carried out by their predecessors. Most farmers cultivate their land as a legacy from their ancestor, so they feel free to cultivate their land to fulfill their daily needs.

However, since the caldera collapsed has caused an abundance of sand, stone and gravel material, the residents have been part of what previous farmers worked as sand and gravel miners. It helps the community in trying to find additional work for their welfare.

Based on 2010 data that 44.85% of the population in the study area have a low level of education that is only up to elementary school level, graduated from elementary school 20.22%, junior high school 9.93%, high school 8.82% and tertiary institutions 2.21%, while the illiterate group was 13.97% (Gowa Regency, 2010).

The low level of education causes people unable to adopt and apply technology. In this regard, efforts are needed to improve the quality of human resources through counseling and training programs. Improving the quality of human resources with the knowledge of technology will provide an understanding of the importance of maintaining each land to reduce the level of erosion and sedimentation in the upstream area of the Bili-bili watershed .

2.5 Landcover change

Land Cover Result from analysis of land use map of study area indicates that most area is dominated by agricultural land with area of 39.57% and secondary forest of 18.77%, followed with paddy field 16.82%, brushes 13.47%, open land 1.43% and settlement area.

From the interpretation of Landsat imagery in 1986/1987, 1995/1996, and 2000/2001, it is known that there has been a decline in the area of forested areas in the Bili-bili watershed over the last few years. In 1986/1987 the area of forest with forest vegetation was 17,450 ha, while in 2003 it was 13,648 ha, which means there was a decrease in the area of forest with forest vegetation by 21.79% or an average of 1.5% per year. Then in 2002 the use of dry land had dominated the Bili-bili watershed area by 69.4%, where the area of forest cover was only 4.4% (Supratman, 2003).

Meanwhile data from Jeneberang watershed agency shows the percentage of forested area in 1990 is very small, only 17.62% and keep decrease by time. Ideally watershed area has a minimal of 30% of forested area to work as a catchment area. Obviously that forested area in Bili-bili watershed is not enough to cover the whole catchment area.

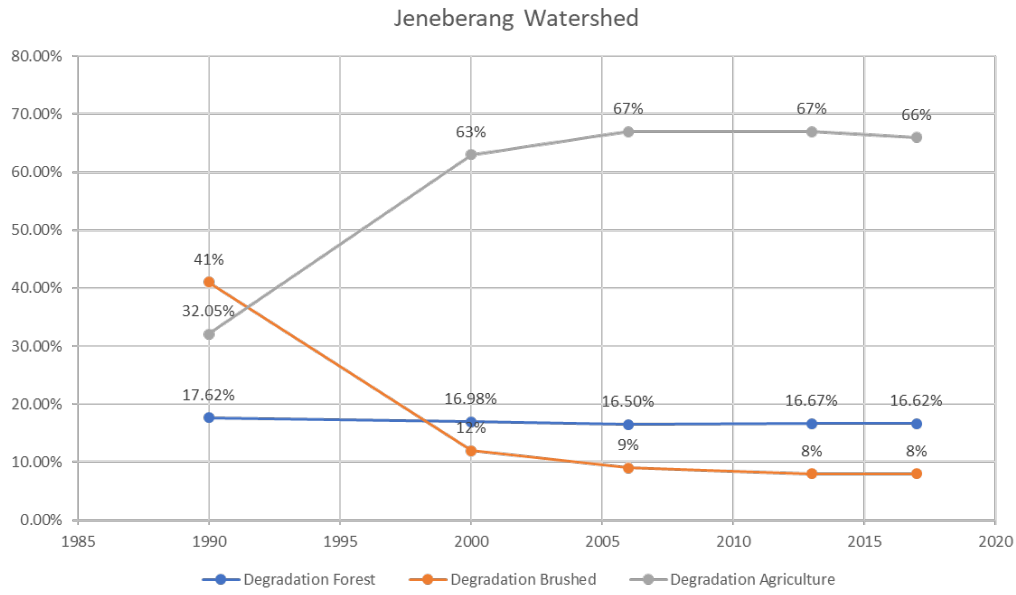

Figure 5 Landcover change from 1990 - 2017

2.6 Jeneberang River and Bili bili dam

Jeneberang River is administratively divided into Gowa regency, Takalar regency and Makassar City. Among others, Gowa regency occupies 95.9 % (730 km2) of the river basin including the whole catchment of Bili-Bili Dam. The share of the river basin by Takalar regency and Makassar City is extremely small; 1.2 % (9.5 km2) and 2.9 % (22.5 km2), respectively. The upstream of Jeneberang river has a very steep slope. At the time of rain, there is torrential flow and materials glide at a high speed, therefore the damaging ability is very high. A series of seven sabo dams (SD) were built to slow down the flow. The existence of sabo dam expected to cause a deposition of material on the upper reaches of the construction, and lead to a gentle slope of the flow, reduced flow speed, and also reduced damaging ability. These deposits also expected to stabilize the cliffs of the river channel.

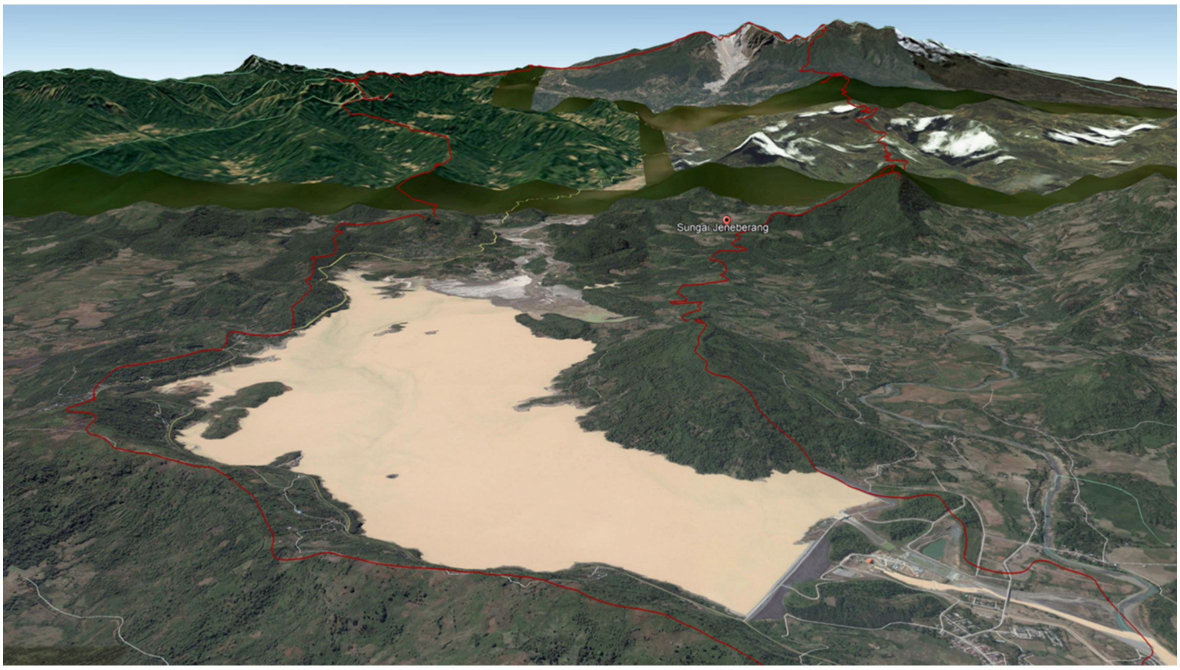

Figure 6 Condition of Bili- bili Dam captured by Google earth

While in middle stream, Eight consolidation dams (CD or KD) also have been built. The main function is to control vertical and horizontal material flows (debris flow, lahar flow) in order to prevent damages and flow deviation. The constructions of the consolidation dams were started in 2007.

Before the landslide of Mount Bawakaraeng, 5 sand pockets (SP) had been built in downstream area from 1997 to 2001 by the Bili-bili Dam Project. After the landslide, these sand pockets were damaged and the material deposition exceeded the sand pockets carrying capacities. It is forecasted that the high possibility of sedimentation occur in this area. If it is not anticipated with the system of dredging, it will be possible to disable the function of Bili-Bili Dam (Samang, 2007)

The Bili-Bili Reservoir, located on the Jeneberang River in South Sulawesi, Indonesia, was completed in 1999, which serves the multipurpose of irrigation, power generation, water supply and flood control. The gross storage of the reservoir is 375,000,000 m3, in which a dead storage of 29,000,000 m3 is provided for detaining 580,000 m3 of the estimated annual inflow of sediment in consideration of the project life of 50 years. The effective storage is 346,000,000 m3.

The Bili-Bili Reservoir Project mainly consists of three rock fill type dams, spillway, intake structure, power plant and outlet works. The area of Bili-Bili irrigation project lies in the downstream basin of the Jeneberang River, and administratively belongs to the two regency of Takalar and Gowa, and Makassar city. Its main objective being to supply drinking water to Ujung Pandang. However, it has also been designed to control floods up to a 50 year return period, irrigate 19,200 ha of land, and generate 69,000 MWh of electric power each year. The Bili-Bili irrigation project comprise three irrigation schemes, namely Bili-Bili, Bissua and Kampili, which cover a total area of 23,660 ha.

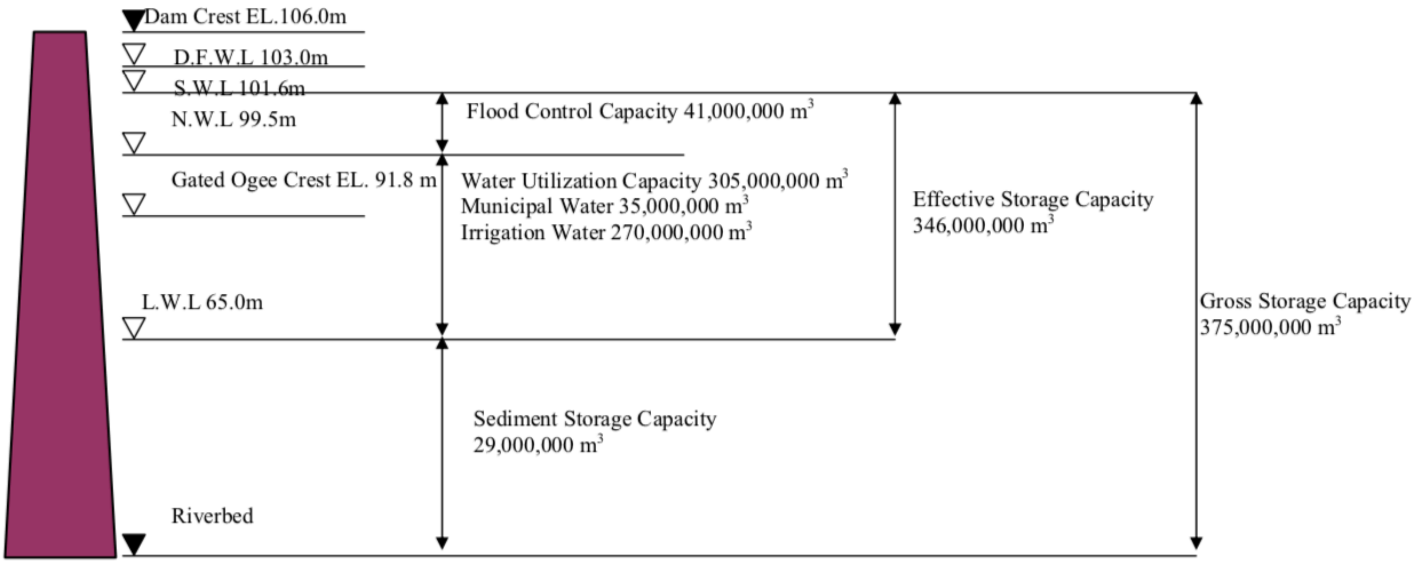

Figure 7 Bili bili dam

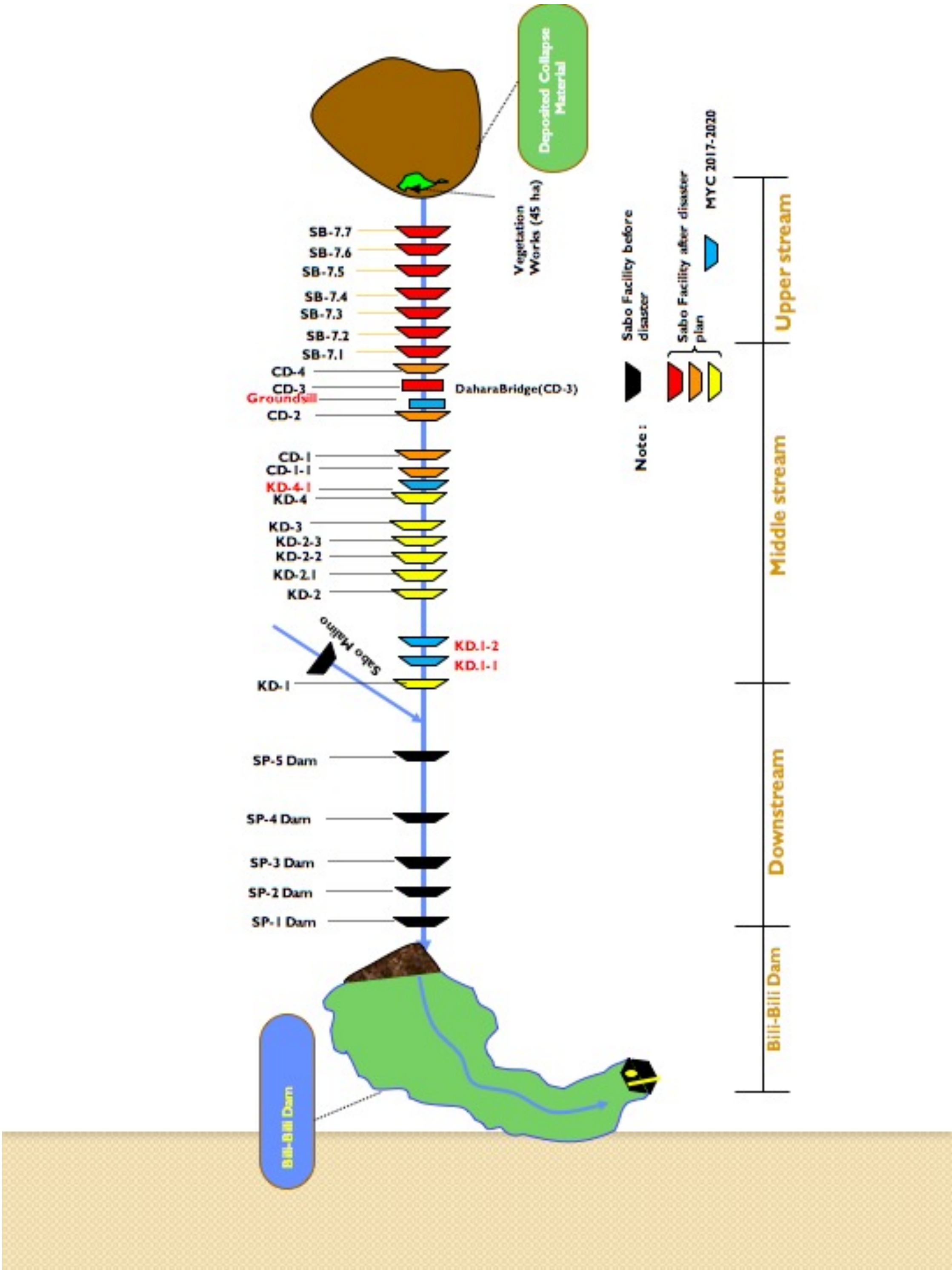

Figure 8 Sediment control structural work

2.7 Particular Issue on river morphology

2.7.1 Sand Mining

Sand mining is now intensively practiced along the downstream reach of Jeneberang River. The annual mining volume in the period (1995 to 2001) was 1,749 thousand m3/year, of which 75 % (or 1,316 thousand m3/year) is mined downstream of Bili-Bili Dam. This downstream extraction volume is more than two times the annual sediment runoff volume of the basin. The excess of sand mining over the natural sediment runoff volume was further aggravated by trapping of sediment runoff by Bili-Bili Dam reservoir, after its completion in 1999. As a result, serious river channel erosion as well as damage to river infrastructure has occurred along the downstream reach of Jeneberang River

Figure 9 Mining activity caused a damage to sand pocket

2.7.2 Sediment Yield

The Jeneberang River has another particular issue regarding sediment runoff as a result of the major collapse of a quay on the caldera of Mt. Bawakaraeng. The collapse occurred on 26 March 2004 and it is now producing a tremendous volume of sediment runoff. The "JICA Sabo Urgent Investigation Team" estimated the volume of these collapses at round 235 million m3 in total, of which about 27 million m3 is expected to accumulate in Bili-Bili Dam reservoir in the next five years. This sediment accumulation corresponds to about 90 % of the dead storage capacity of Bili-Bili Dam reservoir.

Sediment distribution shows the sediment deposition and erosion process in the reservoir bed. Sediment deposit movement from upper reaches of the Jeneberang River, has piled up in the reservoir bottom as illustrated in figure below. At the present, sediment level is above intake pipe, it is very serious condition surrounding intake.

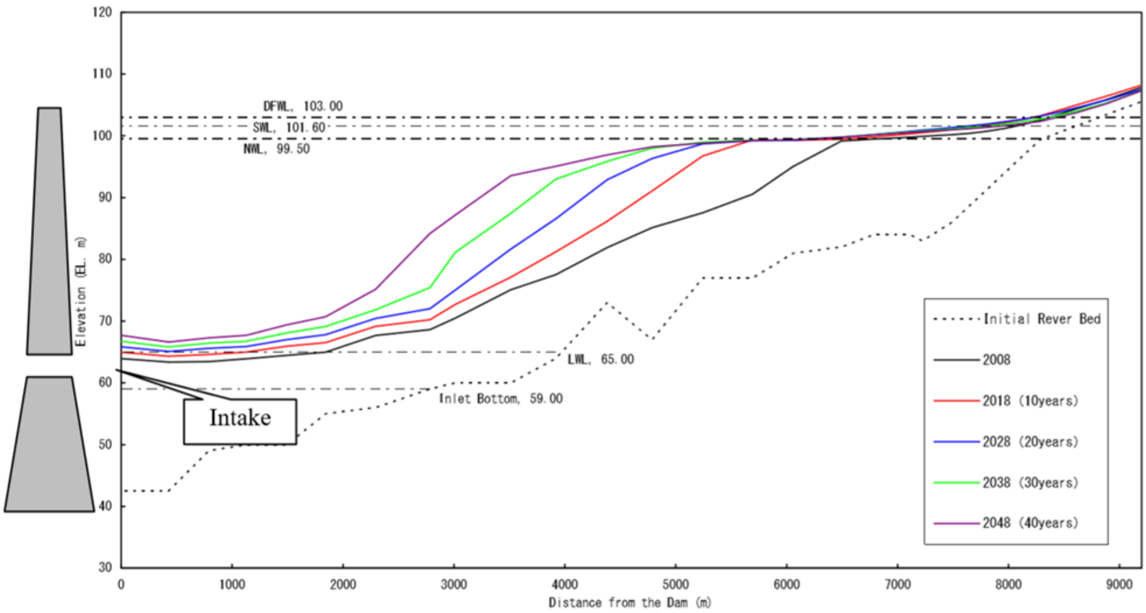

Figure 10 Prediction of Future Reservoir Sedimentation

Based on the one dimensional riverbed fluctuation analysis, the future sediment profile is shown in figure below. In 2048 the 45% of effective reservoir capacity, 54 % of water utilization capacity and about 10 % of flood control capacity could not be utilized. Especially the water utilization function will be badly influenced (Yachio Engineering, 2010).

Based on the analysis of Sedimentation tendency which was entering in 2011 was about 84.81 million m^3 of total sediments with a percentage of 79.17% was in the effective storage area, 18.14% in the area of dead storage and 2.69% in the flood control pool. The depreciation of reservoir storage capacity Bili-Bili that occurred in 2012 was about 24.37%, and it will increase about 31.62% in 2018, meanwhile in 2028 will about 39.92% and 50.33% for the year 2048 (Achsan, 2015).

Figure 11 Sediment deposited in Jeneberang river captured 2019

2.8 Reference

Achsan, 2015, Analisis Kecenderungan Sedimentasi Di Waduk Bili-Bili Dalam Upaya Keberlanjutan Usia Guna Waduk

JICA. 2005. The Study on Capacity Development for Jeneberang River Basin Management in the Republic of Indonesia. Final Report. Volume 1. Japan International Cooperation Agency.

Kompas, 2004: Indonesian National News, August 2005, (Indonesian]

Lundvist, J (1998): "Avert looming hydrocide", pp. 428-433. in 'Ambio', No. 27.

Samang,L., 2007, A Study on Utilization of Jeneberang River's Soil Sediment as the Sub-grade Course Material of Flexible Pavement

Yachiyo Eng. Co. Ltd, 2010, Detailed design report on most urgent maintenance dredging surrounding intake of bili-bili dam, ku.08.08/snvtppsaj/ bpkppsaj-20/viii/2006.

Chapter 3. Effect of Landslide Factor Combinations on the Prediction Accuracy of Landslide Susceptibility Map in Bili-bili Watershed, Indonesia.

3.1 Introduction

Landslide is one of the natural hazards that are unexpected and with a high magnitude that threatens humans and properties. It is a downward movement of rocks and soil, which includes rock, falls, and deep failure of slopes, shallow debris flows, and avalanches. Gravity triggers the movement due to other hazards like an earthquake and high amount of rainfall. Other factors such as geology, morphology, elevation and human activities affect the slope stability of an area. The spatial probability of landslide occurrence, also known as susceptibility (Brabb, 1984), is the probability that any given region will be affected by landslides, given a set of environmental conditions (Guzzetti et al., 2005). Many studies in the field of susceptibility mapping have been conducted in the literature. However, studies on selecting the proper conditioning factors are equally reasonable. The lack of comprehensive research on this topic motivated the authors of this study to conduct such analysis and provide directions for future studies. Landslides occur as a result of the complex interaction between conditioning factors, including meteorology, hydrology, geology, constructions, and geomorphic history (Metternicht, Hurni, & Gogu, 2005; Pradhan & Youssef, 2010).

Van Westen et al. and Guzzetti suggested using all possible factors in the modeling. Meanwhile, there were circumstances where this was not always possible. Some researchers assume that as the number of conditioning factors increases, the precision of the generated susceptibility map increases. By contrast, other case studies prove that a small number of conditioning factors are sufficient to produce landslide susceptibility maps with reasonable quality. Slope instability associated with heavy rainfall or earthquake is a familiar geotechnical problem in Indonesia. Most of Indonesia regions is a mountainous area which frequently experiences a landslide from small to a gigantic scale. Indonesia lies on the convergence of three tectonic plates: Pacific, Indo_Australia and Eurasia plates and it appear like a complicated geologic structure, earthquake belt, and high precipitation.

The main goal of this study was to select the conditioning variables using the application of weights-of-evidence, and certainty factor approach for producing the effective landslide susceptibility maps of a landslide-prone area in Bili-Bili watershed, Indonesia. Rainfall mostly induces the type of landslide events in this area, and its surrounding is selected as the study area.

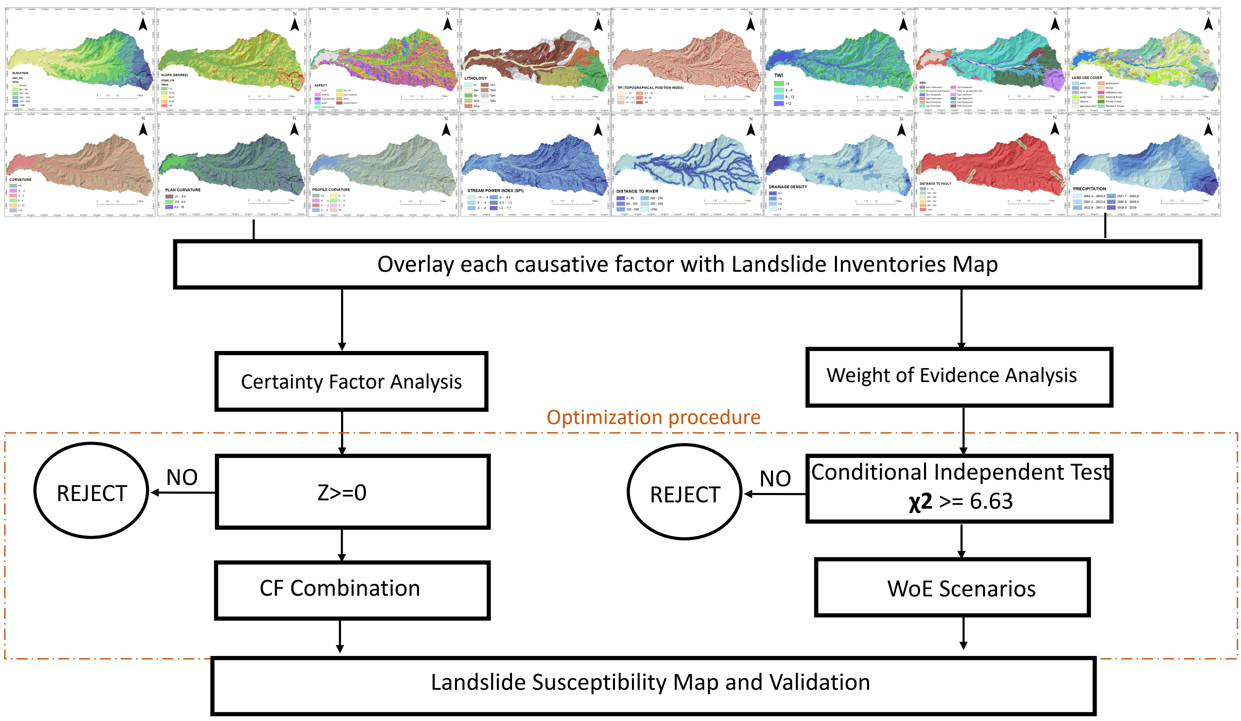

Figure 12 Framework

3.2 Generation of data

3.2.1 Construction of Spatial Database

Data preparation is the first fundamental and essential step for landslide susceptibility analysis. To mapping the potential landslide in sub-watershed Jeneberang, it first conducted studies on the factors that cause landslides. In this study, sixteen landslide causative factors were used, namely: elevation, slope aspect, slope angle, curvature, plan curvature, profile curvature, lithology, drainage density, distance to river, distance to fault, TWI, TPI, SPI, soil texture, rainfall and land cover. Each category was divided into different classes by its value or feature. All data were in prepared in raster format with 12.5 meter spatial resolution.

3.2.2 Landslide Inventory Map

The existing landslide inventory map is essential for studying the relationship between the landslide distribution and the conditioning factors. Moreover, to produce a detailed and reliable landslide inventory map, extensive field surveys and remote sensing were performed resulting a total of 4.466 pixels landslides were observed in the study area.

a. Elevation

A digital elevation model (DEM) can be used to classify the local relief and locate the points of maximum and minimum heights of the study area. The landslides in the study area mainly located along the river in the upper area. Therefore, elevation was used as a parameter to generate the landslide susceptibility map.

b. Slope

Slope angle is directly related to the landslide occurrence, and it is frequently used as a parameter to generate a landslide susceptibility maps. The slope angle is frequently considered to be one of the most influential factors for landslide modeling because it influences the shear forces acting on hill slopes (Dai et al., 2001). Highly sloped areas and cleared areas receive exposure to direct sunlight, which dries the soil and increases the chances of landslides. In this study, the slope angle map is divided into five slope categories.

c. Aspect

Aspect describes the slope direction. Aspect influence the slope stability because it affects moisture retention and vegetation cover, which influence the soil strength. Slope aspect also plays an essential role in exposing the topography to sunlight and drying winds, which control the soil moisture. It is an essential factor in landslide studies (Magliulo et al. 2008).

d. Curvature

Curvature controls the hydrological conditions of the soil cover. Generally, after rainfall, the soil in concave slope will keep and distribute more water than soil in convex slope. However, in many cases, the convex slopes indicate the outcrop of firm bedrock. Concave slopes have a very high prospect for the landslide occurrence than the convex ones (Mezughiet et al. 2012)

e. Plan curvature

Plan curvature controls the convergence or divergence of landslide material and water in the direction of landslide motion (Carson and Kirkby 1972). Plan curvature is described as the curvature of a contour line formed by intersecting a horizontal plane with the surface. The influence of plan curvature on the slope erosion processes is the convergence or divergence of water during downhill flow. For this reason, this parameter constitutes one of the conditioning factors controlling landslide occurrence (Nefeslioglu et al. 2008).

f. Profile curvature

Profile curvature affects the driving and resisting stresses within a landslide in the direction of motion.

g. Lithology

Lithology is the most important parameter in this study of landslides because different lithology units have varying degrees of landslide vulnerability (Dai et al., 2001). The lithological units shown in the surface geologic maps were reclassified according to geology and development center. The result was a generalized geologic map. Finally, the map describes the distribution of six types of lithology:

- TMC (Tertiary Miocene Camba): Marine sediment rocks vary with volcanic rocks, tuff sand varies with sandy tuff and claystone; and have insertion marl, limestone, conglomerate, volcanic breccias, and coal.
- QLVP, QLV, and QLVB (Quarter Lompobatang Volcanic): Agglomerates, lava, breccias, lahar deposition and tuff.

- TPBV, TPBL (Tertiary Pliocene Baturape Cindako Volcanic): Lava and breccias, with insertion tuff and conglomerate.
- QAC (Quarte Aluvium): gravel, sand, clay, mud and coral limestone.

h. TPI

Positive TPI values represent locations that are higher than the average of their surroundings, as defined by the neighborhood (ridges). Negative TPI values represent locations that are lower than their surroundings (valleys). TPI values near zero are either flat areas (where the slope is near zero) or areas of constant slope (where the slope of the point is significantly higher than zero).

i. TWI

Topographic Wetness Index (TWI) describes the steady state index which capable of predicting areas susceptible to saturate land surfaces and areas that carries the potential to produce overland flow.

j. SPI

The stream power index (SPI) is a measure of the erosive power of water flow based on the assumption that discharge (q) is proportional to specific catchment area. Moore et al. (1993) point out that the SPI controls the potential erosive power of overland flow. Therefore, these processes can be considered as one of the components of landslide occurrence (Lee and Min 2001)

k. Distance to river

Rivers play a major role in modifying the terrain by incising different rocks (Meten,2015). Runoff plays an important role and is a triggering factor in landslides. According to Meten (2015), rivers have a significant role in facilitating landslides. The analysis assessed the influence of distance to river and drainage density on a landslide. Gully erosion along the river may initiate landslides. Areas closer to the river network have more erosive forces that erode the base of the slope to a higher degree.

l. Drainage density

Drainage density is the total stream length per unit area of a river basin. Hasegawa et al. (2009) noticed that if precipitation increased, then an area with a higher drainage density is more often prone to a shallow landslide. A large-scale landslide is frequent in areas with less drainage density.

m. Soil

The physical properties of soil are often used for parameter analysis of landslides via a probabilistic approach to soil texture. Soil texture can affect the other physical soil properties such as water infiltration, porosity, and permeability of water and power to pass groundwater. The soil in Indonesia is classified by United States Department of Agriculture system, the Food and Agriculture Organization of the United Nations (FAO), and the Centre of Soil and Agroclimatic Research.

n. Land use cover

Land use also plays an essential role in the stability of the slope. The decrease in the vegetation can make negative influence on the stability slope and probability to landslide occurrence (Soma and Kubota, 2017). Moreover, the land covered by forest regulates continuous water flow. Water regularly infiltrates this area whereas the cultivated land affects the slope stability due to saturation of the covered soil.

o. Distance to fault

It has been observed that the probability of landslide occurrence increases at sites close to lineaments, which not only affect the surface material structures but also make a contribution to terrain permeability causing slope instability.

p. Precipitation

Rainfall is the principal climatic variable that influences landslide distribution. It is affected by topography, elevation, and vegetation—factors that are all interrelated. Mountainous areas especially in the high elevation area, cause the air currents to rise and cool resulting in increased precipitation.

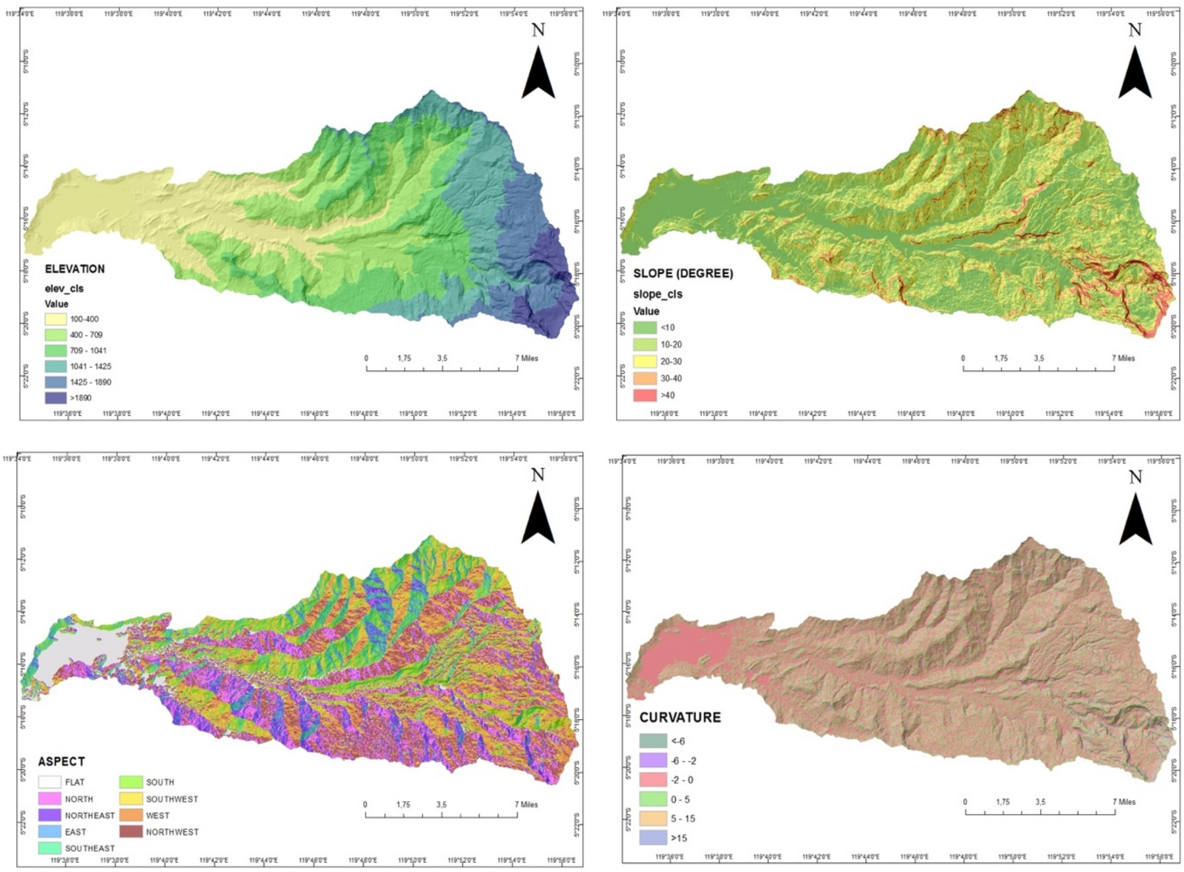

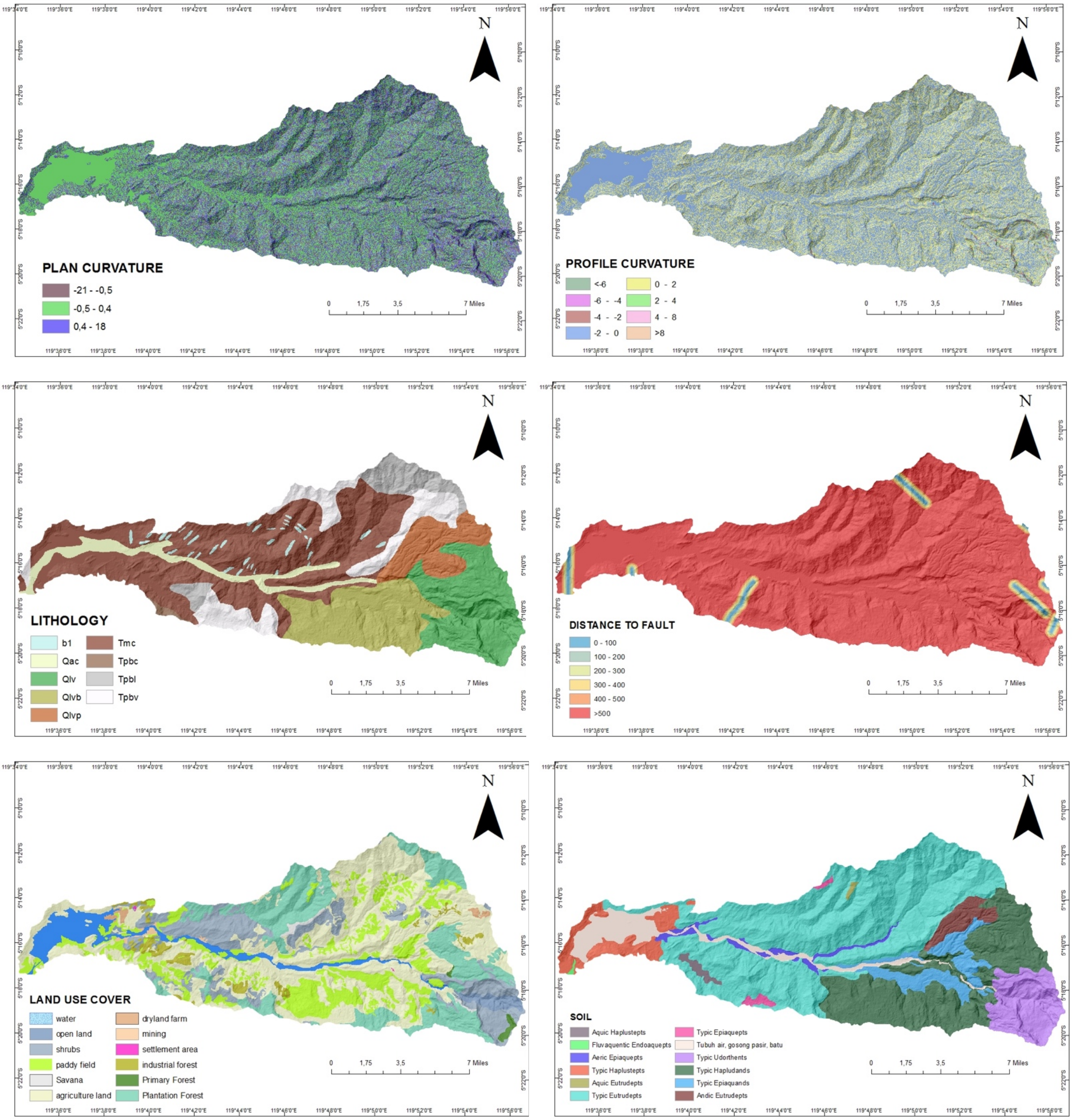

PLAN CURVATURE
-21 - -0,5
-0,5 - 0,4
0,4 - 18
PROFILE CURVATURE
<-6
-6 - -4
-4 - -2
-2 - 0
0 - 2
2 - 4
4 - 8
>8
LITHOLOGY
b1
Qac
Qlv
Qlvb
Qlvp
Tmc
Tpbc
Tpbl
Tpbv
DISTANCE TO FAULT
0 - 100
100 - 200
200 - 300
300 - 400
400 - 500
>500
LAND USE COVER
water
open land
shrubs
paddy field
Savana
agriculture land
dryland farm
mining
settlement area
industrial forest
Primary Forest
Plantation Forest
SOIL
Aquic Haplustepts
Fluvaquentic Endoaquepts
Aeric Epiaquepts
Typic Haplustepts
Aquic Eutrudepts
Typic Eutrudepts
Typic Epiaquepts
Tubuh air, gosong pasir, batu
Typic Udorthents
Typic Hapludands
Typic Epiaquands
Andic Eutrudepts
N
0 1,75 3,5 7 Miles

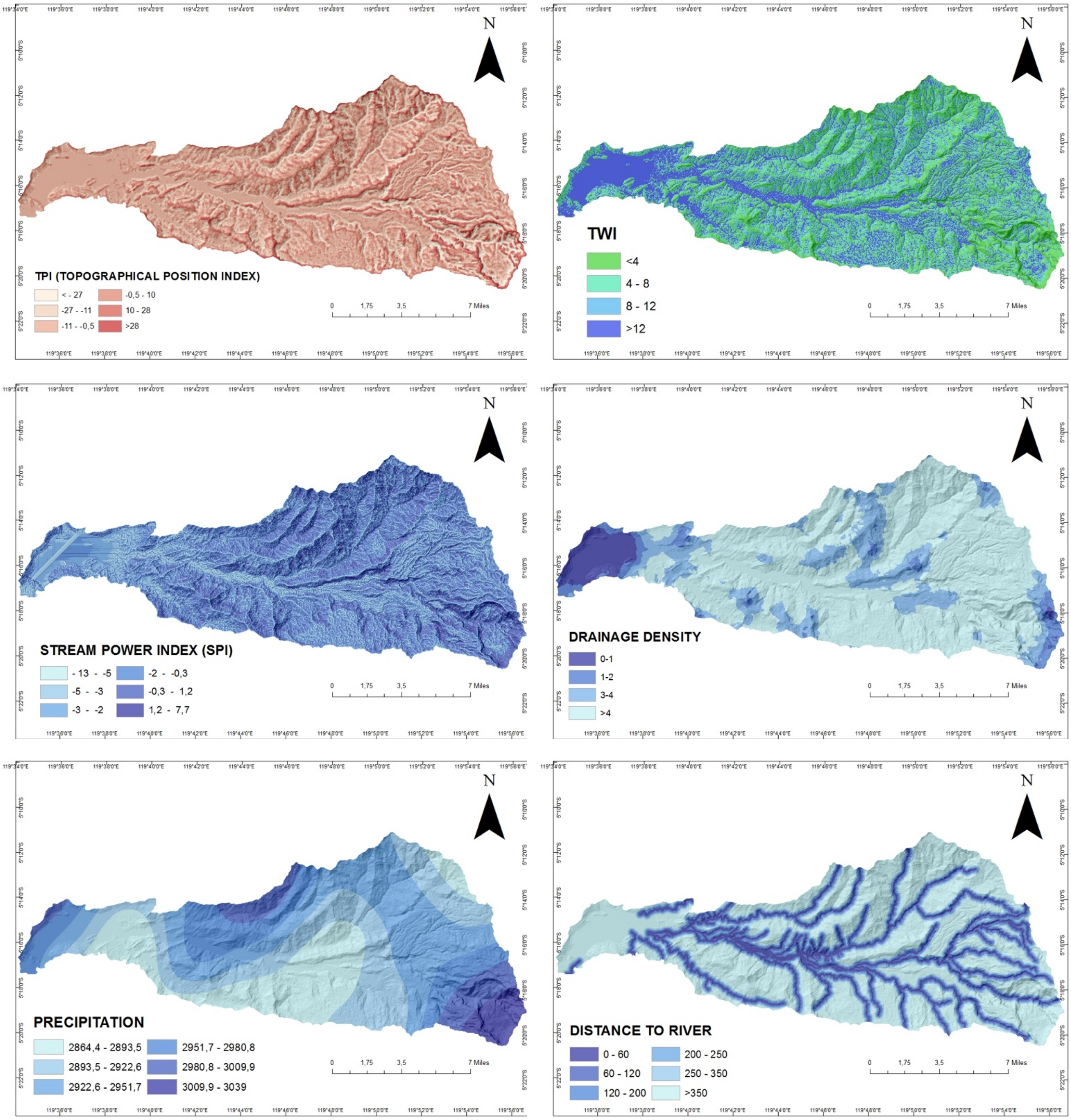

Figure 13 Sixteen causative factors

3.3 Theoretical model

3.3.1 Certainty Factor Analysis

The certainty factor (CF) model is a method for managing uncertainty in rule-based systems. Shortliffe and Buchanan (1975) developed the CF model in the mid-1970s for MYCIN, an expert system for the diagnosis and medical treatment. In this study, CF is applied to selecting the optimal causative factor related to landslide occurrence. CF provides probable favorability functions (FF) for integrating heterogeneous data and can be calculated using the following functions:

$$CF = \begin{cases} \dfrac{PP_a - PP_s}{PP_a(1 - PP_s)} & \text{if } PP_a \geq PP_s \\ \dfrac{PP_a - PP_s}{PP_s(1 - PP_a)} & \text{if } PP_a < PP_s \end{cases} \qquad \textbf{(1)}$$

Where PP_a is the conditional probability of having some landslides event in a class of parameter, a and PP_s is the prior probability of a total number of landslides in the study area. For each of the causative factors, the weights and contrast were calculated using the certainty factor method. The CF approach transforms each class into interval varying between -1 and 1, and it indicates a measure of belief and disbelief. A CF value of -1 indicates that an increasing uncertainty of landslide occurrence or the certainty of the proposition being true is very low, as compared with a high CF near to 1 means that decreasing uncertainty or the indication strongly supports the proposition as true. A value close to 0 means that the prior probability is similar to the conditional one, and is difficult to give any indication about the certainty of the landslide occurrence. The favourability values (ppa, pps) were determined by overlaying each parameter layer with the landslide inventory layer in ArcGIS and landslides falling in each parameter class were determined. These values were used to determine the CF value of each class.

Overlying landslides calculated the CF values for all the condition factors with the parameter class, that is, by calculating the landslide density and the CF values of all the layers using Eq.2 Next, the CF values of the landslide conditioning factors were used for creating various CF layers. Then, the calculated CF layers were combined pairwise. The combination of two CF values, X and Y, due to two different layers of information, is expressed as Z.

$$Z = \begin{cases} CF1 + CF2 - CF1CF2 & CF1,\ CF2 \geq 0 \\ CF1 + CF2 + CF1CF2 & CF1,\ CF2 < 0 \\ \dfrac{CF1 + CF2}{1 - \min(|CF1|,\ |CF2|)} & CF1,\ CF2,\ \text{opposite signs} \end{cases} \quad \textbf{(2)}$$

The pairwise combination is repeatedly performed until all the CF layers are added to obtain the landslide susceptibility index (LSI). Moreover, to make the results easier to interpret, the LSI values are grouped into susceptibility classes to create landslide susceptibility zonation map for the study area. Several authors have applied various methods for dividing the LSI map. In this study, natural break classification method (Constantin et al. 2011; Xu et al. 2012) was used to divide the interval into four classes, and a susceptibility map was prepared. Subsequently, the same classification approach was used for the index of entropy and logistic regression models.

3.3.1.1 Optimization test

The optimization of the model can know by doing optimization test. Eleven out of sixteen causative factor was chosen by certainty factor to generate the landslide susceptibility map. Next step is to generate another two landslide susceptibility maps as a comparison which is, we exclude and adding one factor from eleven selected factor and generate each landslide susceptibility map. We can find out if the optimization is working or not when the validation result shows the eleven causative factor has better accuracy than two other maps.

3.3.2 Weight of Evidence

In this method the weight is calculated for each landslide predictive factor (B) based on the presence or absence of the landslides (S) within the area, as indicated in Bonham-Carter *et al.,* (1994) as follows:

(3)

$$W^{+} = \ln \frac{\dfrac{Npix_1}{Npix_1 + NPix_2}}{\dfrac{NPix_3}{NPix_3 + NPix_4}} \qquad W^{-} = \ln \frac{\dfrac{Npix_2}{Npix_1 + Npix_2}}{\dfrac{Npix_4}{Npix_3 + Npix_4}}$$

W+ and W- are the weights-of-evidence when the factor *B* is present and absent, respectively. A positive weight (W +) indicates the presence of a spatial association between conditioning factor (*B*) and landslides(*S*) while the magnitude of this weight indicates the positive correlation between the presence of the predictive factor and the landslides. A negative weight (W –) indicates an absence of the spatial association between predictive factor (*B*) and landslides (*S*) while the magnitude shows the level of negative correlation. The contrast (C) is the difference between the two weights (C = (W+) – (W-)) where C is positive for a positive spatial association indicating the factor is favorable for the landslides, but C is negative if the spatial association is negative indicating that the factor is unfavorable. The magnitude of the contrast indicates an overall of spatial association between the causative factor and landslides whereas C equal to zero when a class has no spatial relationship with landslides occurrence.

3.3.2.1 Conditional independence test

Weights-of-evidence modeling, the combination of causative factors assumes that the factors are conditionally independent of one another concerning the landslides (Bonham-Carter, 1994). Therefore it is necessary to test the conditional independence (CI) between all causative factors before they can be integrated to create landslide susceptibility index (LSI).

Moreover, to perform CI, all factors maps were converted into binary predictors to apply pair-wise test between all pairs. The contrast (C) was used as a useful measure to convert continuous factors' classes into binary predictors, where the factor's classes having positive values of weight contrasts were assigned as favorable binary predictors to landslides, whereas classes are having negative weight contrast values were assigned as unfavorable.

Table 1 Chi square table

	$P(X \le x)$							
	0.010	0.025	0.050	0.100	0.900	0.950	0.975	0.990
r	$\chi^2_{0.99}(r)$	$\chi^2_{0.975}(r)$	$\chi^2_{0.95}(r)$	$\chi^2_{0.90}(r)$	$\chi^2_{0.10}(r)$	$\chi^2_{0.05}(r)$	$\chi^2_{0.025}(r)$	$\chi^2_{0.01}(r)$
1	0.000	0.001	0.004	0.016	2.706	3.841	5.024	6.635
2	0.020	0.051	0.103	0.211	4.605	5.991	7.378	9.210
3	0.115	0.216	0.352	0.584	6.251	7.815	9.348	11.34
4	0.297	0.484	0.711	1.064	7.779	9.488	11.14	13.28
5	0.554	0.831	1.145	1.610	9.236	11.07	12.83	15.09
6	0.872	1.237	1.635	2.204	10.64	12.59	14.45	16.81
7	1.239	1.690	2.167	2.833	12.02	14.07	16.01	18.48
8	1.646	2.180	2.733	3.490	13.36	15.51	17.54	20.09
9	2.088	2.700	3.325	4.168	14.68	16.92	19.02	21.67
10	2.558	3.247	3.940	4.865	15.99	18.31	20.48	23.21

3.4 RESULT AND DISCUSSION

3.4.1 Correlation between conditioning factors and landslide occurrence

The correlation between the location of landslide and landslide causative factors was performed. The certainty factor values were calculated by overlaying all the causative factors and landslide training data. The results of the spatial relationship between causative factors and landslide using certainty factor and weight of evidence can be seen on Table 1.

The elevation class more than 1890 has the highest value of CF and contrast (CF=0.804, contrast=1.828) followed by elevation class 1425 – 1890 and 1041 – 1425. The CF and contrast values decrease with the decrease in altitude and become negative after 1041 – 1425. It shows that the probability of landslide occurrence increase as the altitude becomes higher than 1425 m. In case of slope class, slope gradient more than 40 degrees has the highest CF and contrast values (CF=0.941, contrast= 2.449), followed by slope class 30 – 40 and 20 – 30. The CF and contrast value is negative for the slope from 20 degrees, so it is obvious that few landslides occurs on a very gentle slope and landslide occurrences increase by the increase in slope gradient. For aspect, south-west facing slope has the highest CF and contrast value (CF=0.372, contrast=0.561) followed by north-facing slope (CF=0.332, contrast=0.491). East and west facing slope are less prone to landslide occurrence as they have a negative CF and contrast value.

In case of curvature, curvature class less than -6 has the highest CF and contrast values (CF=0.921, contrast=2.551). Profile curvature class more than 8 has the highest CF and contrast value (CF=0.911, contrast=2.737). The highest CF and contrast values (CF=0.239, contrast=0.384) is goes to plan curvature with class -21 - -0.5. In case of stream power index, landslide mostly occurred at -0.3 – 1.2 (CF = 0.163, contrast=0.244) and 1.2 – 7.7 (CF = 0.607, contrast=1.235) respectively. For topographic position index, the highest CF and contrast values is less than -27 class (CF=0.820, contrast=1.968) and the lowest CF and contrast values is -11 - -0.5 class (CF=-0.582, contrast= -1.179). And for topographic wetness index, CF and contrast value is positive only for class less than 4 (CF=0.529, contrast=1.394).

Lithology and distance to faults are considered because they affect the strength and permeability that are associated with landslide occurrence. For lithology, the result shows that landslide mostly occurs at QLV (CF=0.754, contrast=2.168) and QLVB (CF=0.524, contrast=0.940) class and only these class has a positive CF and contrast values. In case of distance to faults, class 300 – 400 meters has the highest CF and contrast value (CF=0.516, contrast=0.739). In case of soil class, typic Udorthents has a highest CF and contrast value (CF=0,813, contrast=2.122).

About distance to rivers, the area close to the river is prone to landslide occurrence. From the table as we can see that class 0 – 60 had the highest CF and contrast value and followed with 60 – 120 (CF=0.513, contrast=0.849) and 120 – 200. After 200 meters the CF value is negative. It may relate to the gully erosion that often occurs near the rivers. In case of drainage density, CF and contrast value is positive for class 1 – 2 (CF=0.562, contrast=0.885) and more than 4 meters. The topography change caused by gully erosion might affect the landslide occurrence. For the land cover, the primary forest has the highest CF and contrast value (CF=0.927, contrast=2.676). About precipitation, the probability of landslide occurrence is increasing as the precipitation increase. From the table, we can see that CF and contrast value is positive (CF=0.505, contrast=0.896) start from 2951.7 – 2980.8 class. So, it is evident that landslide is prone to occur after precipitation 2,951.7 mm/year.

Table 2 Spatial relationship between landslide occurrence and causative factors by certainty factor and weight of evidence.

Factors	Class	Certainty Factor		Weight of evidence		
		CF	Z	W+	W-	C
Elevation (m)	100-400	-0.988147551	-2.614963843	-4.43522	0.278909	-4.71413
	400-709	-0.818257322	-3.525377712	-1.70516	0.241301	-1.94646
	709-1041	-0.251845913	-0.955608002	-0.29015	0.065519	-0.35567
	1041-1425	0.567857508	0.152426718	0.839	-0.27913	1.118134
	1425-1890	0.566593468	0.834084273	0.836079	-0.14601	0.982088
	>1890	0.804246157		1.630897	-0.19807	1.828968
Slope (degree)	<10	-0.781583754	-1.863295883	-1.52135	0.328385	-1.84974
	20	-0.60716322	-1.166398533	-0.93436	0.304888	-1.23925
	30	0.243389918	0.466074409	0.278907	-0.08593	0.36484
	40	0.753542304	0.941190413	1.400565	-0.25261	1.653178
	>40	0.889854339		2.205952	-0.24366	2.449611
Aspect	FLAT	-0.624834951	-0.084265595	-0.98039	0.040926	-1.02132
	NORTH	0.332691857	0.075244157	0.404503	-0.08652	0.491023
	NORTHEAST	0.147113173	-0.17208535	0.159128	-0.01453	0.173654
	EAST	-0.267453846	-0.988485001	-0.31123	0.014553	-0.32578
	SOUTHEAST	-0.696536009	-1.24111574	-1.19249	0.063161	-1.25565
	SOUTH	-0.127046842	-0.406228993	-0.13587	0.017598	-0.15347
	SOUTHWEST	0.37253174	-0.460221049	0.466062	-0.09554	0.561602
	WEST	-0.038394925	-0.703732299	-0.03915	0.00664	-0.04579
	NORTHWEST	-0.166763279		-0.18244	0.035131	-0.21757
Curvature	<-6	0.921177034	0.976921324	2.540551	-0.01142	2.551971
	-6 - -2	0.70720873	0.971554852	1.228295	-0.0832	1.311493
	-2 - 0	-0.232529448	0.974464773	-0.26466	0.304123	-0.56878
	0 - 5	0.102299398	0.995822022	0.107919	-0.06637	0.174287
	5 - 15	0.836383756	0.999446306	1.810232	-0.01056	1.820796
	>15	0.867473112		2.02097	-0.00039	2.021358
Profile Curvature	<-6	0.807790626	0.977014723	1.64917	-0.00145	1.650619
	-6- -4	0.88041542	0.99600091	2.123731	-0.00614	2.129866
	-4 - -2	0.826015136	0.995331142	1.748787	-0.04191	1.790695
	-2 - 0	-0.167480084	0.995157515	-0.1833	0.198852	-0.38215
	0 - 2	-0.03718835	0.999137834	-0.0379	0.025685	-0.06358
	2 - 4	0.82195806	0.999943261	1.725736	-0.04543	1.771163
	4 - 8	0.934190415	0.999994967	2.72099	-0.0169	2.737886
	>8	0.911302944		2.422529	-0.00143	2.423958
Plan Curvature	-21 - -0,5	0.23951475	0.03003514	0.273799	-0.11111	0.38491
	-0,5 - 0,4	-0.275455191	0.196917567	-0.32221	0.231058	-0.55327
	0,4 - 18	0.172049972		0.188802	-0.07754	0.266339
Stream Power Index (SPI)	-13 - -5	-0.808944209	-1.991343112	-1.65519	0.042034	-1.69722
	-5 - -3	-0.653640337	-3.438801246	-1.06028	0.086575	-1.14685
	-3 - -2	-0.48388235	-4.393388245	-0.66142	0.121286	-0.78271
	-2 - -0,3	-0.215055134	-3.511946361	-0.24214	0.061456	-0.3036
	-0,3 - 1,2	0.163430082	-0.77482643	0.178445	-0.06564	0.24408
	1,2 - 7,7	0.606638402		0.933026	-0.30212	1.235148
Topographic Position Index (TPI)	> -27	0.820480986	0.825576979	1.717474	-0.25144	1.968918
	-27 - -11	0.028386923	0.723995521	0.028798	-0.00731	0.036106
	-11 - -0,5	-0.582385609	0.64794322	-0.8732	0.306	-1.1792
	-0,5 - 10	-0.275547344	0.754253726	-0.32234	0.085275	-0.40761
	10 - 28	0.301969773	0.886514775	0.359493	-0.05407	0.413563
	>28	0.538201645		0.772627	-0.02505	0.797675

Topographic Wetness Index (TWI)	<4	0.52935075	0.419969885	0.753642	-0.64047	1.394112
	4-8	-0.232404208	0.064892461	-0.26449	0.096284	-0.36078
	8-12	-0.61217067	-0.566932371	-0.94719	0.088743	-1.03593
	>12	-0.67567077		-1.126	0.22231	-1.34831
Lithologi type	Tmc	-0.943348867	-2.886697734	-2.87084	0.49941	-3.37025
	Tpbl	-1	-6.157967468	NaN	0.056442	NaN
	Tpbv	-0.841657869	-7.119488088	-1.843	0.093826	-1.93682
	Qlvp	-0.134328722	-0.99256182	-0.14425	0.010354	-0.1546
	Qlv	0.754595142	-2.985123639	1.404846	-0.76368	2.168522
	b1	-1	-6.922606072	NaN	0.013829	NaN
	Qac	-0.988045238	-2.768267025	-4.42663	0.057159	-4.48378
	Qlvb	0.524365216	-6.53653405	0.743105	-0.19789	0.940998
	Tpbc	-1		NaN	0.003514	NaN
Soil type	Aquic Haplustepts	-1	-3	NaN	0.00621	NaN
	Fluvaquentic End	-1	-7	NaN	0.000779	NaN
	Aeric Epiaquepts	-1	-15	NaN	0.017641	NaN
	Typic Haplustepts	-1	-31	NaN	0.046643	NaN
	Aquic Eutrudepts	-1	-61.10672959	NaN	0.00151	NaN
	Typic Eutrudepts	-0.9408353	-123.2134592	-2.82743	0.640534	-3.46796
	Typic Epiaquepts	-1	-68.73914693	NaN	0.005697	NaN
	Water bodies, Sar	0.438554023	-12.00285437	0.57724	-0.05287	0.630112
	Typic Udorthents	0.813550137	-6.897643237	1.679593	-0.44276	2.122351
	Typic Hapludands	0.392622342	-3.469248271	0.498605	-0.19401	0.692614
	Typic Epiaquands	0.43410355	-7.938496542	0.569344	-0.04795	0.617299
	Andic Eutrudepts	-1		NaN	0.025401	NaN
Distance to Faults (m)	0-100	0.351238749	0.299401009	0.432691	-0.00534	0.438026
	100-200	-0.079902645	0.520515829	-0.08328	0.000765	-0.08404
	200-300	0.315608248	0.768375781	0.379225	-0.00465	0.383875
	300-400	0.516930416	0.811009765	0.727595	-0.01177	0.739365
	400-500	0.184065313	0.806390164	0.203421	-0.00255	0.205967
	>500	-0.024443597		-0.02475	0.373957	-0.3987
Distance to Rivers (m)	0-60	0.51358204	0.761677026	0.720687	-0.12913	0.849819
	60-120	0.510044872	0.825489577	0.713441	-0.11106	0.824504
	120-200	0.267756607	0.78945958	0.311642	-0.04327	0.354911
	200-250	-0.206463292	0.782135855	-0.23126	0.012921	-0.24418
	250-350	-0.034785367	0.69058085	-0.0354	0.004026	-0.03943
	>350	-0.420238974		-0.54514	0.398865	-0.944
Drainage Density	0-1	-0.375011596	0.399016946	-0.47002	0.020634	-0.49066
	1-2	0.562925102	0.154175902	0.827651	-0.05795	0.885605
	3-4	-0.407400912	0.206117048	-0.52324	0.095617	-0.61885
	>4	0.061408921		0.063375	-0.17258	0.235954
Landcover type	Brushes	0.356095886	-0.287808227	0.440205	-0.08988	0.530081
	Plantation	-1	0.639865804	NaN	0.024361	NaN
	Openland	0.720351067	0.725407453	1.27422	-0.03802	1.312242
	Water bodies, Sar	0.237527151	0.746997662	0.271188	-0.01951	0.290695
	Savana	0.078626346	0.551506361	0.08189	-0.00041	0.082297
	Paddy Field	-0.772685748	0.445521498	-1.48142	0.145413	-1.62683
	Peatland	-0.236312968	-0.108957003	-0.2696	0.143943	-0.41354
	Mining	-1	-1.217914006	NaN	0.003023	NaN
	Settlement area	-1	-0.569457684	NaN	0.000255	NaN
	Secondary Forest	0.292372166	-2.138915369	0.345837	-0.10028	0.446112
	Agriculture land	-1	0.77293286	NaN	0.005069	NaN
	Primary Forest	0.927660637		2.626387	-0.05024	2.676628
Rainfall	2864,4 - 2893,5	-0.876803078	-2.306719926	-2.09397	0.222995	-2.31697
	2893,5 - 2922,6	-0.761889655	-2.903543162	-1.43502	0.22342	-1.65844
	2922,6 - 2951,7	-0.180487991	-0.931821245	-0.19905	0.065128	-0.26417
	2951,7 - 2980,8	0.505110828	-0.042118446	0.703421	-0.19354	0.896958
	2980,8 - 3009,9	0.460551307	0.846895365	0.617208	-0.07149	0.688695
	3009,9 - 3039	0.853083269		1.917889	-0.25677	2.174655

3.4.2 Factor Selection by Certainty Factor

The landslide distribution for each class is expressed by the number of occurring pixels and was used to calculate CF values. The table 1 shows the Z value of each causative factor. Based on the Certainty Factor method, eleven out of sixteen causative factors were detected with high influence to landslide occurrences in the study area: profile curvature (0.9999), curvature (0.9994), slope (0.9411), TPI (0.8865), rainfall (0.8468), elevation (0.8340), distance to fault (0.8063), land-use (0.7729), distance to river (0.6905), drainage density (0.2061), plan curvature (0.1969). Therefore, these eleven factors were selected for further processing to create a landslide susceptibility map of the four causative factors.

As mention earlier, Z values describes how strong the relationship between causative factors and landslide occurrence. The result shows profile curvature, and curvature has a highest Z value. Meanwhile, the soil has the lowest Z value (-7.938) which means that based on certainty factor analysis, soil type in the study area has a very low influence on landslide occurrences.

3.4.3 Weight of evidence

First, for the ease of the analysis, all of the factors causing landslides were converted into a binary pattern (presence or absence of landslides) based on weight contrast. Second, Contingency tables (shown in Table 1) were used to test conditional independence for all possible pairs of 16 binary predictor patterns using pair-wise analysis. Then the chi-square (x^2) test was applied to all possible predictor pattern pairs to assess the variation between the expected and observed landslide frequencies of the patterns in the two factors as shown in table 1.

Table 3 An example of the contingency table testing conditional independence between slope and elevation.

		Elevation					
SLOPE	Oi	favorable	unfav	total			
	favorable	2830	640	3470			
	unfav	739	274	1013			
	total	3569	914	4483			
SLOPE	Ei	Elevation					
		favorable	unfav	total			
	favorable	2762.532	707.4682	3470			
	unfav	806.4682	206.5318	1013	1.608466	7.112437	
	total	3569	914	4483	6.159621	16.61299	31.49352

$$\chi^2 = \sum_{i=1}^{i=4} \frac{(O_i - E_i)^2}{O_i}$$

The $\chi 2$ values for testing the conditional independence between pairs of binary patterns were calculated at the 99% significance confidence level and 1 degree of freedom. If the calculated $\chi 2$ value between pairs of binary patterns is below 6.63, then the pair is independent, and they can be used together to map the landslide susceptibility. Otherwise, the pairs are dependent factors need to be rejected.

Table 4 Calculated chi-squared (X2) for testing the conditional independence between all factors.

FACTOR	ELEV	SLO	ASP	CURV	PROF	PLAN	LITHO	RAIN	LUSE	DRAIN	DISRIV	FAULT	SOIL	SPI	TPI	TWI
ELEVATION		31.49	3.87	37.37	0.15	28.90	206.74	4862.61	524.13	13.90	446.82	16.72	NaN	1.01	0.73	85.07
SLOPE	31.49		90.58	64.58	100.41	65.94	22.24	118.24	4.24	24.49	1691.66	92.82	3.19	568.49	31.31	1151.56
ASPECT	3.87	90.58		26.49	6.52	2.57	108.90	39.38	60.57	120.84	121.45	0.39	97.92	19.47	55.94	84.29
CURVATURE	37.37	64.58	26.49		1472.85	199.65	4.29	32.85	2.69	463.74	1.49	0.01	6.47	38.06	0.11	185.13
PROF CURVATURE	0.15	100.41	6.52	1472.85		34.33	85.26	5.17	1.91	827.70	1.46	2.48	249.92	21.49	35.24	39.15
PLAN CURVATURE	28.90	65.94	2.57	199.65	34.33		0.70	19.99	1.35	337.50	0.26	10.32	1.30	0.31	3.43	44.74
LITHO	206.74	22.24	108.90	4.29	85.26	0.70		NaN	43.56	138.39	19.29	NaN	146.87	0.28	10.63	67.52
RAIN	4862.61	118.24	39.38	32.85	5.17	19.99	NaN		305.58	35.75	270.44	NaN	67.79	11.01	21.72	171.51
LUSE	524.13	4.24	60.57	2.69	1.91	1.35	43.56	305.58		29.93	753.13	1816.46	NaN	8.98	316.77	0.45
DRAINDEN	13.90	24.49	120.84	463.74	827.70	337.50	138.39	35.75	29.93		468.00	34.13	78.34	100.58	13.01	5.82
DISRIV	446.82	1691.66	121.45	1.49	1.46	0.26	19.29	270.44	753.13	468.00		NaN	146.77	0.29	0.65	4.97
FAULT	16.72	92.82	0.39	0.01	2.48	10.32	NaN	NaN	1816.46	34.13	NaN		NaN	58.70	0.88	2.33
SOIL	NaN	3.19	97.92	6.47	249.92	1.30	146.87	67.79	NaN	78.34	146.77	NaN		0.12	36.68	50.31
SPI	1.01	568.49	19.47	38.06	21.49	0.31	0.28	11.01	8.98	100.58	0.29	58.70	0.12		2.52	49.24
TPI	0.73	31.31	55.94	0.11	35.24	3.43	10.63	21.72	316.77	13.01	0.65	0.88	36.68	2.52		32.66
TWI	85.07	1151.56	84.29	185.13	39.15	44.74	67.52	171.51	0.45	5.82	4.97	2.33	50.31	49.24	32.66	

The values in highlighted area indicate the independent binary patterns pair related to landslide occurrences and vice versa. For example, the relation between elevation and slope, as shown in the table the X^2 values is 31.49, it means that these parameters is influencing each other's in triggering landslide that's why it has to be rejected. Table 3 shows there are 16 possible scenarios chosen by conditional independence test as an independent variable, which are :

1. Elevation – aspect - profile curvature – SPI - TPI
2. Slope – land use - soil
3. Elevation - aspect - profile curvature - plan curvature - fault
4. Curvature - lithology – land use – distance to river – fault – soil - TPI
5. Elevation – aspect - profile curvature – land use – distance to river – fault – rain
6. Aspect - plan curvature – lithology – land use – distance to river – soil – SPI – TPI
7. Curvature - plan curvature – lithology – SPI
8. Profile curvature - rain
9. Slope – curvature - profile curvature - plan curvature – land use - TWI
10. Drainage density – TWI
11. Curvature - profile curvature - plan curvature – distance to river – SPI – TPI – TWI
12. Aspect – curvature - profile curvature – fault – TPI – TWI
13. Slope – curvature - plan curvature – soil - SPI
14. Elevation - plan curvature – lithology – distance to river – soil – SPI – TPI
15. Elevation – curvature - plan curvature – distance to river – fault – SPI – TPI
16. Land use – drainage density – distance to river – fault - TWI

3.4.4 Accuracy assessment of susceptibility maps

Landslide susceptibility maps without validation are of little meaningful (Chung and Fabric 1998). For validation purpose landslide in the study area was divided into the random partition. This partition falls into two categories 70% for the training and 30% for the validation. The receiver operating characteristics (ROC) curve is a useful method for representing the quality of deterministic and probabilistic detection and forecasting systems (Swets 1988). The area under the curve (AUC) of the ROC characterizes the quality of a forecast system by describing the system's ability to anticipate the correct occurrence or non-occurrence of pre-defined events. The best model has a curve with largest AUC which it varies from 0,5 to 1. The quantitative–qualitative relationship between AUC and prediction accuracy can be classified as follows: 0.9–1, excellent; 0.8–0.9, very good; 0.7–0.8, good; 0.6–0.7, average; and 0.5–0.6, poor.

In this study both the training and validation datasets were selected to assess the models. The training data was used for the LSM success rate, and the validation data was used for prediction. The success rate and prediction rate can be obtained by comparing the landslide susceptibility results at known landslide locations.

Table 5 Optimization test and CF models validation

MODEL	AUC	PREDICTION ACCURACY
10 CAUSATIVE FACTOR	0.901	0.904
11 CAUSATIVE FACTOR	0.903	0.902
12 CAUSATIVE FACTOR	0.901	0.9

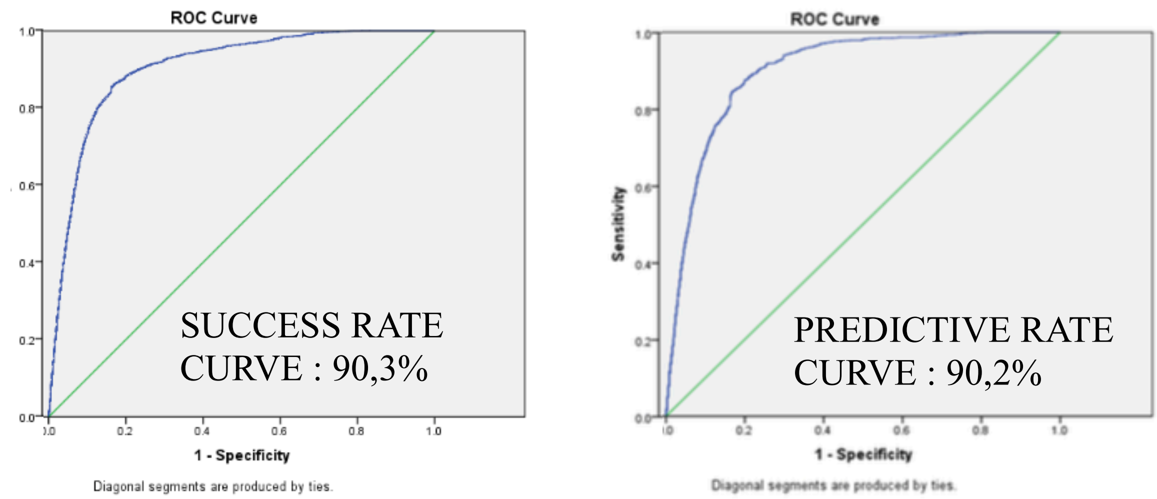

Figure 14 Validation result by ROC for eleven causative factors

The identified eleven landslide conditioning factors (profile curvature, curvature, slope, TPI, rainfall, elevation, distance to fault, land use, distance to river, drainage density, plan curvature) all have a high correlation with landslide occurrence. The results were also validated by the success rate and prediction rate.

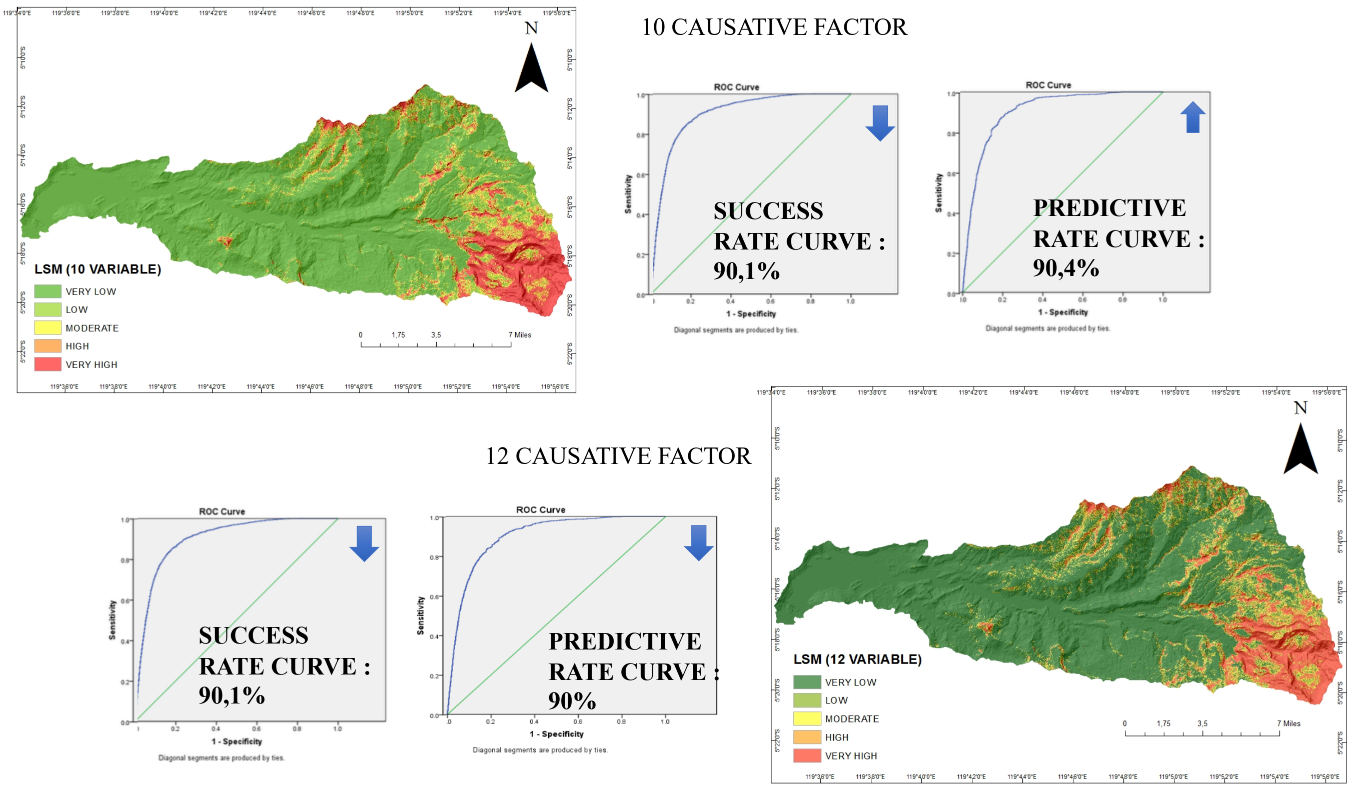

Figure 15 Optimization test (CF)

Moreover, also optimization test was held by excluding and including one conditioning factors in accuracy assessment. It is found that the LSM produced from eleven factors have higher accuracy than ten and twelve models. It is assumed that eleven chosen landslide conditioning factors have a strong influence on landslide occurrences.

Table 6 Sixteen scenarios of independent conditional factors with their validations.

SCENARIO	FACTORS	AUC	PREDICTION ACCURACY (%)
1	ELEVATION,ASPECT,PROF CURVATURE,SPI,TPI	0.86	0.856
2	SLOPE,LUSE,SOIL	0.897	0.885
3	ELEVATION,ASPECT,PROF CURVATURE,PLAN CURVATURE,FAULT	0.825	0.798
4	CURVATURE,LITHO,LUSE,DISRIV,FAULT,SOIL,TPI	0.894	0.897
5	ELEVATION,ASPECT,PROF CURVATURE,LUSE,DISRIV,FAULT,RAIN	0.882	0.874
6	**ASPECT,PLAN CURVATURE,LITHO,LUSE,DISRIV,SOIL,SPI,TPI**	**0.901**	**0.903**
7	CURVATURE,PLAN CURVATURE,LITHO,SPI	0.87	0.866
8	PROF CURVATURE,RAIN	0	0
9	SLOPE,CURVATURE,PROF CURVATURE,PLAN CURVATURE,LUSE,TWI	0.808	0.787
10	DRAINDEN,TWI	0	0
11	CURVATURE,PROF CURVATURE,PLAN CURVATURE,DISRIV,SPI,TPI,TWI	0.835	0.881
12	ASPECT,CURVATURE,PROF CURVATURE,FAULT,TPI,TWI	0.794	0.797
13	SLOPE,CURVATURE,PLAN CURVATURE,SOIL,SPI	0.894	0.855
14	**ELEVATION,PLAN CURVATURE,LITHO,DISRIV,SOIL,SPI,TPI**	**0.901**	**0.899**
15	ELEVATION,CURVATURE,PLAN CURVATURE,DISRIV,FAULT,SPI,TPI	0.877	0.887
16	LUSE,DRAINDEN,DISRIV,FAULT,TWI	0.803	0.794

In case of WOE, the fourteen scenarios were validated by comparing each with the landslide validation set. In this study, we exclude scenario number eight and ten because the pair is too small. According to AUC values, each landslide susceptibility index of models showed a prediction accuracy as shown in Table 5. Among these models, model fourteen comprise of combination: elevation, plan curvature, lithology, distance to river, soil, SPI, and TPI showed the highest accuracy (AUC = 90,1%). Therefore, LSI of this model was chosen as more accurate than others to prepare a landslide susceptibility map.

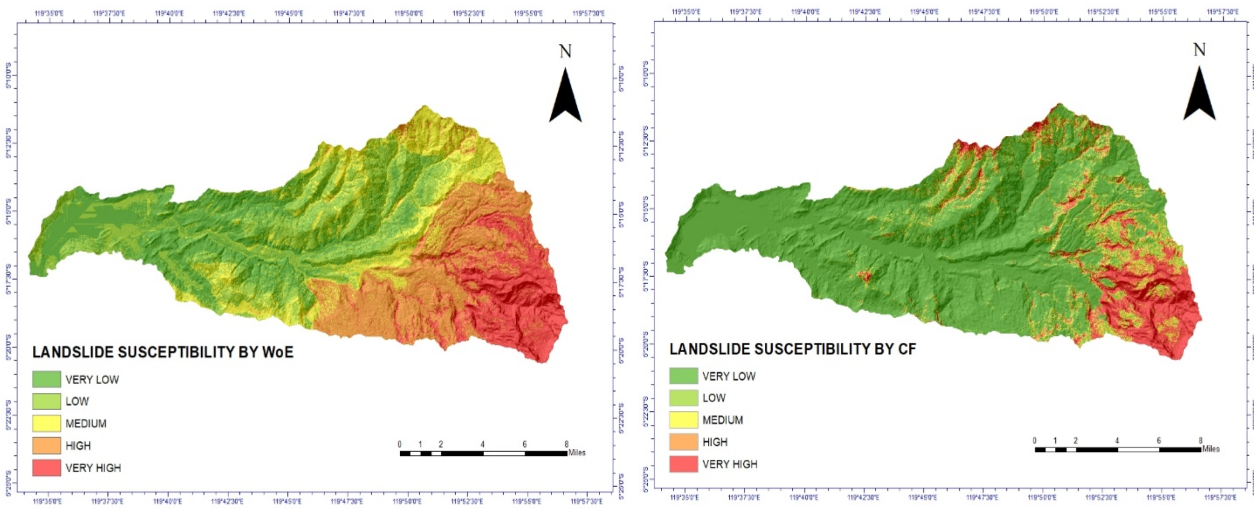

Figure 16 Landslide susceptibility map generated by WoE (left) and CF (right).

The pixel values obtained are then classified based on natural breaks in Arc GIS 9.3 software into low, moderate, high and very high susceptibility groups to determine the class intervals in the landslide susceptibility map as shown in figure 3. From the visual observation, an area classified as the high and very high area is distributed widespread for the landslide susceptibility map generated by WoE. Meanwhile, for the landslide susceptibility that generated by CF, the area which classified as high and very high is distributed in the specific area.

Lastly, the landslide susceptibility map was overlayed with the landslide data set for validation to assess the landslide distribution for each class of susceptibility. Figure 4 shows for WoE models, 97% of total landslides took place in the area which classified as high and very high area. While for CF, 80% of total landslides accumulated in the high and very high area using the eleven conditional factors.

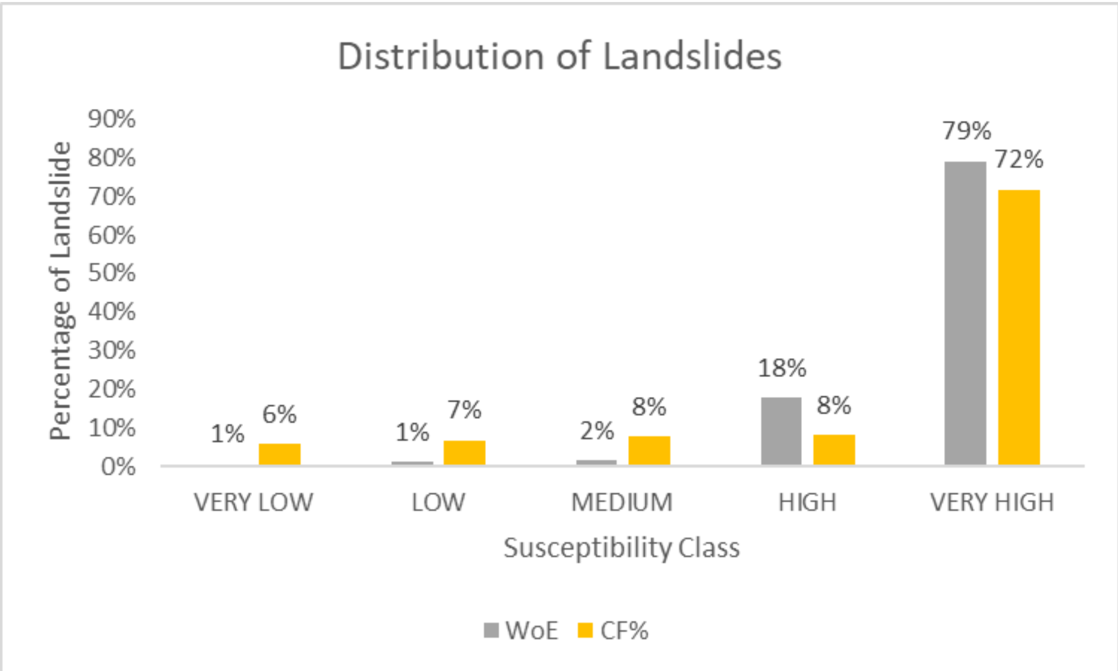

Figure 17 Comparison of landslide distribution for each susceptibility class

3. 5 CONCLUSION

This study demonstrates the usefulness of the certainty factor and weight of evidence to identifying the better-fitted conditioning factors to generate effective landslide susceptibility map. Based on the Certainty Factor method, eleven out of sixteen causative factors were detected with high influence to landslide occurrences in the study area: profile curvature (0.9999), curvature (0.9994), slope (0.9411), TPI (0.8865), rainfall (0.8468), elevation (0.8340), distance to fault (0.8063), land-use (0.7729), distance to river (0.6905), drainage density (0.2061), plan curvature (0.1969). Meanwhile Weight of Evidence shows the dependence correlation in pair of causative factors, whereas rain – elevation has the greatest chi square values 4862.61, followed by fault – land use with chi square values 1816, distance to river – slope 1691, profile curvature – curvature 1472, TWI – slope 1151.

Based on the CF, eleven conditional factors (profile curvature, curvature, slope, TPI, rainfall, elevation, distance to fault, land use, distance to river, drainage density, plan curvature) has a high correlation to landslide occurrence were selected from sixteen factors. Meanwhile weight of evidence applied the conditional independent test to assess the independence of each factor and produce a combination of elevation, plan curvature, lithology, distance to river, soil, SPI, and TPI. Both models have a high accuracy, but the CF models has slightly higher ROC result (AUC = 90.3%, prediction = 90.2%) than WoE (AUC = 90.1%, prediction = 89.9%). The results of this research may provide planners and researchers with a proper perspective about the effect of conditioning factors in the future analysis. The complexity of obtaining high accuracy is related to the fact that each kind of landslide has its own set of conditioning factors, which should be evaluated separately.

3.6 REFERENCES

Brabb, E.E., 1984, Innovative approaches to landslide hazard and risk mapping. Proceedings of the 4th International Symposium on Landslides, 16–21 September, Toronto, Ontario, Canada 1. Canadian Geotechnical Society, Toronto, Ontario, Canada, pp. 307–324.

Carson, M.A., Kirby, M.J., 1972, Hillslope Form and Process. Cambridge University Press, Cambridge

Constantin M, Bednarik M, Jurchescu MC, Vlaicu M., 2011, Landslide susceptibility assessment using the bivariate statistical analysis and the index of entropy in the Sibiciu Basin (Romania). Environ Earth Sci 63 :397–406

Chung CJF, Fabbri AG., 1998, Three Bayesian prediction models for landslide hazard. In: Buccianti A, Nardi G, Potenza R (eds.) Proceedings of International Association for Mathematical Geology 1998 Annual Meeting (IAMG'98), Ischia, Italy, October 1998. pp. 204–211

C. J. Van Westen, N. Rengers, M. T. J. Terlien, and R. Soeters, 1997, "Prediction of the occurrence of slope instability phenomenal through GIS-based hazard zonation," Geologische Rundschau, vol. 86, pp. 404-414

Dai FC, Lee CF, Li J, Xu ZW., 2001, Assessment of landslide susceptibility on the natural terrain of Lantau Island, Hong Kong. Environ Geol 40:381–391

F. Guzzetti, 2002, "Landslide Hazard Assessment and Risk Evaluation: Limit and Prospectives," in The 4th EGS Plinius Conf. on Mediterranean Storms, Mallorca, Spain

Guzzetti, F., Reichenbach, P., Cardinali, M., Galli, M., Ardizzone, F., 2005, Probabilistic landslide hazard assessment at the basin scale. Geomorphology 72 (1–4), 272–299.

Hasegawa S., Yamanaka M., Mimura T., Dahal R.K., Nonomura A., 2009, Drainage density as rainfallinduced landslides susceptibility index. International Seminar on Hazard Management for Sustainable Development in Kathmandu, Nepal (pp. 72-75)

Lee S, Min K., 2001, Statistical analysis of landslide susceptibility at Yongin, Korea. Environ Geol 40:1095–1113.

Magliulo P, Di Lisio A, Russo F, Zelano A. , 2008, Geomorphology and landslide susceptibility assessment using GIS and bivariate statistics: a case study in southern Italy. Nat Hazards. 47: 411–435. doi: 10.1007/s11069-008-9230-x

Meten, M., N.P. Bhandary, and R. Yatabe., 2015, Effect of Landslide Factor Combinations on the Prediction Accuracy of Landslide Susceptibility Maps in the Blue Nile Gorge of Central Ethiopia. Geoenvironmental Disaster 2: 9. doi:10.1186/s40677-015-0016-7

Mezughi TH, Akhir JM, Rafek AG, et al., 2012, Analytical Hierarchy Process Method for Mapping Landslide Susceptibility to an Area along the E-W Highway (Gerik-Jeli), Malaysia. Asian Journal of Earth Sciences 5: 13-24. DOI: 10.3923/ajes.2012.13.24

Metternicht, G., Hurni, L., & Gogu, R., 2005, Remote sensing of landslides: an analysis of the potential contribution to geo-spatial systems for hazard assessment in mountainous environments. Remote Sensing of Environment, 98, 284–303.

Moore ID, Grayson RB, Ladson AR., 1991, Digital terrain modeling: a review of hydrological, geomorphological, and biological applications. Hydrol Process 5:3–30

Moore ID, Gessler PE, Nielsen GA, Peterson GA., 1993, Soil attribute prediction using terrain analysis. Soil Sci Soc Am J 57:443–452

Nefeslioglu HA, Duman TY, Durmaz S., 2008, Landslide susceptibility mapping for a part of tectonic Kelkit Valley (Eastern Black Sea region of Turkey). Geomorphology 94:401–418

Pradhan, B., & Youssef, A.M., 2010, Manifestation of remote sensing data and GIS on landslide hazard analysis using spatial-based statistical models. Arabian Journal of Geosciences, 3, 319–326.

Soma, A.S., Kubota, T., 2017, Land Use Changes on the Slopes and the Implications for the Landslide Occurrences in Ujung-Loe Watersheds South Sulawesi Indonesia. Int. J. Ecol. Dev. 32, 33–42.

Xu C, Xu X, Lee YH, Tan X, Yu G, Dai F., 2012, The 2010 Yushu earthquake triggered landslide hazard mapping using GIS and weight of evidence modeling. Environ Earth Sci. doi:10.1007/s12665- 012-1624-02

Chapter 4. Improved landslide susceptibility map integration with critical land map for revegetation priority in Bili-bili watershed area.

4.1 Introduction

The watershed damage in Indonesia shows an increasing trend from time to time. The watershed damage in Indonesia is reflected in the large number of watersheds that are categorized as having high priority. In 1984, there were 22 super-priority watersheds (Joint Decree of Three Ministers, Minister of Home Affairs, Minister of Forestry, and Minister of Public Works No: 19 of 1984 - No: 059/Kpts-II/1984 - No: 124/Kpts/1984 date April 4, 1984, referred to in Arsyad 2006). In 1999, there were 62 priority I Watersheds, 232 Priority II watersheds, and 178 Priority III watersheds (Ditjen RRL, 1999). In 2004, the number of first-priority watersheds increased to 65 (Ditjen sumber daya air, 2004). In 2009, there were a total of first-priority 108 watersheds in accordance with the Minister of Forestry Decree No. 238/Menhut-II/2009 watershed targets that require action.

The accumulation of critical land areas in South Sulawesi has now reached 682,784 ha, which consists of 369,956 ha in forest areas and 312,828 ha outside forest areas. This critical land has been degraded such that the cover is in the form of shrubs or stands with few trees. The area of this critical land will increase if it is not reforested by a rehabilitation method that can restore land conditions quickly on a large scale.

Erosion occurs on open and critical land, which decreases the land's productivity. If it is not controlled, erosion will worsen and quickly create bigger problems in the future. Erosion on degraded soil can cause landslides that not only damage the land, but can also be a threat to the survival of humans who live in the vicinity. Landslides can be a serious ecological concern because they negatively impact aquatic ecosystems by increasing sediment loadings in streams

(Ziemer et al., 1991, Brosofske et al., 1997, Lewis, 1998, Smith et al., 2003, Constantine et al., 2005).

Landsat imagery in 1986/1987, 1995/1996, and 2000/2001 shows that there has been a decline in the area of forested areas in the Bili-bili watershed over the last few years. In 1986/1987, the area with forest vegetation was 17,450 ha, while in 2003, it was 13,648 ha, which means there was a decrease by 21.79% with an average of 1.5% per year. In 2002, the use of dry land dominated 69.4% of the Bili-bili watershed area, and the area of forest cover was only 4.4% (Supratman, 2003).

Mappa et al. (1987) suggested that the area of critical land in the Bili-bili watershed is 65,620 ha, of which 5,250 ha are severely eroded, 37,400 ha are moderately eroded, and 6,563 ha are moderately eroded. Tangkaisari's (1987) research on erosion rates in the upstream Bili-bili watershed area showed that the total eroded land in the conservation plot was 80 tons/ha/year and that the terraced terraces were 9 tons/ha/year, with both exceed the allowable erosion of 8 tons/ha/year. In 1993-1994, the erosion that occurred upstream of the Bili-bili watershed was 21.53 tons/ha/year, and in 1999, erosion increased to 25.00 tons/ha/year (Makaheming, 2003).

Vegetation plays a very important role in reducing landslide hazards, not only by reducing the impact of rainfall and runoff water, but also by withholding the soil from being carried away. The roots anchor the topsoil and its cover tightly to the substratum, which is essential for landslide prevention on steep slopes. Vegetation recovery on a steep slope can reduce runoff on the slope surface (Ren et al., 2016, Alvarenga et al., 2016), increase water infiltration (Huang et al., 2010), reduce soil erosion (Wang et al., 2016, Huang et al., 2012, Gao et al., 2013), and increase water-use efficiency. Different vegetation types have somewhat different responses to water (Duan et al., 2016).

The most prominent issue regarding upper watershed conservation is the decreasing trend of forest area. Soil conditions affect the efficiency of vegetation reconstruction and recovery (Wang et al., 2016). In addition, vegetation recovery will improve the physical and chemical properties of the soil, such as the soil nutrient content (SNC) (Deng et al., 2016; He et al., 2016) and the soil structure (D. Zhao et al., 2016; Cheng et al., 2013; Tang et al., 2016). Therefore, vegetation recovery on an exposed slope can result in a mutually beneficial relationship between the soil and plants (Chen et al., 2016), which improves the regional ecological environment.

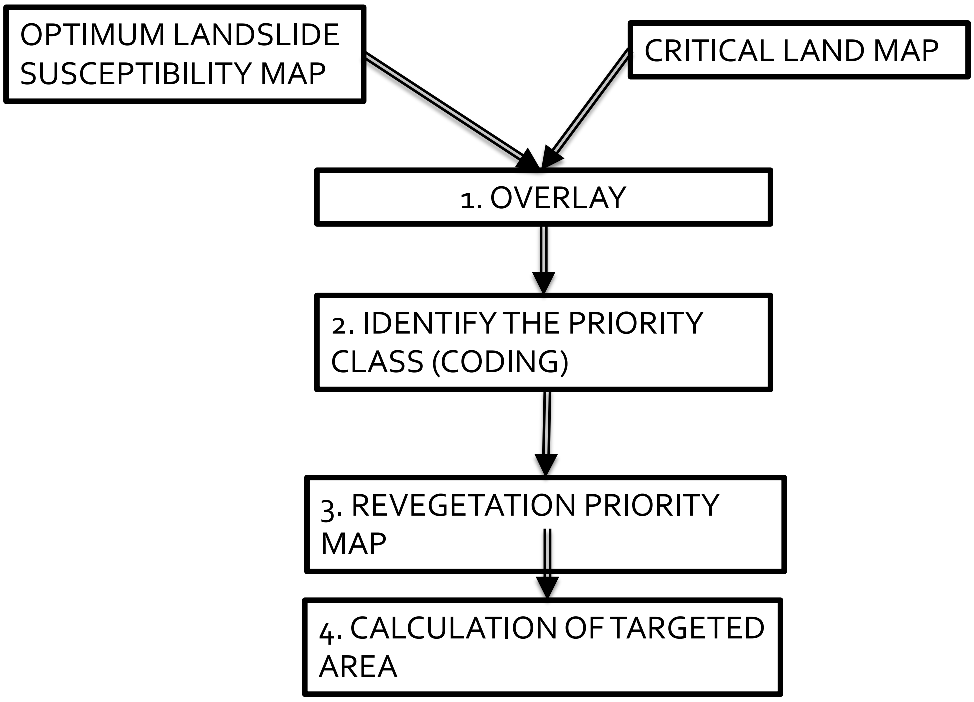

Figure 18 Framework

Susceptibility mapping provides information about vulnerable locations and thus helps to potentially decrease infrastructure damage due to mass wasting. There is a need to investigate potential management plans that simultaneously protect the forest and the ecosystem services of the forest. Hence, one effort to minimize these problems involves incorporating all disaster-related information by preparing a susceptibility map and detecting the critical areas that need prioritized management plans.

This chapter shows an effort to improve the function of the landslide susceptibility map to detect landslide-prone areas and as supporting maps for zoning the highest-priority areas for rehabilitation. The maps could be used to reduce the erosion rate and susceptibility of landslides.

3.2 Material and Methods

3.2.1 Landslide Susceptibility Map

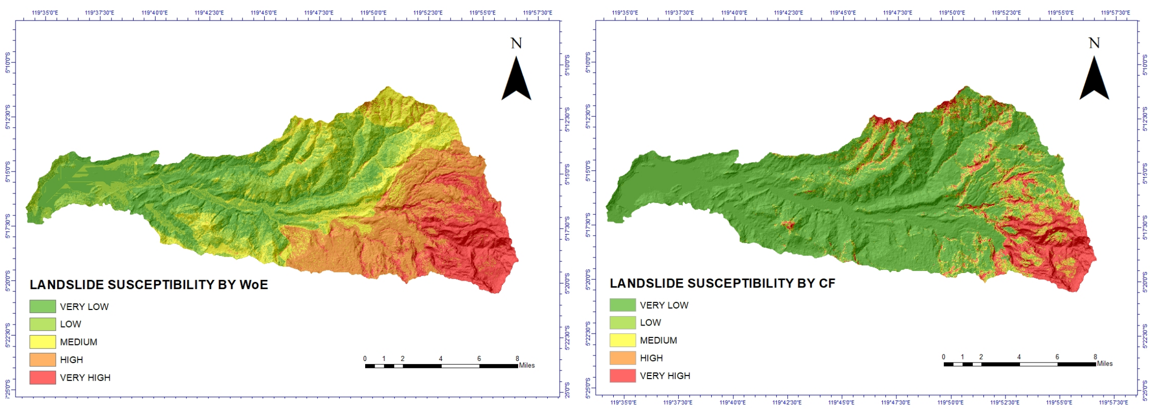

ROC RESULT WoE	
SUCCESS RATE	PREDICTIVE RATE
90.10%	89.90%

ROC RESULT CF	
SUCCESS RATE	PREDICTIVE RATE
90.30%	90.20%

Figure 19 Optimized landslide susceptibility map by WoE and CF

The spatial information related to a landslide susceptibility map is derived from remote sensing data, ground-based information, and several other data sources. Geographic information systems (GISs) are a very powerful tool for the integration of different types of data. Over the past few years, there have been significant developments in GISs for spatial data analysis. Efficient landslide susceptibility mapping can be carried out by combining a GIS with image processing capabilities.

Chapter 3 discussed two landslide susceptibility maps (LSMs) as shown in figure 17 that were generated based on information collected from available maps, satellite data, and field investigations. LSMs with better accuracy will be utilized to integrate with a critical land map from the government of South Sulawesi. The causative factors employed were the elevation, slope, aspect, curvature, plan curvature, profile curvature, lithology, TPI (Topographical Position Index), TWI (Topographical Wetness Index), SPI (Stream Power Index), distance to a river, drainage density, soil, land use cover, distance to a fault, and precipitation. All maps were subdivided into different classes by their value or feature and then converted to a raster format in ArcGIS 9.3.

A certainty factor was used to select 11 out of 16 factors. A combination of seven factors was also selected as independent factors by WoE using a conditional independence test. The validation results were graphically expressed by success-rate curves, and the model's global quality was quantified by calculating the Area Under the Curve (AUC). The validation results showed that the CF model has a slightly greater AUC at 90.3% and a predictive rate curve of 90.2%, which is better than that of WoE (AUC of 90.1% and a predictive rate curve of 89.9%). Therefore, the CF model was chosen for use in the next procedures.

3.2.2 Critical Land Map

In accordance with Indonesian Government Regulation No. 37 of 2012, the carrying capacity of a watershed is its ability to realize sustainability and harmony of the ecosystems and the increasing use of natural resources for humans and other living things in a sustainable manner. A watershed that has been restored for carrying capacity is one where the land conditions, the quantity, quality, and continuity of water, socioeconomics, investment in water construction, and spatial use of the region are not functioning properly. Those that need to be maintained still function as they should. It is necessary to establish a watershed classification throughout Indonesia that divides watershed management into two classifications as follows:

- A watershed that has been restored for carrying capacity is one where the land conditions, the quantity, quality, and continuity of water, socioeconomics, investment in water construction, and spatial use of the region are not functioning
- In watersheds that have sustained carrying capacity, the land conditions, the quantity, quality, and continuity of water, socioeconomics, investment in water construction, and spatial use of the region are functioning properly.

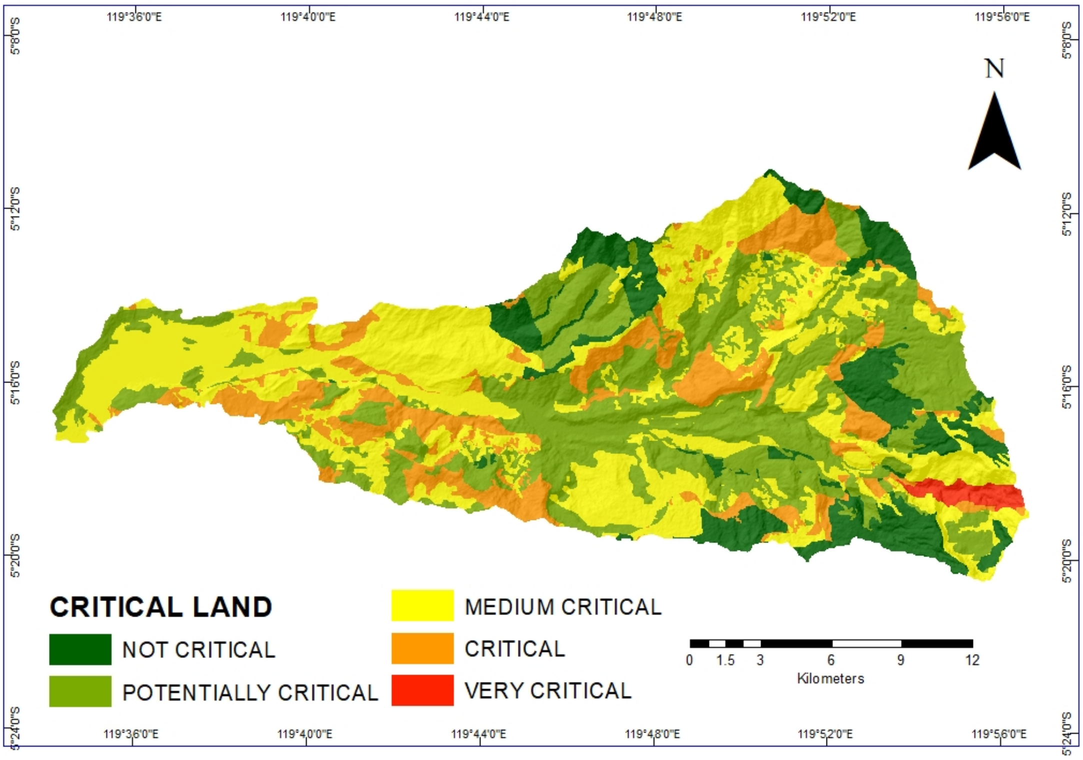

Figure 20 Critical land map of study area

In land exploitation for agricultural activities in Indonesia, little attention is given to appropriate land use planning. For agricultural activities, proper land use planning can only be conducted by the evaluation of land suitability. Critical land is defined as land that has experienced a functional decline (degradation) up to a certain level due to land damage. "Function" in this definition is related to production and water system function.

- Production function relates to land functions such as providing a nutrient source for plants.
- Water system function relates to land function such as provided is a root base and storing ground water.

The critical land map as shown in figure 18 is employed in this study has been verified and validated by the Ministry of Public Work and the Pompengan Jeneberang Watershed Agency. This critical land map was generated by the parameters shown in Figure 17.

Criteria	Sub criteria
Land Condition	Vegetation cover
	Critical land
	Erosion index
Quality, quantity and continuity of water	Flow regim coefficient
	Annual flow
	Sediment flow
	Flood
	Water usage index
Social	Population pressure to land
	Population welfare
	Existance and enforcement of rules
Water building investment	
Land Cover	Protected zone
	Cultivation area

Figure 21 Parameters of critial map

By restoring and maintaining the watershed's carrying capacity, goals can be achieved in terms of realizing productive land conditions in accordance with the carrying capacity and environmental capacity of the watershed in a sustainable manner, realizing the quantity, quality, and sustainability of optimal water availability according to space and time, and improving community welfare.

3.2.3 The relationship Matrix

A relationship matrix is a tool that can identify the presence and strengths of relationships between two or more lists of items. It provides a compact way of representing many-to-many relationships of varying strengths. Relationships between things are often complex (many-to-many) and require thinking in more than one-dimension. The relationship matrix is a simple tool that allows relatively complex situations to be analysed in a simple and straightforward way. It helps to expose interactions and dependencies between things, which helps help us to understand complex causal relationships

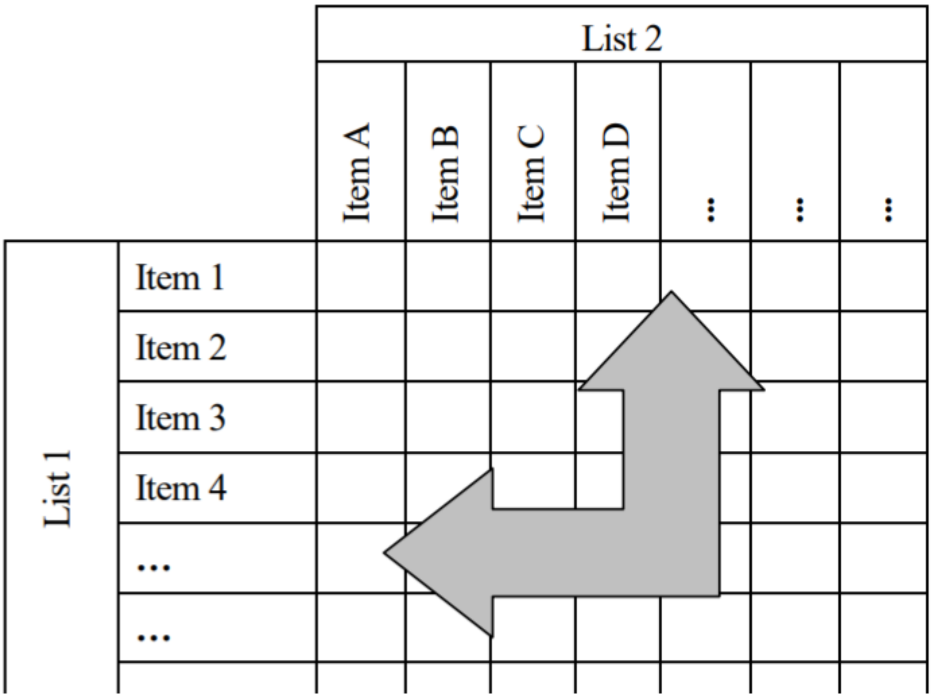

Figure 22 Matrix L type

A matrix diagram can be used to identify and assess the strength of relationships between two or more lists of items. It is particularly useful for examining the relationships between the following:

- A set of vague and un-measurable items with a set of precise and measurable items
- Two sets of items that are physically different

In this study, an L-type matrix was utilized, as shown in Figure 18.

3.3 Result and Discussion

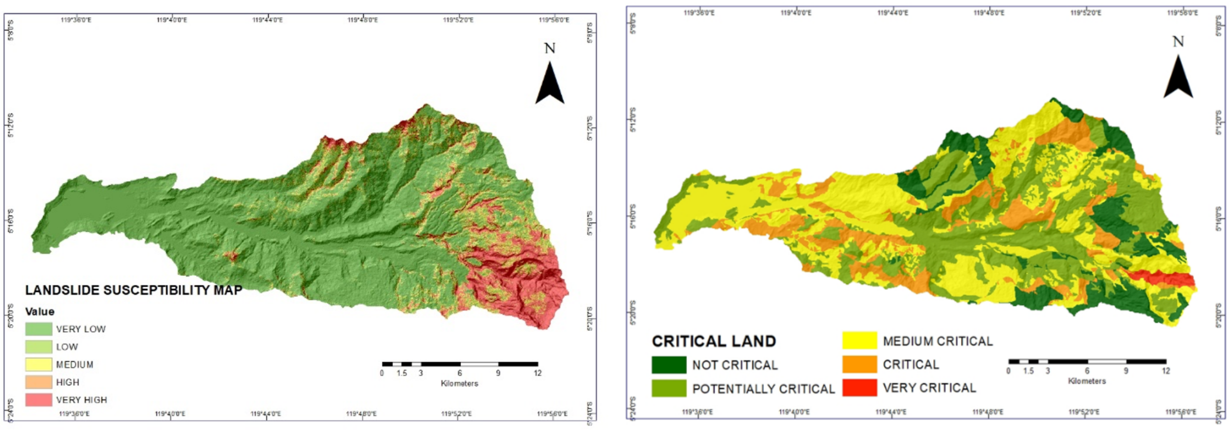

Figure 23 Landslide susceptibility map and critical land map

Numerical data layers were generated to represent the weight values of the factor classes as attribute information from the thematic data layers for data integration and spatial analysis. This analysis uses an objective based on an optimized landslide susceptibility map and critical land map. These two maps were integrated in GIS 10.3 by using the "multi value to point extract" function for a total of 384,815,151 points.

The integrated map was then divided into five classes, which were each divided into four subclasses based on the critical rate. The next step is to define the priority class of each subclass. The purpose of this map is to define zoning based on the critical level and vulnerability to landslides, so the next step is to perform the coding for each sub-class.

A matrix relationship was applied to obtain the code. The factors were then multiplied and assigned a numerical ranking on a scale of 1 to 25 in order of importance, where higher weight indicates more influence toward a critical condition and landslide susceptibility. Then, the result is divided into three priority classes. First priority is a value greater than 16, second priority is a value of 8-16, and third priority is value less than 8.

Critical land classes and landslide susceptibility classes are described by values of 1-5, where critical land classes are 1 = uncritical, 2 = potentially critical, 3 = medium critical, 4 = critical, and 5 = very critical. Each landslide type-based susceptibility map was classified into five classes: 1 = Very high, 2 = High, 3 = Moderate, 4 = Low and 5 = Very low.

x	CRITICAL LAND				
LANDSLIDE	1	2	3	4	5
1	1	2	3	4	5
2	2	4	6	8	10
3	3	6	9	12	15
4	4	8	12	16	20
5	5	10	15	20	25

Figure 24 Result of matrix relationship

The priority class that is generated from the matrix relationship calculation is then applied to the map to be processed in GIS to produce revegetation recovery maps. The first and second priorities are targeted areas that need immediate treatment for a revegetation recovery plan, and third-priority areas can be treated later after the first and second-priority areas have been addressed.

This final Revegetation priority map shows that in study area, 9,856,260.32 m^2 are associated to area that needs an immediate rehabilitation and classified as first priority, and 33,364,481.74 m^2 which corresponds to second priority. The total area that needs immediate handling is 43,220,742 m2.

Table 7 Result of GIS analysis for priority area

LS CLASS	CRITICAL LAND CLASS	Sum of Area_m2	CLASS PRIORITY
VERY LOW	1	265,397,422.63	
	UNCRITICAL	14,447,544.79	3
	POTENTIALLY CRITICAL	94,739,244.55	3
	MEDIUM CRITICAL	111,361,883.40	3
	CRITICAL	44,848,749.89	3
LOW	2	40,484,288.80	
	UNCRITICAL	8,132,643.73	3
	POTENTIALLY CRITICAL	16,284,374.83	3
	MEDIUM CRITICAL	9,290,567.55	3
	CRITICAL	6,774,592.74	3
	VERY CRITICAL	2,109.94	3
MEDIUM	3	18,332,036.46	
	UNCRITICAL	5,123,649.23	3
	POTENTIALLY CRITICAL	6,646,981.85	3
	MEDIUM CRITICAL	3,908,933.76	3
	CRITICAL	2,634,235.23	2
	VERY CRITICAL	18,236.39	2
HIGH	4	17,990,316.58	
	UNCRITICAL	5,844,235.67	3
	POTENTIALLY CRITICAL	6,049,211.92	2
	MEDIUM CRITICAL	3,814,296.45	2
	CRITICAL	2,171,792.09	1
	VERY CRITICAL	110,780.45	1
VERY HIGH	5	42,611,086.77	
	UNCRITICAL	14,188,897.24	3
	POTENTIALLY CRITICAL	7,984,025.70	2
	MEDIUM CRITICAL	12,864,476.05	2
	CRITICAL	3,557,663.96	1
	VERY CRITICAL	4,016,023.82	1
Grand Total		384,815,151.24	

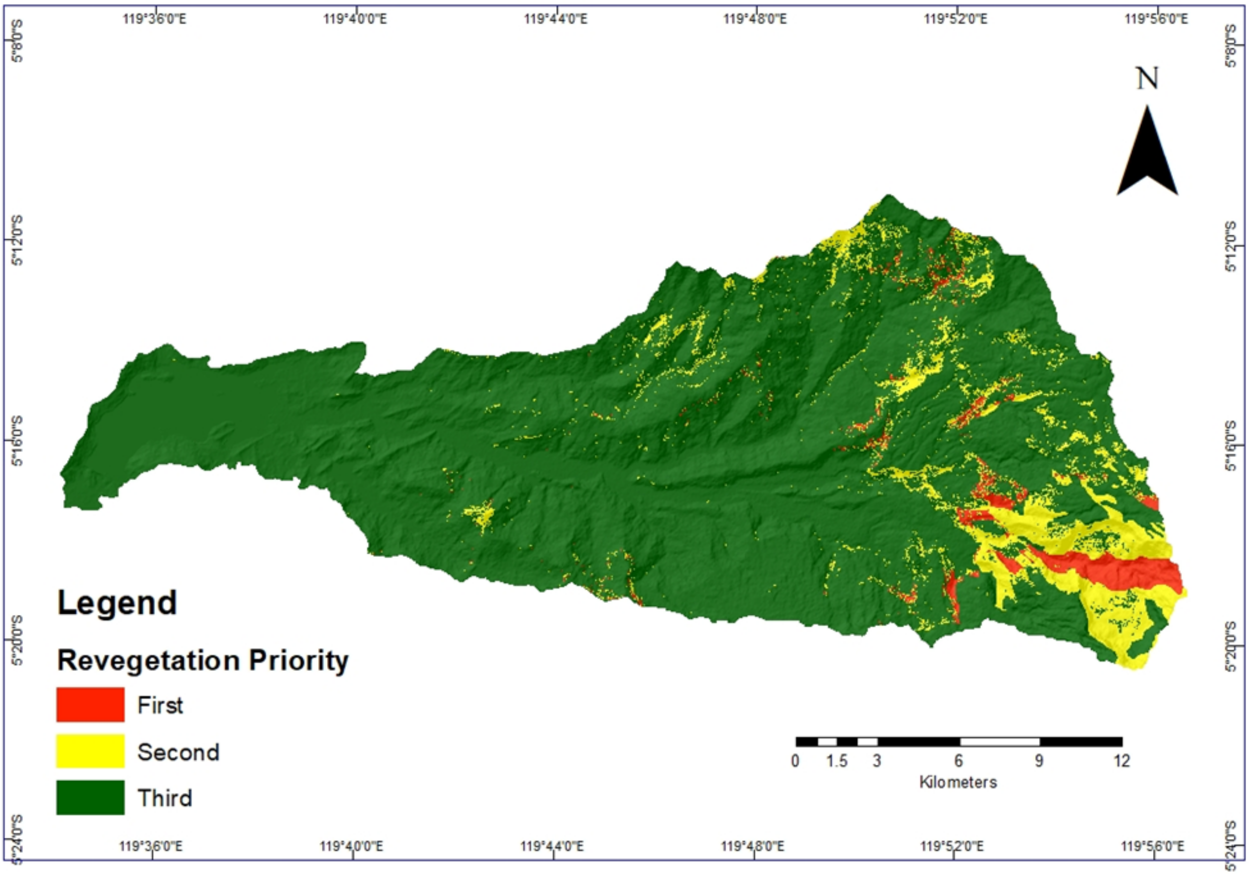

PRIORITY LEVEL	AREA (M^2)
FIRST PRIORITY	9,856,260.32
SECOND PRIORITY	33,364,481.74
THIRD PRIORITY	341,594,409.18
TOTAL AREA	384,815,151.24

Figure 25 Revegetation priority map and area classification

3.4 Conclusion

This chapter has shown an effort to improve the function of a landslide susceptibility map to detect landslide-prone areas and for use as supporting maps for zoning the highest-priority areas for rehabilitation. The maps could be used to reduce the erosion rate and susceptibility of landslides. The new map was generated by integrating an optimized landslide susceptibility map and a critical land map to zone areas for revegetation recovery. The critical land map was verified and validated by the Ministry of Public Work and Pompengan Jeneberang Watershed Agency. Coding for the revegetation recovery map was done using the matrix relationship method, and the zoning areas were divided into three classes of first, second, and third priority. The first and second priorities are targeted areas that need immediate treatment for a revegetation recovery plan, and third-priority areas can be treated later. The results showed that 43,220,742 m^2 are categorized as first and second-priority areas that need an immediate treatment from a total of 384,815,151.24 m^2.

3.5 References

Alvarenga, L.A., de Mello, C.R., Colombo, A., Cuartas, L.A., Bowling, L.C., 2016. Assessment of land cover change on the hydrology of a Brazilian headwater watershed using the Distributed Hydrology-Soil-Vegetation Model. Catena 143, 7–17

Arsyad, S. 2010. Konservasi Tanah dan Air. IPB Press. Bogor.

Brosofske, K.D., Chen, J., Naiman, R.J., Franklin, J.F., 1997. Harvesting effects on microclimatic gradients from small streams to uplands in Western Washington. Ecol. Appl. 7 (4), 1188–1200

Cheng, M., Zhu, Q.L., Liu, L., An, S.S., 2013. Effects of vegetation on soil aggregate stability and organic carbon sequestration in the Ningxia Loess Hilly Region of northwest China. Acta Ecol. Sin. 33, 2835–2844.

Chen, S.N., Ai, X.Y., Dong, T.Y., Li, B.B., Luo, R.H., Ai, Y.W., Chen, Z.Q., Li, C.R., 2016. The physico-chemical properties and structural characteristics of artificial soil for cut slope restoration in Southwestern China. Sci Rep 6, 20565.

Constantine, J.A., Pasternack, G.B., Johnson, M.L., 2005. Logging effects on sediment flux observed in a pollen-based record of overbank deposition in a northern California catchment. Earth Surf. Process. Landf. 30, 813–821.

Deng, J., Sun, P.S., Zhao, F.X., Han, X.H., Yang, G.H., Feng, Y.Z., Ren, G.X., 2016. Soil C, N, P and its stratification ratio affected by artificial vegetation in subsoil, Loess Plateau China. PLoS One 11, e0151446

Departemen Kehutanan, Direktorat Jenderal Reboisasi dan Rehabilitasi Lahan. 1999. Pedoman Penyusunan Rencana Teknik Rehabilitasi Teknik Lapangan dan Konservasi Tanah Daerah Aliran Sungai.

Departemen Kehutanan, 2009. Rencana Strategis Direkorat Jenderal Rehabilitas Lahan dan Perhutanan Sosial 2010-2014. Jakarta.

Duan, L.X., Huang, M.B., Zhang, L.D., 2016. Differences in hydrological responses for different vegetation types on a steep slope on the Loess Plateau, China. J. Hydrol. 537, 356–366.

He, S.X., Liang, Z.S., Han, R.L., Wang, Y., Liu, G.B., 2016. Soil carbon dynamics during grass restoration on abandoned sloping cropland in the hilly area of the Loess Plateau, China. Catena 137, 679–685.

Huang, J., Wu, P.T., Zhao, X.N., 2010. Impact of slope biological regulated measures on soil water infiltration. Trans. Chin. Soc. Agri. Eng. 26, 29–37.

Huang, R., Huang, L., He, B.H., Zhou, L.J., Wang, F., 2012. Effects of slope forest and grass vegetation on reducing rainfall-runoff erosivity in Three Gorges Reservoir Region. Trans. Chin. Soc. Agri. Eng. 28, 70–76.

Gao, Z.L., Fu, Y.L., Zhang, J.J., Zhang, X.P., Wan, L., 2013. Responses of streamflow and sediment load to vegetation restoration in catchments on the Loess Plateau. Trans. Chin. Soc. Agri. Eng. 29, 99–105.

Lewis, J., 1998. Evaluating the impacts of logging activities on erosion and suspended sediment transport in the Caspar Creek Watersheds. In: General Technical Report PSW-GTR-169, . fs.fed.us

Makaheming, Y. 2003. Pola Pengelolaan Hutan pada Hulu DAS Jeneberang Kabupaten Gowa. [Tesis]. Program Pascasarjana, Universitas Hasanuddin. Makassar.

Mappa, H., S. Paembonan, R. Mustaqiem. 1987. Pengembangan Wilayah Terpadu Daerah Aliran Sungai Jeneberang. Bulletin Universitas Hasanuddin. Vol.4. Ujung Pandang.

Ren, Z.P., Zhu, L.J., Wang, B., Cheng, S.D., 2016. Soil hydraulic conductivity as affected by vegetation restoration age on the Loess Plateau, China. J. Arid. Land 8, 546–555.

Smith, D.W., Prepas, E.E., Putz, G., Burke, J.M., Meyer, W.L., Whitson, I., 2003. The forest watershed and riparian disturbance study: a multi-discipline initiative to evaluate and manage watershed disturbance on the Boreal Plain of Canada. J. Environ. Eng. Sci. 2, S1–S13

Supratman dan C. Yudilastiantoro. 2003. Analisis Sistem Kelembagaan Pengelolaan DAS Jeneberang (Analysis of Institutional System of Jeneberang Watershed Management). Jurnal Sosekhut [serial online]. 2(4):1-10. http://puslitsosekhut.web.id/download.php?page=publikasi&sub= jurnal&di=108 [10 Maret 2009]

Tang, J., Dang, T.H., Xue, J., Wen, Y.R., Xu, N., Wu, D.F., 2016. Effect of vegetation restoration on soil aggregate characteristics of an opencast coal mine dump in the loess area. Acta Ecol. Sin. 36, 5067–5077.

Tangkaisari, R. 1987. Tingkat Erosi di Sub DAS Jeneberang. Bulletin Penelitian Universitas Hasanuddin. Ujung Pandang.

Wang, H.D., Wang, J.M., Cao, Y.G., Lu, Y.Q., Qin, Q., Wang, Y., 2016. Effect of soil and topography on vegetation restoration in an opencast coal mine dump in a loess area. Acta Ecol. Sin. 36, 5098–5108.
Wang, H.D., Wang, J.M., Cao, Y.G., Lu, Y.Q., Qin, Q., Wang, Y., 2016. Effect of soil and topography on vegetation restoration in an opencast coal mine dump in a loess area. Acta Ecol. Sin. 36, 5098–5108.
Zhao, D., Xu, M.X., Liu, G.B., Zhang, R.R., Tuo, D.F., 2016. Characterization of soil aggregate microstructure under different revegetation types using micro-computed tomography. Trans. Chin. Soc. Agri. Eng. 32, 123–129

Ziemer, R.R., Lewis, J., Rice, R.M., Lisle, T.E., 1991. Modeling the cumulative watershed effects of forest management strategies. J. Environ. Qual. 20, 36–42.

Chapter 5. Investigation of flood and landslide in the Jeneberang catchment area, Indonesia in 2019

5.1 Overview of extreme flood and landslide

On January 22, 2019, ten regencies in the province of South Sulawesi experienced an extreme flood. The Jeneberang River is one of the major rivers and has the most extensive impact on flooding. The Jeneberang River has a length of 75 km and the area of the Jeneberang Watershed is 727 km^2. The Jeneberang River originates from Mount Bawakaraeng at an altitude of 2,833 above sea level. Bili-bili Dam is a multipurpose dam located on Jeneberang River, Gowa regency. The heavy rainfall that occurred on January 22 was marked by heavy rainfall from January 21 to January 23. The peak rainfall recorded at three measuring stations including 329 mm at Lengkese station, 308 mm at Bawakaraeng station, and 328 mm at Limbungan station. These numbers exceed the normal limit for daily precipitation in this area (150 mm/day). As a result of heavy rainfall, the discharge runoff from the upstream watershed was estimated to be 3500 m^3/s.

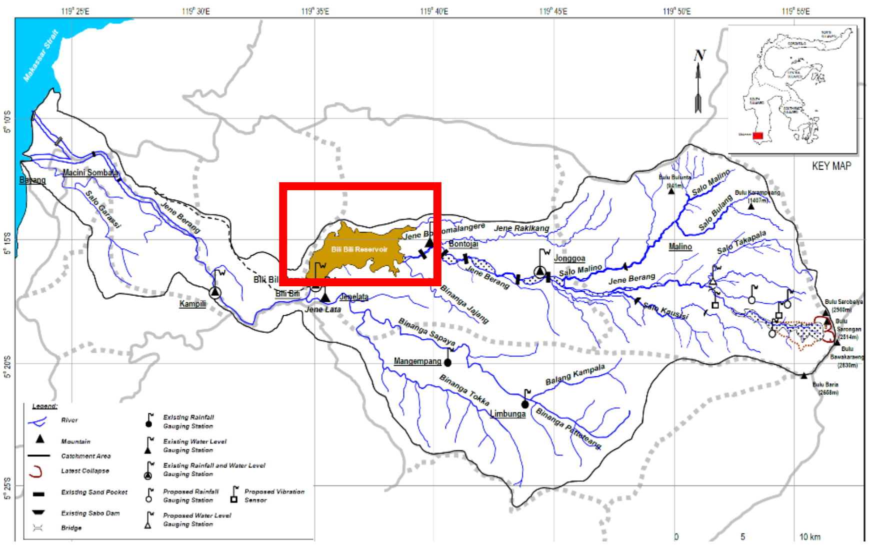

Figure 26 Location of Bili-Bili Dam (Source : Indonesia Ministry of Public Works.

The heavy rainfall caused the Jeneberang River to overflow, resulting in the overfilling of Bili-Bili dam on the Jeneberang River. The inlet data show that the discharge released

Figure 27 Aerial image of the flood (January 24, P. Nurdin).

through the spillway dam ranges from 1200 m^3/s to the maximum spill way capacity of 2200 m^3/s. This shows that the dam can function well even though the water level in the dam is close to the maximum height. However, the spillway door must be opened to avoid overtopping the dam; the water level in the dam reached 101.8, which is the maximal level of Bili-Bili dam (+103). Bili-bili reservoir had been suffered from silting since the gigantic caldera wall collapsed in 2004, which produced 230 million m^3 of sediment deposited on the river and reduced the reservoir capacity. Jeneberang watershed is the 15th highest national priority in terms of Indonesian critical watersheds.

Figure 28 Additional discharge from Jenelata river

The flood downstream was a result of the river basin not being able to accommodate the water discharge from the spillway dam; there was additional discharge from the Jenelata river (1000 m^3/s). The flood hit the settlement area on the banks of the Jeneberang river, which should not be used for residences according to flood maps.

According to the Indonesian National Board for Disaster Management (BNPB), the water level reach roof level (1.5 meters to 4 meters), killed 78 people, and affected 5,825 people; 32 houses were swept away, 25 houses were heavily damaged, 14 were damaged, and 55 were buried under landslides. In addition, 2,694 houses and 11,433 hectares (28,250 acres) of farmland were inundated (as shown in **Fig. 2**) along with damage to various public facilities.

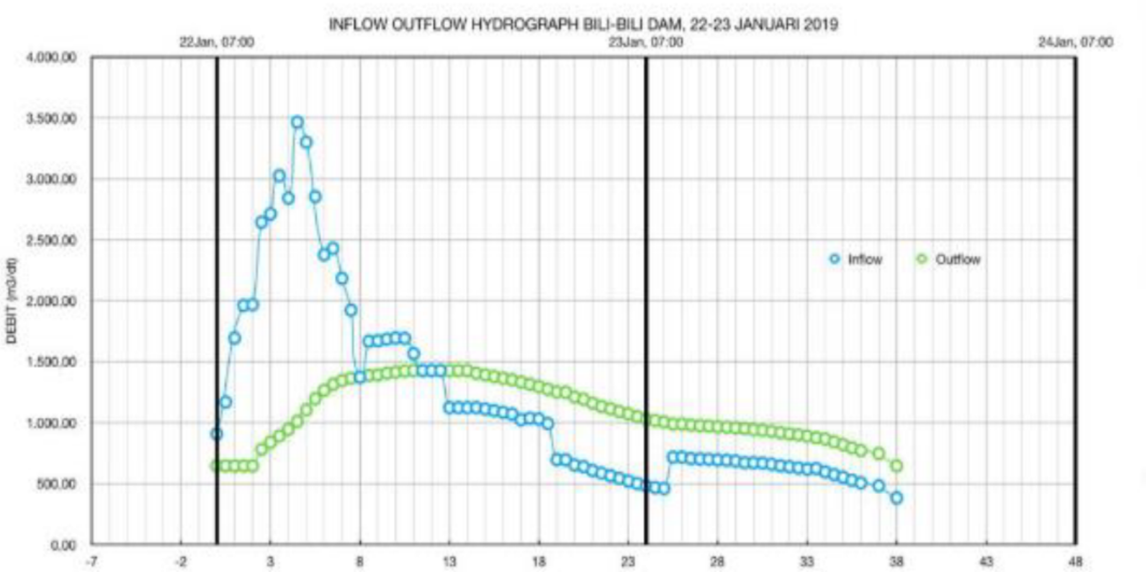

Figure 29 Hydrograph of Bili Bili Dam. Source : BBWS PPJ

5.2 CAUSES OF FLOOD

In addition to an extreme weather upstream, there were also problems in the middle and downstream.

5.2.1 Sedimentation in Bili-Bili Dam

The Bili-Bili Dam is located in Gowa Regency, South Sulawesi, Indonesia, on the Jeneberang River, about 30 km from the city of Makassar. It serves several purposes include flood control, irrigation, and hydroelectric power generation. Based on existing data, the Bili-Bili Dam is planned to accommodate a total volume of 375 million m^3 of water. It is an effective reservoir with 345 million m^3 and sediment storage of 29 million m^3 including a flood control reservoir of 41 million m^3 with spillway release rates of

Sedimentation in the reservoir has been a concern since the gigantic landslide on Bawakaraeng mountain in 2004. The total volume of sediment deposits in 2009 was estimated to be more than 244.9 million m^3, and the unstable sediment deposits remaining in the caldera were estimated to be 82.7 million m^3. The total volume of sediment flowing along the Jeneberang main river channel is 162.2 million m^3. This condition causes an increase in the sedimentation in the Bili-Bili reservoir, which causes silt build-up in the reservoirs that can threaten the sustainability of reservoir functions. To control the sediment flow, a number of sediment control buildings were constructed, i.e., a sabo dam (SD; check dam), consolidated dam (CD), and sand pocket (SP) buildings.

Figure 30 Aerial image of sediment deposited along the river (January 24, P. Nurdin).

5.2.2 Mining Activity

Mining is another problem along the river, but is an important income source for local people and governments. There are sediment control structures like SD, SP, and CD along the Jeneberang River, and these are expected to reduce sediment transport to the Bili-bili reservoir. These dams will optimally work as long as the pools holding the sediments upstream are empty.

Figure 32 Damaged sand pocket (January 30, A. Soma).

Figure 31 Aerial image of shallow landslide (January 24, P. Nurdin).

Mining activity releases sediments in accordance with the recommendations given. This can be controlled when the done properly but our observations in the field suggest that the mining did not follow the prescribed technical recommendations. As a result, a number of sediment control structures have collapsed due to material extraction that is too close to building construction. Hence, the stability is disrupted leading to building collapse (**Fig. 30**). There are shallow landslides in some areas along the river bank (**Fig. 29**).

5.2.3 Land cover change

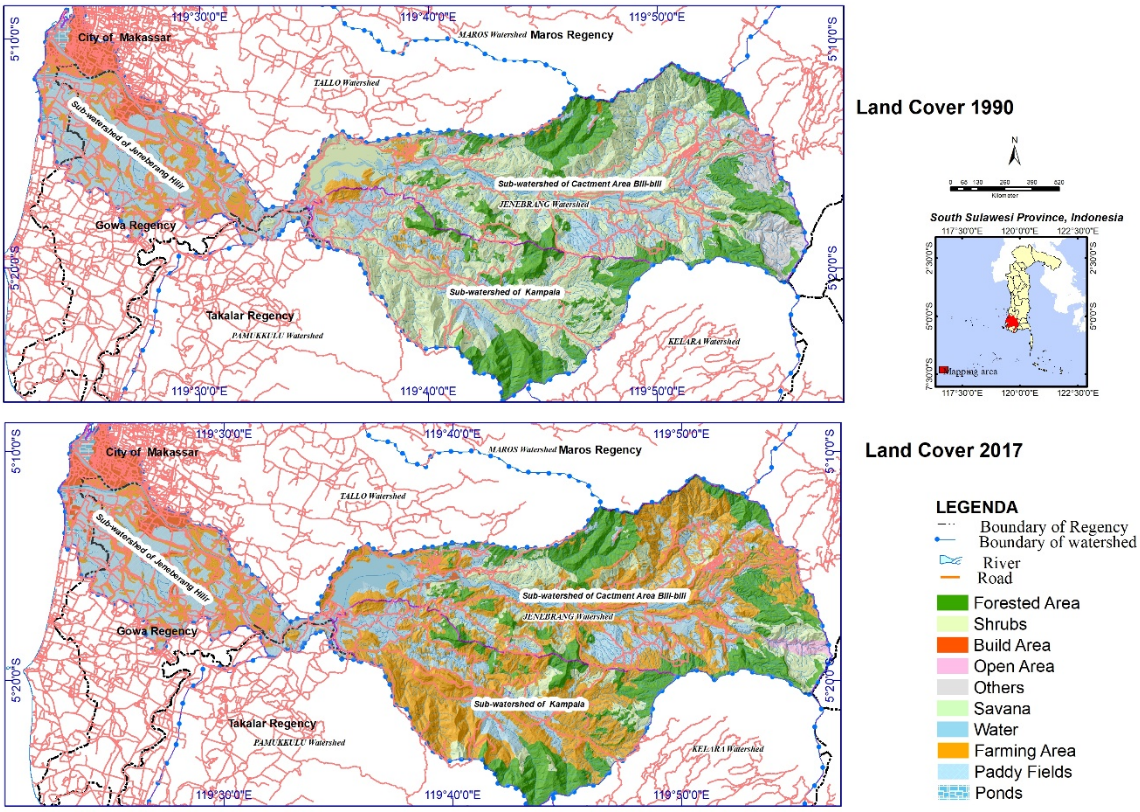

Figure 33 Map of land cover 1990 and 2017.

The Jeneberang watershed is divided to three sub-watersheds, i.e. catchment areas: Bili-Bili Dam, Kampala, and downstream Jeneberang. From 1990 to 2017, the Jeneberang watershed experienced a very significant number of land cover change (**Fig. 31**). Shrub cover changed from 32,222.02 (40%) to 6,339.69 hectares (8%), and the farming area increased from 6,396.98 (8%) to 33,254.11 hectares (42%). Farming areas are dominated with corn, potatoes, carrots, cabbage, etc. located on a steep slope. In 1990, 17% of the area was covered by forest including primary forest, secondary forest, and plantation forest. This decreased to 16.6% in 2017. Land use changed from high vegetation to medium vegetation or low vegetation. This affected the stability of the slope and may lead to landslides (Hasnawir et al., 2017; Soma and Kubota, 2017a, 2017b).

The average population growth rate is 1.31%, and the population density is 398.83 people/ km^2, which is higher than the average population growth rate of South Sulawesi

Province. The impact on land demand continues to increase due to the high socio-economic activity of the population in this region. The main occupation of people in this region is agriculture, which requires land.

The reduced water catchment areas increase flood discharge. Dense residential areas impact the soil and have little water infiltration. During intense rainfall, most of the water will become surface runoff—this exceeds the capacity of the system and causes flooding.

5.2.4 Landslide

The condition of the rain catchment area in the upstream area continues to decline due to land management that does not heed the conservation aspects of the land. This increase

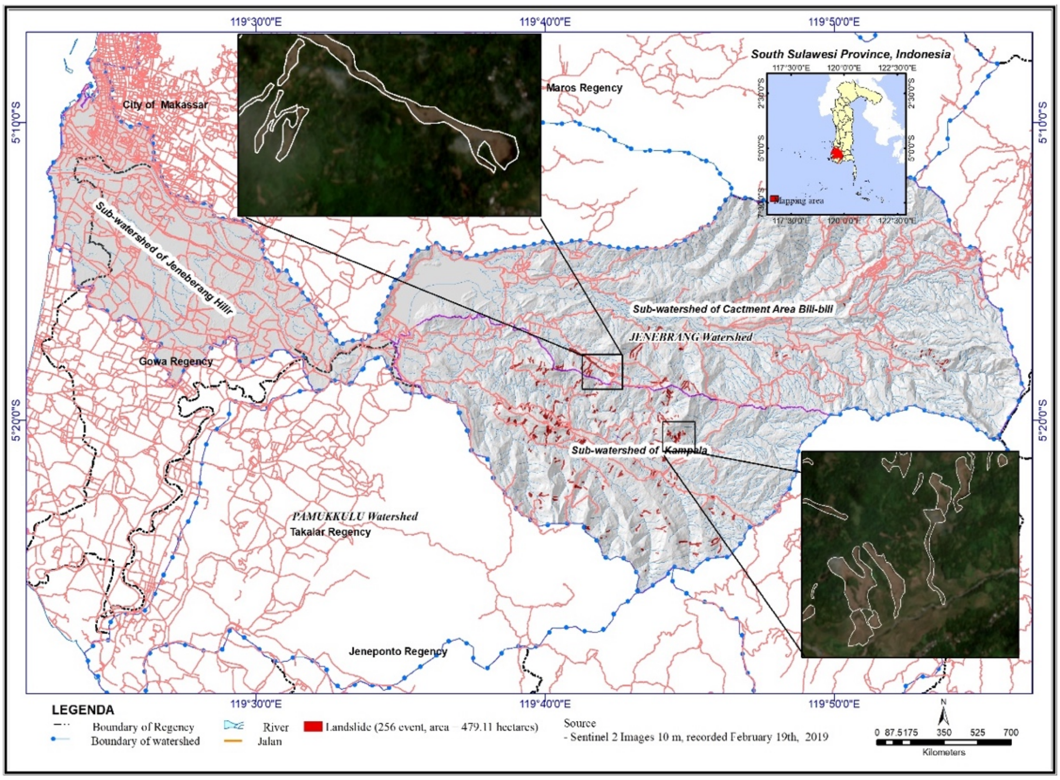

Figure 34 Landslide evidence on January 2019 using sentinel imaging resolution 10 m, recorded February 19th, 2019

soil erosion and impacts sedimentation in the downstream area. This leads to reduced river drainage capacity due to siltation, drought in the dry season, and flooding in the rainy season.

The field observations showed that there was a significant change in land use. There was mostly seasonal plants that further increased runoff and caused landslides and erosion in the upper watershed area.

The classification of the slope class for the Jeneberang watershed area is 0 < 8 degrees. This slope class is 32.38% of the area; slopes above 25 degrees are 28.72% of the area. There are 254 landslides, and the biggest area was 34.96 hectares. The total area of the landslide is 479.11 hectares (as shown in **Fig. 32**). Landslides caused a flash flood in the sub-watershed of Kampala, and this destroyed a bridge downstream. Landslides with extensive impacts occurred in the settlement area and buried half of the village in Pattalikang.

Figure 35 Landslide in agricultural land

Figure 36 Shallow landslide along the road (January 30, P. Nurdin).

5.3 REFERENCES

Government of the Republic of Indonesia Ministry of Public Works Directorate General pf Water Resources. 2010.

Detailed design report on most urgent maintenance dredging surrounding intake of Bili-Bili dam, JBIC LOAN NO.: IP-524 (KU.08.08/SNVTPPSAJ/ BPKPPSAJ-20/VIII/2006)

Hasnawir, Kubota, T., Sanchez-Castillo, L., Soma, A.S., 2017. The influence of land use change and rainfall on shallow landslide in Tanralili Sub-watwrshed, Indonesia. J. Fac. Agric. Kyushu Univ. 62, 171–176.

Soma, A.S., Kubota, T., 2017a. Land use changes on the slopes and the implications for the landslide occurrences in Ujung-Loe Watersheds South Sulawesi Indonesia. Int. J. Ecol. Dev. 32, 33–42.

Soma, A.S., Kubota, T., 2017b. The performance of land use change as a causative factor on landslide susceptibility map in Upper Ujung-Loe Watersheds in South Sulawesi, Indonesia. Geoplanning J. Geomatics Plan. 4, 157–170. doi:10.14710/geoplanning.4.2.157-170

Chapter 6. The Cost and Benefit Analysis of Sediment Based on Landslide and Erosion model in Bili-bili Dam, Indonesia.

6.1 Introduction

Dams have contributed to human development by providing reliable sources of drinking water, irrigation, hydropower, recreation navigation, income, and other important benefits (World commission on Dams, 2000). In the presence of climate change, dams may play an increasingly important role in protecting water resources. For example, areas affected by drought and floods will likely increase in the coming decades.

In 2004, a gigantic landslide occurred on Mount Bawakaraeng, which drastically changed the quality of raw water input to Bili-Bili Multipurpose Dam. This resulted in extreme turbidity, which reached 219 000 nephelometric turbidity units (NTU). A water treatment plant also had difficulties during operation and maintenance. The volume of mass collapse was estimated to be between 200 - 300 million m^3 (Hasnawir et al., 2006). The results of echosounding measurements conducted in June 2004 showed that the volume of sediment deposited in the Bili-Bili Reservoir was 4,763,229 m^3 (Bapro PSDA, 2004). Increased sedimentation occurred in 2005 with the influx of sediment from landslides of the G. Bawakaraeng caldera wall, which amounted to 22,686,654 m^3 (Bapro PSDA, 2005).

All of the area upstream was covered with a deposition of material across 1 to 3 km in width, 30 km in length, and 40 to 200 m in height. The impact of the landslide has not finished and has just started to begin. The destabilized soil materials of landslides were physicality changed by the rain intensity level, which gradually influenced the water quality input of the dam. Soil erosion leads directly to an increase in the amount of sediment in rivers. The Jeneberang River carries sediments to the Bili-Bili Reservoir and causes an increase in sedimentation there. The resulting siltation of the reservoir ultimately reduces the life of the reservoir operation and threatens the sustainability of its functions.

The calculation of the capacity of Sabo-Dam and Sand-Pocket with sediments originating from the collapse of a caldera wall reached 300 million m^3. The additional sediment originating from land erosion each year which reached 5200 m^3. This illustrates that Sabo-Dam and Sand-Pocket cannot accommodate the remaining landslide material, and sediment will flow into the Bili-Bili Reservoir.

According to Lubis and Syafiuddin (1992), the area upstream of the Jeneberang Watershed forest area has reached critical symptoms because the level of erosion exceeds the permissible level. Therefore, we need mechanical and vegetative land conservation actions to prevent soil loss. Studies have shown that the more closely an agricultural system resembles a natural forest in its canopy structure, tree spacing, and ground cover, the less chance there is of soil erosion.

The vegetation indeed plays a very important role in reducing the chance of landslides by reducing the impact of rainfall and runoff water and by stopping the soil from being carried away. Roots anchor the topsoil and its cover tightly to the substratum, which is essential for landslide prevention on steep slopes. Rainfall energy is the prime cause of erosion from tilled or bare land, which occurs when the soil lacks protective vegetative cover. Plants shelter and fix the soil with their roots (Gyssels et al., 2005; de Baets et al., 2007a, b) and reduce the energy of raindrops with their canopy (Bochet et al., 1998; Durán et al., 2007). Vegetation can also act as a physical barrier that alters sediment flow at the soil surface (Van Dijk et al., 1996; Lee et al., 2000; Martínez et al., 2006).

Cost–benefit analysis can be used to select efficient measures for natural disaster risk management in hazard-prone areas. In the context of scarce resources, cost–benefit analysis are useful for selecting the most profitable projects in terms of damages avoided and rejecting projects that are not cost-effective

6.2 Study Area

The main river basin in South Sulawesi Province is Jeneberang River, which has with a catchment area covering 760 km^2. It originates from Mount Lompobatang (el. 2.874 m) and flows into Makassar Strait. Administratively, it is divided into three-part boundaries of basins: Gowa Regency (96.3%, Takalar Regency (2.1%), and Makassar City (1.6%). Jeneberang River catchment is in a tropical climate with high and constant air temperature.

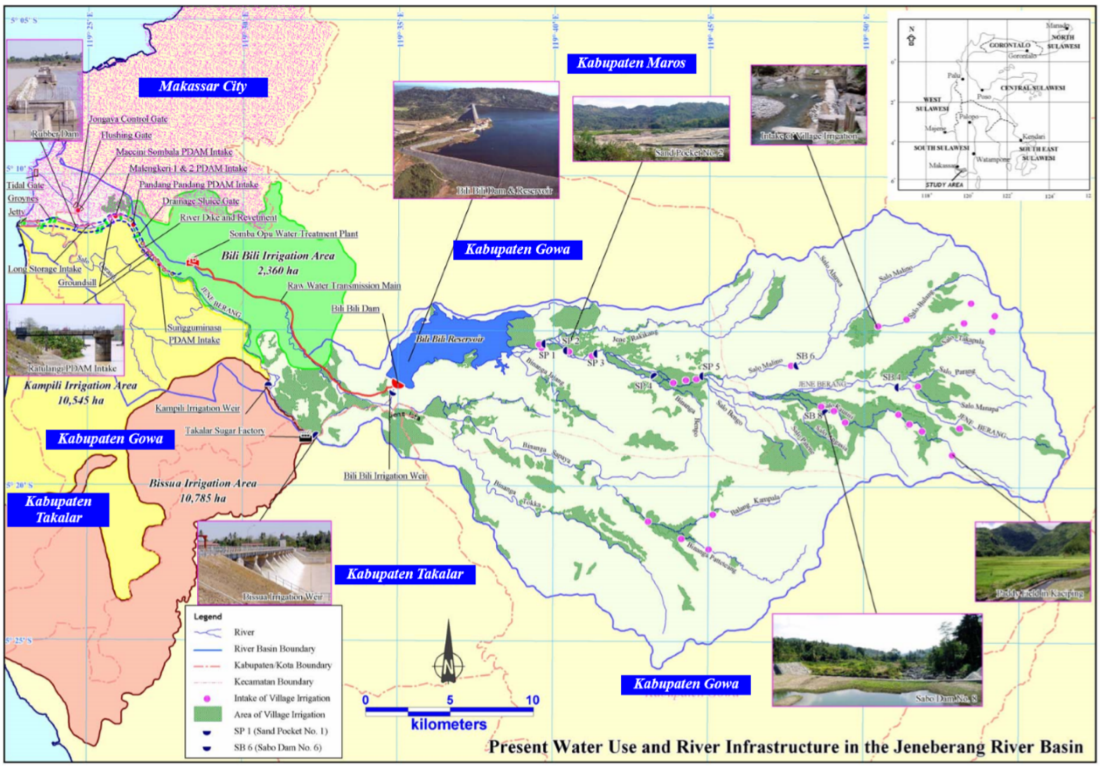

Figure 37 Jeneberang catchment area (Source : JICA, 2005)

The Bili-Bili Reservoir is located on the Jeneberang River in South Sulawesi, Indonesia (5º15' LS and 119 º 37' BT). It was completed in 1999, but initial impounding was started in 1996. It serves the multiple purposes of irrigation, power generation, water supply, and flood control. The gross storage of the reservoir is 375,000,000 m^3, and the effective storage is

346,000,000 m^3. A dead storage of 29,000,000 m^3 is provided for detaining 580,000 m^3 of the estimated annual inflow of sediment.

Jeneberang River Basin is administratively divided into several areas. The Gowa area occupies a substantial part of the river basin and the whole catchments of Bili-Bili multi-purpose dam. The shite area on the top-right side of the map shows the dam's location. Each color indicates each irrigation scheme: pink, yellow, and green indicate the boundary of the Bissua scheme (10.785 ha), Kampili scheme (10.540 ha), and Bili-Bili Irrigation scheme (2.360 ha).

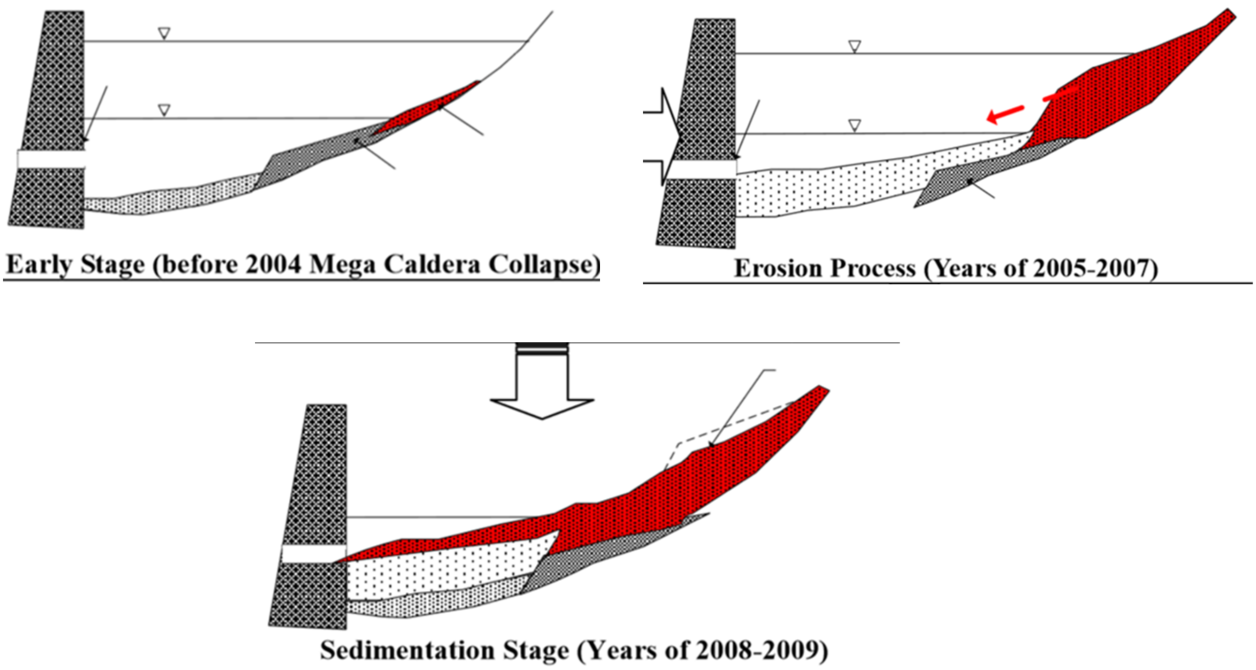

Figure 38 Process of sedimentation movement in DAM

Based on a one-dimensional riverbed fluctuation analysis by Pompengan, the future sediment profile is shown in the figure below. In 2048, 45% of the effective reservoir capacity, 54% of the water utilization capacity, and about 10% of flood control capacity could not be usable. The water utilization function will be badly influenced in particular (Indonesia Ministry of Public work, 2010), which has already occurred in recent years. Although the urgent sediment disaster project work is completed, sediment inflow cannot be stopped, and the reservoir capacity will gradually decrease. Moreover, continuous sediment inflow into reservoir is leading to serious problems, especially for the intake, which might be buried with sedimentation because of its low location.

6.2.1 Objectives

1. Which scenario will optimally reduce the sediment level in Bili-Bili Dam?
2. Which scenario has the most beneficial return according to cost–benefit analysis analysis?

6.3 Material and Methods

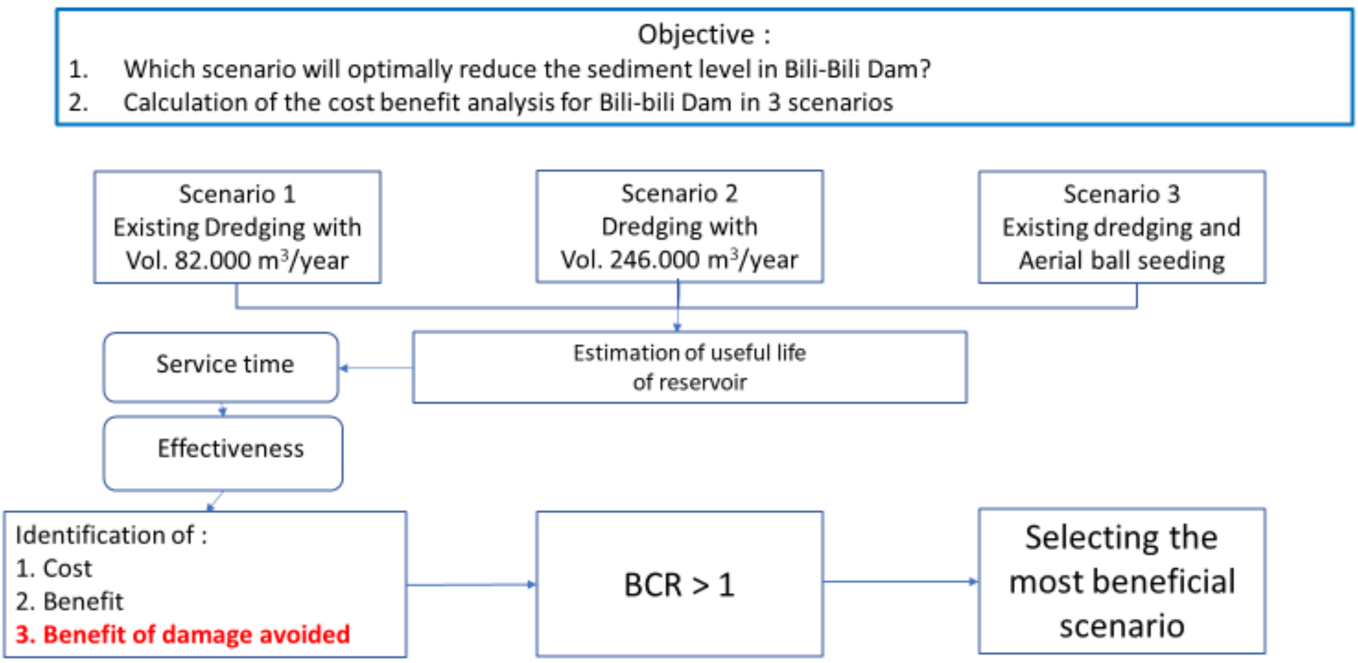

Figure 39 Research framework for cost benefit analysis

6.3.1 Scenario

6.3.1.1 Dredging

Dredging can be performed using one cable-suspended dredge pump. The aims of the project are not to maintain or increase the reservoir capacity but to maintain the function of the existing intake by preventing clogging. The annual dredging sediment volume is 75,000 – 95,000 m^3/year, and the total capacity of the sedimentation pond is 98,000 m^3. The period of the working season is 6 months in the rainy season to minimize the negative impact on downstream water quality and to consider the necessary period for drying up and disposal work.

6.3.1.2 Aerial seeding

Planting seedlings is the technique most used for reforestation as it has the highest guarantee of success. There are, however, some cases where direct sowing is preferable for economic or technical reasons. On the other hand, there may be conditions of urgency or difficult access to a given site where sowing cannot be carried out according to traditional techniques. These situations make aerial sowing a valid alternative.

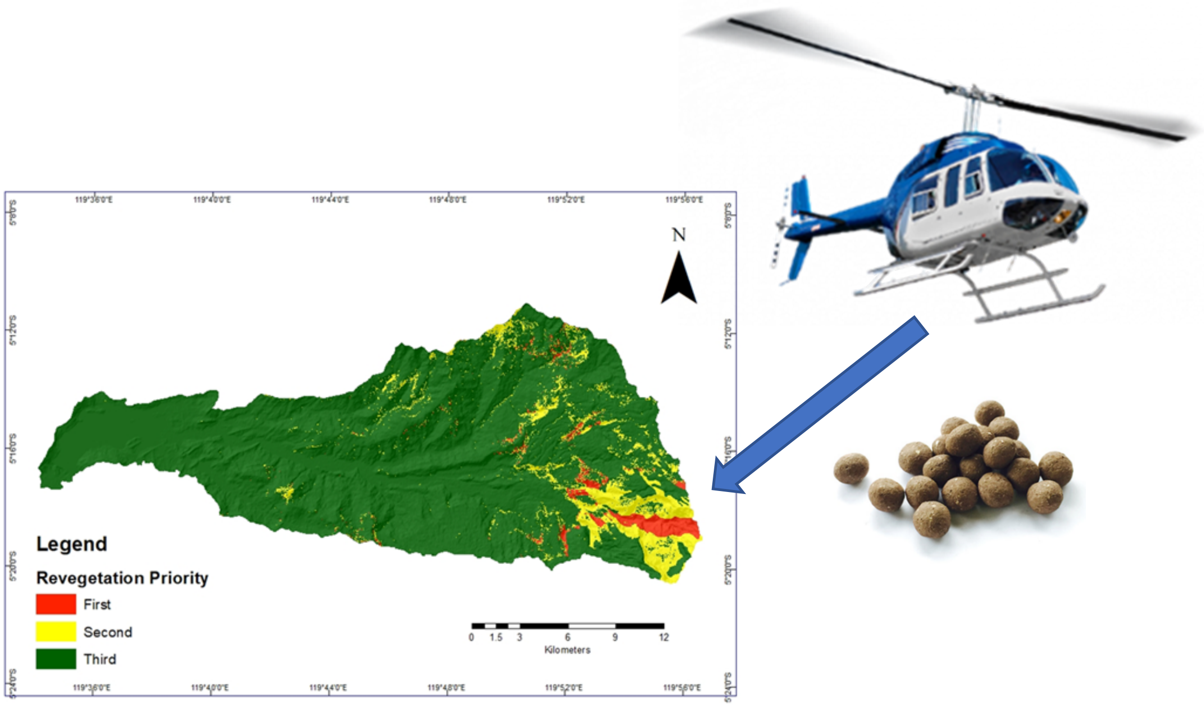

Figure 40 Aerial seeding procedure

Aerial seeding is best suited to sites whose remoteness, ruggedness, inaccessibility, or sparse population make seedling planting difficult. It is particularly appropriate for "protection forests" because helicopters or planes can easily spread seed over steep slopes, remote watersheds, and isolated dryland areas. Seed balls are a conglomeration of clay, sifted dirt, and seeds (mostly the grass family), which are mixed with water and are thrown from helicopters. The balls are between 10 and 80 mm (about 0.4 to 3.15 inches) in diameter. The vegetation types are pioneers that are able to grow in land conditions that have experienced physical, chemical, and biological degradation. The advantage of an airplane or helicopter is its ability to quickly seed large areas, even remote areas, when conditions for prompt germination and survival are best. On steep strip-mine spoils in West Virginia and in Indonesia, slopes of more than 30° (about 70 percent slope) have been successfully revegetated from the air.

There are three scenarios being considered to reduce the sediment level in Bili-Bili Dam:

a. **Scenario 1: Dredging work volume of 82.000 m^3/year – existing condition**

Cable-suspended dredge pump with dredging volume of 82,000 m^3/year.

b. **Scenario 2: Dredging work volume of 246.000 m^3/year**

Multiply the dredging volume to be three times bigger than the existing volume.

c. **Scenario 3: Dredging work volume of 82.000 m^3/year and aerial bomb seeding**

Dredging work and a vegetation recovery plan are combined. The proposed vegetation plan uses aerial bomb seeding. Due to the limitations of planting conditions (steep slopes), aerial seeding is chosen for vegetation recovery in the study area.

6.3.2 Estimation of Useful life of reservoir

The primary functions of a reservoir are to smoothen the variability of surface water flow through control and regulation and to make water available when and where it is needed. Reservoirs have well known primary purposes, such as water supply, irrigation, flood control, hydropower, and navigation. The total storage capacity of reservoirs in the world has been estimated by various sources.

The useful life is an important design parameter of a reservoir that may affect the economic feasibility and sustainability of a water resources project (Gill, 1979). In general, the useful life of a reservoir is the time period when the reservoirs are depleted by 50% of its storage capacity or the dead storage is completely filled with sediment. In this study, the useful life of Bili-Bili Dam was calculated using a volume approach.

$$\text{Useful life of reservoir} = \frac{\text{Remaining Dead Storage Capacity}}{\text{Sediment rate}}$$

6.3.3 Cost Benefit Analysis related to disaster

A cost–benefit analysis is a main economic appraisal technique and is commonly used by governments and public authorities for public investments. The basic idea is to render comparable all the costs and benefits of an investment accruing over time and in different sectors from the viewpoint of society. A cost–benefit analysis has its origins in the rate-of return assessment/financial appraisal methods undertaken in business operations to assess whether investments are profitable or not.

According to ISDR, main principles of a cost–benefit analysis are:

- With-and-without approach: The cost–benefit analysis compares the situation with and without the project/investment, not the situation before and after.
- Focus on selection of "best option": A cost–benefit analysis is used to single out the best option rather than calculating the desirability to undertake a project.
- Societal point of view: The cost–benefit analysis takes a social welfare approach. The benefits to society have to outweigh the costs in order to make a project desirable. The question addressed is whether a specific project or policy adds value to all of society, not to a few individuals or businesses.
- Clearly define boundaries of analysis: We only count losses within the geographical boundaries in the specified community, area, region, or country defined at the outset. The impacts or offsets outside these geographical boundaries should not be considered.

In the context of disaster risk, benefits are probabilistic and arise only in cases of events occurring.

6.3.3.1 Cost of project

is the total funds needed to complete the project or work that consists of a Direct Cost and Indirect Cost. The Project Costs are any expenditures made or estimated to be made, or monetary obligations incurred or estimated to be incurred to complete the project which are listed in a project baseline as shown in figure 41 and more details in appendix 11-15.

6.3.3.2 Benefit of Dam

- Irrigation

  The Bili-Bili multi-purpose dam has an storage capacity of 305 million cubic meters for water supply allocation, providing water to 23.685 ha of agricultural land or the equivalent of 327 million cubic meters, with a river maintenance flow of 1.000 m^3/s. It supplies 107.3 million cubic meters of municipal water at 3.4 m^3/s. The raw water of transmission main with a capacity of 3.3 m^3/s was completed in 1999.

- Hydropower

  Another benefit of the dam is hydropower. According to the State Power Authority-PLN, it is rated at 16.6 MW with an annual output of 77 GWh.

- Raw water purification
- Paddy field purification
- Sediment selling

6.3.3.3 Damage avoided benefit

In this study, the cost–benefit analysis was done using a backward-looking assessment (impact based). Time series data of past damages (10 years) were employed. A cost–benefit analysis related to natural disaster risk was applied in this study, where the damage avoided is estimated and included as a benefit. In a conventional cost–benefit analysis of investment projects, the benefits are the additional outcomes generated by the project compared to the situation without the project. In this study, however, benefits arise due to the savings in terms of avoided damage in the variability of the project outcome.

6.3.4 Discounting

(P/A, *i*, *N*)	**Uniform Series Present Worth Factor**	$\frac{(1+i)^N - 1}{i(i+1)^N}$
(P/F, *i*, *N*)	**Single payment present worth factor**	$\frac{1}{(1+i)^N}$

In a cost–benefit analysis (and economics in general), costs and benefit streams occurring in future periods need to be discounted. This entails adjusting future benefits and costs by the discount factor. Present Value (PV) is used in finance by calculating the present-date value of an amount that is received at a future date. The premise of the equation is that there is a time value of money, which is the concept that receiving something today is worth more than receiving the same item at a future date.

Discounting is considered as people putting a higher value on the present. Funds invested now offer profit opportunities in the future, and there is generally uncertainty about the future. The discount rate represents the average expected return of a public investment into alternatives projects.

6.3.5 Project evaluation decision criteria

There are different types or methods of analysis to determine the economic efficiency of a project. The types that will be covered in this study are:

6.3.5.1 Benefit Cost Ratio

All benefits and costs should be expressed in discounted present values. Costs and benefits have to be compared in order to be able to arrive at a decision. This is the ratio of project benefits versus project costs. It involves summing the total discounted benefits for a project over its entire duration/life span and dividing it over the total discounted costs of the project. A scenario with a benefit-cost ratio greater than one has greater benefits than costs, so it has positive net benefits. The higher the ratio, the greater the benefits relative to the costs are.

BCR < 1.0	BCR = 1.0	BCR > 1.0
In this criterion, the project should not proceed.	Cost equals the benefits, means the project should be allowed to proceed but with little viability	The project should be allowed to proceed.

6.3.5.2 Net Present value

This method considers the difference between the total discounted benefits minus the total discounted costs, which gives the Net Present Value of a project. Projects with positive net benefits are considered to be viable and a project with a higher NPV as compared with another project with a lower NPV is measured to be less lucrative. In other words, the higher the NPV, the greater the calculated benefits of the project.

6.4 Result

6.4.1 Service life time of Dam

The main differences between the three proposed scenarios is that scenarios 1 and 2 only focus on reducing sediment in the reservoir through dredging, while scenario 3 also proposes revegetation recovery, which is expected to reduce the erosion rate upstream and the possibility of landslides in that area. Vegetation coverage influences the entire process of soil erosion. Further investigations on the effect of plant roots in preventing shallow mass movements are of major interest, especially at the early stages of development, where plants offer the lowest protection and where soil should be the most vulnerable. Grass strips of different widths can reduce soil loss by 50 to 99%, and grass density is identified as a key factor affecting sediment reduction (Van Dijk, Kwaad, & Klapwijk, 1996). Runoff and sediment loss have been shown to decrease exponentially with vegetation coverage (Moore et al., 1979, SnelderandBryan, 1995).

In this study, a simulation of reducing erosion rates is based on the lifecycle of vegetation. The first year of planting is at stage C7 with the assumption that there are no plants at all, and then the second year to the seventh year are stage C6, with the assumption that plants grow into young plants, and the root system is developing. Years eight and nine are in C5 stage, where plants have begun to mature and are functioning optimally in preventing erosion. In the tenth year, the plants have entered stage 4, where the root and body functions of the plant are considered to be mature and can minimize erosion very well.

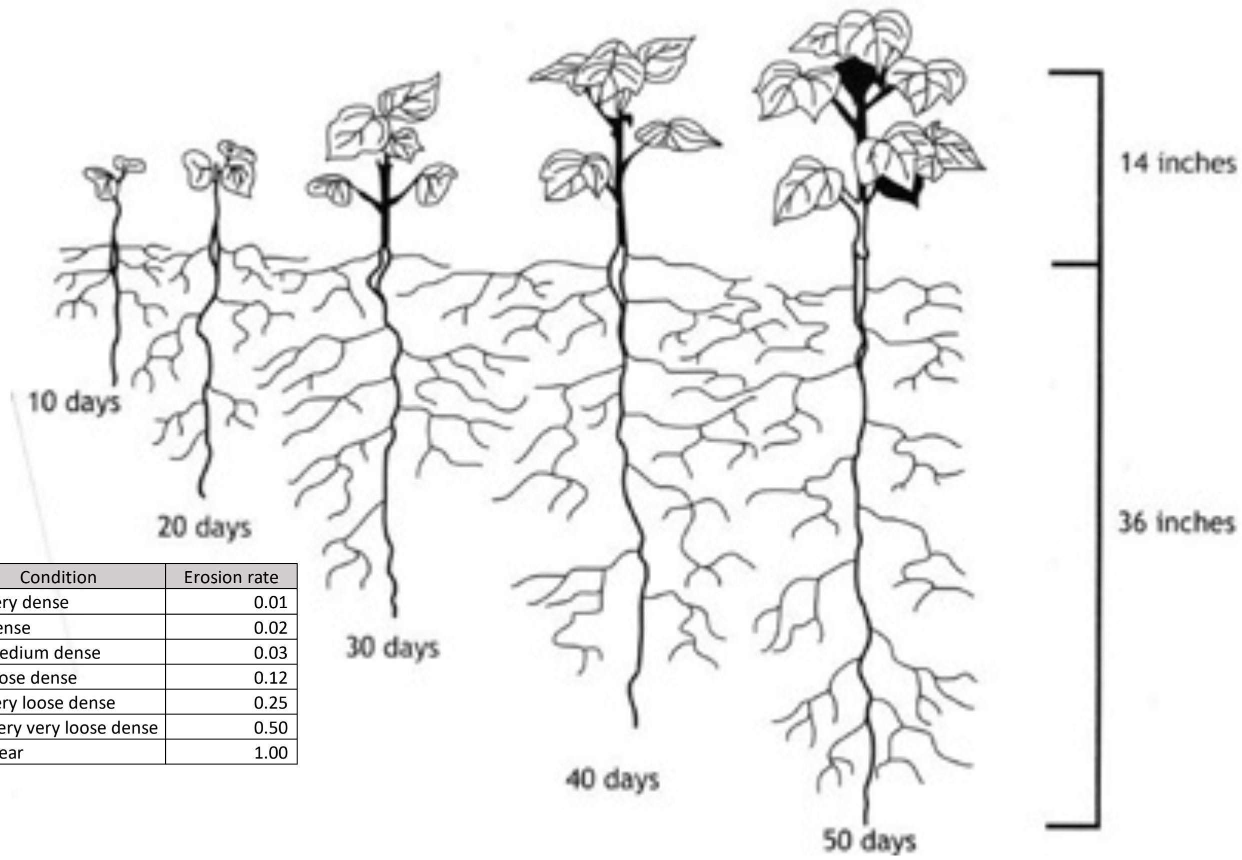

Condition	Erosion rate
C1 very dense	0.01
C2 dense	0.02
C3 medium dense	0.03
C4 loose dense	0.12
C5 very loose dense	0.25
C6 very very loose dense	0.50
C7 Clear	1.00

Figure 41 Ilustration of erosion rate by lifecycle of vegetation (Soil and water conservation)

Table 8 Illustration of annual sediment volume before and after revegetation

No	Year	Annual Sediment Vol. (m3)	
		Without Revegetation	With Revegetation
1	2000	222,861	222,861
2	2001	362,699	362,699
3	2002	315,711	315,711
4	2003	292,780	292,780
5	2004	4,951,896	4,951,896
6	2005	559,365	559,365
7	2006	496,132	496,132
8	2007	622,599	622,599
9	2008	632,880	632,880
10	2009	329,880	329,880
11	2010	259,961	259,961
12	2011	306,949	306,949
13	2012	298,930	298,930
14	2013	314,968	314,968
15	2014	245,049	245,049
16	2015	292,037	292,037
17	2016	222,118	222,118
18	2017	230,137	230,137
19	2018	547,848	547,848
20	2019	547,848	547,848
21	2020	547,848	547,848
22	2021	547,848	493,063
23	2022	547,848	438,278
24	2023	547,848	383,493
25	2024	547,848	328,709
26	2025	547,848	273,924
27	2026	547,848	219,139
28	2027	547,848	164,354
29	2028	547,848	136,962
30	2029	547,848	136,962
31	2030	547,848	65,742
total sediment 2030		**18,078,971**	**15,241,120**
sediment rate		**583,193**	**491,649**

The results show that if the aerial seeding is done in 2019, then in 2020, the seeds that spread will be growing into a young plants and play a role in reducing the erosion rate. In 5-10 years, plants that succeed in growing will effectively reduce the erosion rate upstream.

Table 9 Lifetime service of Bili-bili dam

Item	Scenario 1	Scenario 2	Scenario 3
Dead storage capacity year 1997	29,000,000	29,000,000	29,000,000
Sediment volume in year 2030	18,626,818	18,626,818	15,306,862
Operating period	33	33	33
Sediment rate	582,088	582,088	478,339
Total of dredging volume	2,283,711	4,087,711	2,283,711
Dead storage volume in 2019	19,208,904	19,208,904	15,469,497
Remaining dead storage capacity	12,656,893	14,460,893	15,976,849
Remaining operating year	**22**	**25**	**34**
Final operate year	**2,052**	**2,055**	**2,064**

Using the sediment volume data, we calculated the lifetime of reservoir and applied dead storage formulas. The results show that if scenario 1 continues to be applied with a volume of dredging of 82,000 m^3/year, Bili-Bili Dam will effectively work until 2052. For scenario 2, if the dredging volume is 3 times greater (246,000 m^3/year), then the lifetime of Bili-Bili Dam will extend to 2055. In scenario 3, the dredging volume is 82,000 m^3/year, but there are additional revegetation recovery efforts in critical areas, so the dam's age will increase significantly until 2064. From these data, the effectiveness of the dam can be calculated by dividing the remaining service life by the additional service life.

Table 10 Effectivity of Bili-bili dam

Variable	Without dredging	Scenario 1	Scenario 2	Scenario 3
Remaining service life	17.82	22	25	34
Additional service life		3.92	7.02	12.34
Effectivity		18%	28%	36%
Finish Operating	2,048	2,052	2,055	2,064

The results show that scenario 1 with an additional lifetime of 3.92 years will increase the dam effectiveness by 18%. Scenario 2 has an additional lifetime of 7.02 years and will increase the dam effectiveness by 28%. Scenario 3 shows a significant increase of effectiveness with additional lifetime of 12.34 years, and the effectiveness of the dam will increase by 36%.

6.4.2 Cost Benefit Analysis

After calculating the effectiveness of the dam, the next step is to calculate the cost–benefit analysis. In this calculation, the first step is to determine the costs and benefits of the project. For scenarios 1 and 2, there are initial costs and operational costs for dredging activities. The cost for scenario 3 is scenario 1 added to the initial cost for revegetation and operational activities.

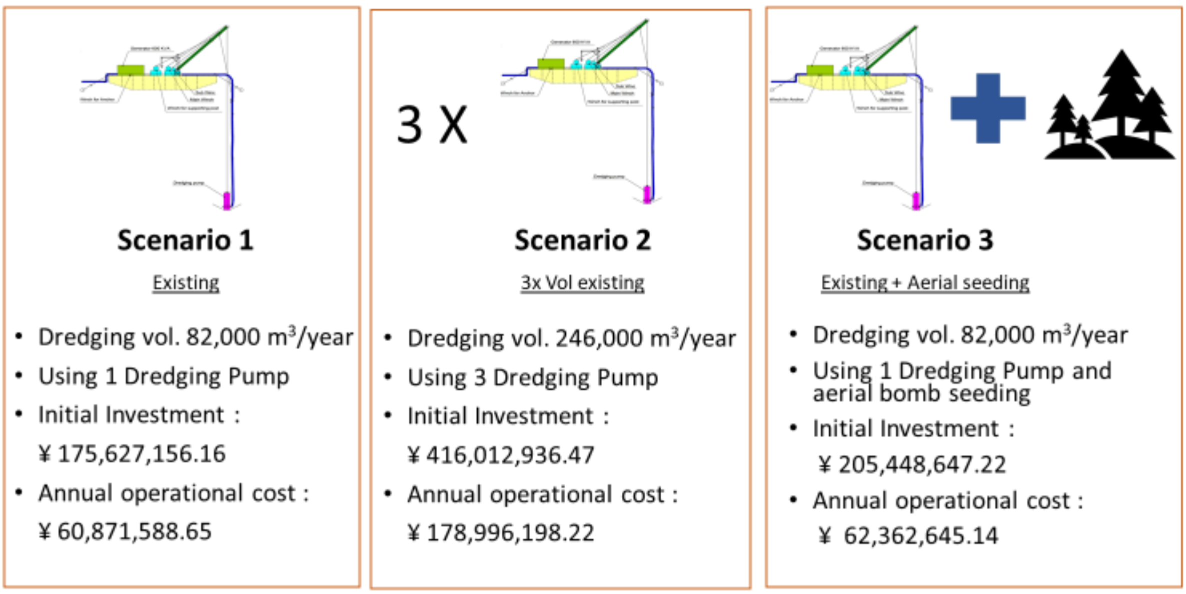

Figure 42 Scenario to reduce the sedimentation in Bili-bili dam

The benefits of the dam are related to the increase of the effectiveness of the dam. The implementation of scenarios to reduce the level of sedimentation in dams is expected to have an impact on increasing the effectiveness of the dams. The benefits come from irrigation, hydropower generation, raw water purification, paddy field protection, and material sales.

One of the original values of this study is the risk reduction benefit. The value of risk reduction is taken from the time series of events for 20 years. Specifically for risk reduction, benefits are not converted to present value because they are only generated if a disaster occurs. Therefore, the risk reduction benefit will be added later after everything has been converted.

6.4.3 Discounting

As explained earlier, all cost and benefit calculations will be converted into a present value calculation. The conversion value represents the expected return and service life of the dam. This conversion value will change the value of the cost and benefit to the present value.

Table 11 Deflators for cost and benefit

P/F,I,n COST

Scenario	Service Life	Interest rate						
		4	5	6	7	8	9	10
3	34	3.97	5.56	7.76	10.79	14.97	20.69	28.53
2	25	3.79	5.25	7.25	9.98	13.69	18.73	25.55
1	22	2.65	3.36	4.25	5.37	6.77	8.51	10.67

P/A,I,n BENEFIT

Scenario	Service Life	Interest rate						
		4	5	6	7	8	9	10
3	34	18.70	16.40	14.52	12.96	11.66	10.57	9.65
2	25	18.41	16.19	14.37	12.85	11.59	10.52	9.61
1	22	15.56	14.05	12.75	11.63	10.65	9.81	9.06

6.4.4 Benefit Cost Ratio and Net Present Value

Scenario 3 (dredging + revegetation) shows an increase in dam effectiveness and reduced sedimentation rates in the dam. Based on economic calculations using the cost–benefit analysis formula, all scenarios would be profitable (BCR > 1). If the expected rate of return is 4-5%, scenario 3 achieves a greater profit compared to scenarios 1 and 2. But if the expected rate of return is higher than 5%, the maximum profit is generated by scenario 1. It is important to note that the result of this cost–benefit analysis only concerns the reservoir.

While all scenarios provide a net positive outcome, the NPV and BCR methods provide slightly different outcomes. Using NPV suggests project scenario 2 provides the best outcome as the NPV of ¥ 16,692,837,000 is greater than the NPV of scenarios 1 and 3. However, when using the BCR method, scenario 3 has the highest a BCR of 16.9.

In this case, the overall result of the cost–benefit analysis may be determined by considering the costs involved in scenario 2, which are much greater, or may be determined by considering the much greater overall benefits (in monetary terms) obtained by choosing scenario 2. So in my humble opinion, I considered to choose the scenario 3 as a best option. Because In this case, the decision maker is a government, not a private sector. So their final decision is not only considering about the benefit in economic aspect but also the benefit for the society. The CBA result shows the every scenario offer a positive outcome, but the scenario 3 has an additional value, benefit in environment aspect which not calculated in CBA but we can see the positive trend from the effectivity calculation.

It should be noted that although both NPV and BCR provide the same positive or negative outcome for an alternative, where a number of options are considered, the two methods will not always give the same preferred outcome. This is important as the choice of calculating the outcome of the cost–benefit analysis using only one of these methods could result in the analysis not considering an alternative that actually offers a positive outcome. Presenting both sets of results may therefore be most appropriate to provide the most information with which to make a final decision.

Table 12 Result of cost benefit analysis

Scenario			Present Value		Risk Reduction Benefit	BC Ratio	B-C
Alternatives	Efective age	Interest Rate	Cost	Benefit			
Scenario 1	22	4	¥ 589,519,070	¥ 8,250,567,695		14.0	¥ 7,661,048,625
Vol. 82.000 m3		5	¥ 725,880,023	¥ 7,521,491,208		10.4	¥ 6,795,611,185
		6	¥ 892,021,369	¥ 6,885,934,494		7.7	¥ 5,993,913,125
		7	¥ 1,094,070,194	¥ 6,329,652,307		5.8	¥ 5,235,582,113
		8	¥ 1,339,338,232	¥ 5,840,813,400		4.4	¥ 4,501,475,168
		9	¥ 1,636,536,524	¥ 5,409,558,789		3.3	¥ 3,773,022,265
		10	¥ 1,996,026,409	¥ 5,027,645,878		2.5	¥ 3,031,619,468
Scenario 2	25	4	¥ 1,701,632,781	¥ 18,394,469,781	¥ 1,683,333,846	11.8	¥ 16,692,837,000
Vol. 246.000 m3		5	¥ 2,158,305,557	¥ 16,603,223,104	¥ 1,683,333,846	8.5	¥ 14,444,917,547
		6	¥ 2,731,375,154	¥ 15,065,796,164	¥ 1,683,333,846	6.1	¥ 12,334,421,010
		7	¥ 3,448,970,652	¥ 13,739,530,564	¥ 1,683,333,846	4.5	¥ 10,290,559,912
		8	¥ 4,345,654,834	¥ 12,589,724,412	¥ 1,683,333,846	3.3	¥ 8,244,069,577
		9	¥ 5,463,814,104	¥ 11,588,034,387	¥ 1,683,333,846	2.4	¥ 6,124,220,284
		10	¥ 6,855,331,404	¥ 10,711,217,724	¥ 1,683,333,846	1.8	¥ 3,855,886,320
Scenario 3	34	4	¥ 1,076,986,003	¥ 16,370,899,861	¥ 1,796,061,538	16.9	¥ 15,293,913,857
Existing + Veg2%		5	¥ 1,492,295,118	¥ 14,395,397,454	¥ 1,796,061,538	10.9	¥ 12,903,102,336
		6	¥ 2,061,373,808	¥ 12,770,937,154	¥ 1,796,061,538	7.1	¥ 10,709,563,346
		7	¥ 2,838,843,029	¥ 11,423,444,319	¥ 1,796,061,538	4.7	¥ 8,584,601,290
		8	¥ 3,897,921,658	¥ 10,296,141,061	¥ 1,796,061,538	3.1	¥ 6,398,219,402
		9	¥ 5,336,490,824	¥ 9,345,217,272	¥ 1,796,061,538	2.1	¥ 4,008,726,448
		10	¥ 7,285,050,074	¥ 8,536,643,165	¥ 1,796,061,538	1.4	¥ 1,251,593,091

6.5 REFERENCES

Bapro PSDA. 2004. Laporan Hasil Echosounding Waduk Bili-Bili. Bagian Proyek Pengelolaan Sumber Daya Air Jeneberang. Makassar.

Bapro PSDA. 2005. Laporan Hasil Echosounding Waduk Bili-Bili. Bagian Proyek Pengelolaan Sumber Daya Air Jeneberang. Makassar.

CTI Engineering Co. Ltd. (2001): Comprehensive Water management Plan Study for Maros-Jeneponto River Basin. Volume I-III. Directorate General of Water Resources, Ministry of Public Works, Jakarta.

CTI Engineering Co. Ltd. (2005): Final Report on Environmental Management Monitoring in Bili bili multi purpose dam Project (Phase II). Directorate General of Water Resources, Ministry of Public Works, Jakarta.

de Baets S., Poesen J., Knapen A., Barbera G.G., Navarro J.A. (2007a) Root characteristics of representative Mediterranean plant species and their erosion-reducing potential during concentrated runoff, Plant Soil 294, 169–183.

de Baets S., Poesen J., Knapen A., Galindo P. (2007b) Impact of root architecture on the erosion-reducing potential of roots during concentrated flow, Earth Surf. Proc. Land. 32, 1323–1345.

DuránZ.V.H.,RodríguezP.C.R.,FranciaM.J.R.,CárcelesR.B.,Martínez R.A., Pérez G.P. (2007) Harvest intensity of aromatic shrubs vs. soil-erosion: an equilibrium for sustainable agriculture (SE Spain), Catena (in press)

Gill M.A. (1979) Sedimentation and Useful Life of Reservoirs, Journal of Hydrology, 44, 89-95.

Gyssels G.,Poesen J.,Bochet E.,LiY.(2005)Impact of plant roots on the resistance of soils to erosion by water: a review, Prog. Phys. Geog. 2, 189–217.

Hasnawir, H. Omura and T. Kubota. 2006. Landslide Disaster at Mt. Bawakaraeng Caldera, South Sulawesi, Indonesia. Kyushu Journal 59:269- 272.

Japan International Cooperation Agency (JICA), (2004): Executive Summary, The Study on Capacity Development for Jeneberang River Basin Management in Rep. Indonesia, Nippon Koei Co-CTI Engineering Int.Co [In Indonesian].

Japan International Cooperation Agency (JICA), (2004): Draft Final Report of Capacity Development of Jeneberang River Basin.

Kompas, 2005: PDAM Makassar Stop Distribusi Air Bersih Pengolah Air Tercemar Sisa Longsor. Dated 16 January 2005. http://www.kompas.com/kompas%2Dcetak/0501/17/daerah/1503582.htm

Kompas, 2004: Indonesian National News, August 2005, (Indonesian]

Lee K.H., Isenhart T.M., Schultz C., Mickelson S.K. (2000) Multispecies riparian buffers trap sediment and nutrients during rainfall simulations, J. Environ. Qual. 29, 1200–1205.

Lubis, R., dan Syafiuddin. 1992. Penghitungan Biaya Erosi (On-Site Cost) di Daerah Aliran Sungai Jeneberang Hulu, Sulawesi Selatan. Jurnal Ekonomi Lingkungan. 2:36-43.

Moore, D.B. Thomas, R.G. BarberInfluence of grass cover on runoff and soil erosion from soils in the machakos area, Kenya Tropical Agriculture, *56* (4) (1979), pp. 339-344

MartínezR.A.,DuránZ.V.H., FranciaF.R. (2006) Soil erosion and runoff response to plant cover strips on semiarid slopes (SE Spain), Land Degrad. Dev. 17, 1–11

Van Dijk P.M., Kwaad F.J.P.M., Klapwijk M. (1996) Retention of water and sediment by grass strips,Hydrol. Process. 10, 1069–1080.

World Commission on Dams, 2000. Dams and Development: a New Framework for Decision-Making. Earthscan, London

Chapter 7. Conclusion and future works

7.1 Conclusions

Based on the previous chapters and the subsequent discussions the following major conclusion are presented:

1. Based on the Certainty Factor method, eleven out of sixteen causative factors were detected with high influence to landslide occurrences in the study area: profile curvature (0.9999), curvature (0.9994), slope (0.9411), TPI (0.8865), rainfall (0.8468), elevation (0.8340), distance to fault (0.8063), land-use (0.7729), distance to river (0.6905), drainage density (0.2061), plan curvature (0.1969). Meanwhile Weight of Evidence shows the dependence correlation in pair of causative factors, whereas rain – elevation has the greatest chi square values 4862.61, followed by fault – landuse with chi square values 1816, distance to river – slope 1691, profile curvature – curvature 1472, TWI – slope 1151.
2. Based on the CF, eleven conditional factors (profile curvature, curvature, slope, TPI, rainfall, elevation, distance to fault, land use, distance to river, drainage density, plan curvature) has a high correlation to landslide occurrence were selected from sixteen factors. Meanwhile weight of evidence applied the conditional independent test to assess the independence of each factor and produce a combination of elevation, plan curvature, lithology, distance to river, soil, SPI, and TPI. Both models have a high accuracy, but the CF models has slightly higher ROC result (AUC = 90.3%, prediction = 90.2%) than WoE (AUC = 90.1%, prediction = 89.9%).
3. The improved landslide susceptibility map is generated by integrating an optimized landslide susceptibility map and the critical land map to zoning the area for revegetation recovery. The critical land map employed in this study has been verified and validated by the Ministry of Public Work and Pompengan Bili-bili watershed Agency. Coding

for the revegetation recovery map using the matrix relationship method, the zoning area is divided into three classes; first, second, and third priorities. The first and second priority is the targeted area that needs immediate treatment for a revegetation recovery plan, and the third priority area is classified as an area that can be treated later after the first and second priority areas have been addressed. The result shows 43,220,742 m^2 is categorize as first and second priority that needs an immediate treatment from total of 384,815,151.24 m^2 area.

4. The result shows the calculation of service time and effectivity, scenario 3 (existing dredging + revegetation) shows an increase in dam effectiveness and reduced sedimentation rates in the dam. While all scenarios provide a net positive outcome, the NPV and BCR methods provide slightly different outcomes. Using NPV suggests project scenario 2 provides the best outcome as the NPV of ¥ 16,692,837,000 is greater than the NPV of scenarios 1 and 3. However, when using the BCR method, scenario 3 has the highest a BCR of 16.9. Presenting both sets of results may therefore be most appropriate to provide the most information with which to make a final decision.

7.2 Future Works

1. Improving the landslide inventory as the base data for landslide susceptibility assessments in the study area by using remote sensing analysis. Landslide inventory is one of the key input in landslide susceptibility mapping.
2. Detail weather data especially rainfall data were needed to ensure accurate slope stability analysis and more of data related to damage cost by landslide and flashflood will improving the accuracy of result.
3. Improving the cost and benefit data of the Dam will be challenging to ensure the accurate optimization result in cost benefit analysis for future research.

Appendices

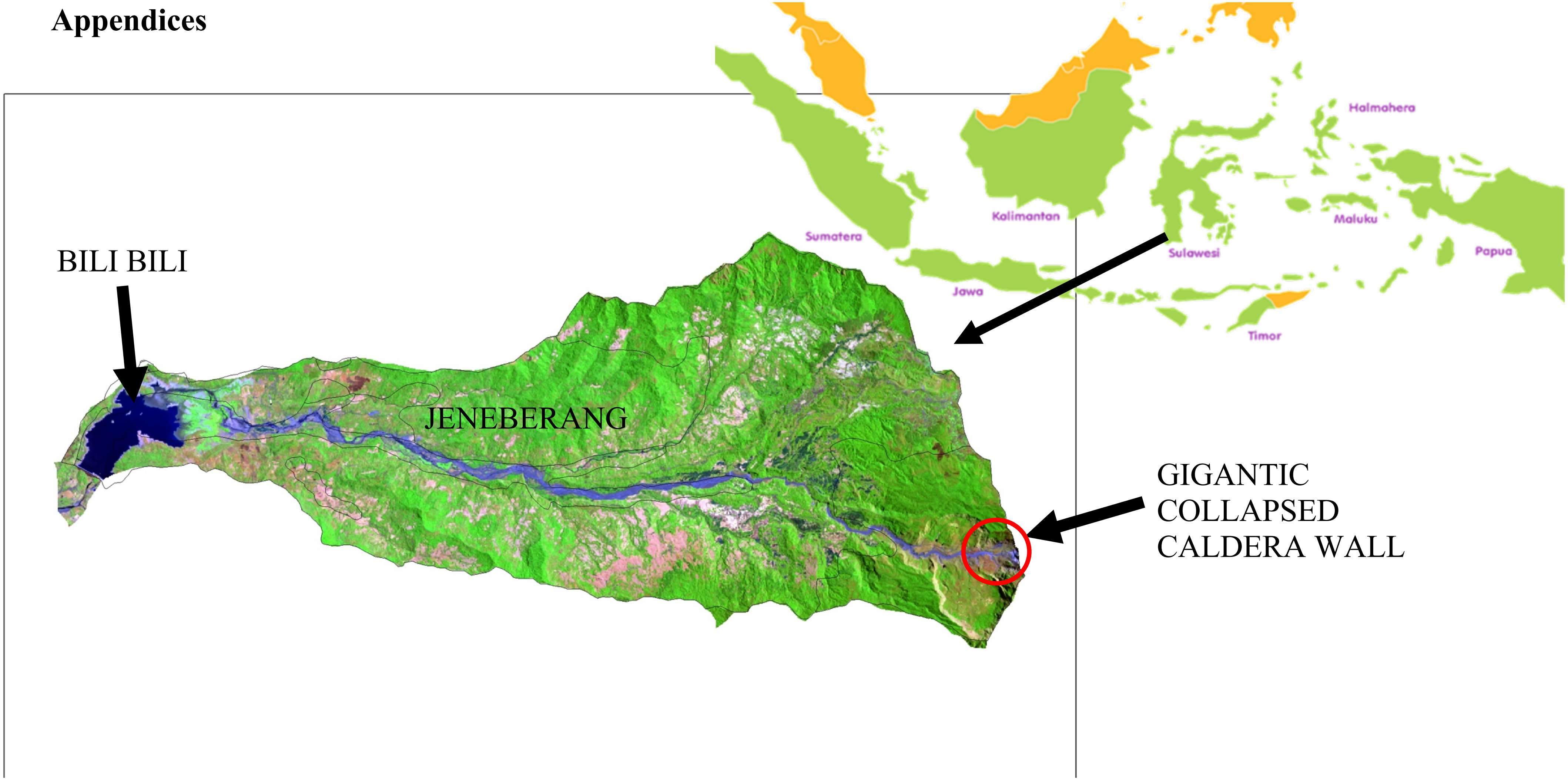

Appendix 1 Study area located in Jeneberang sub-Watershed

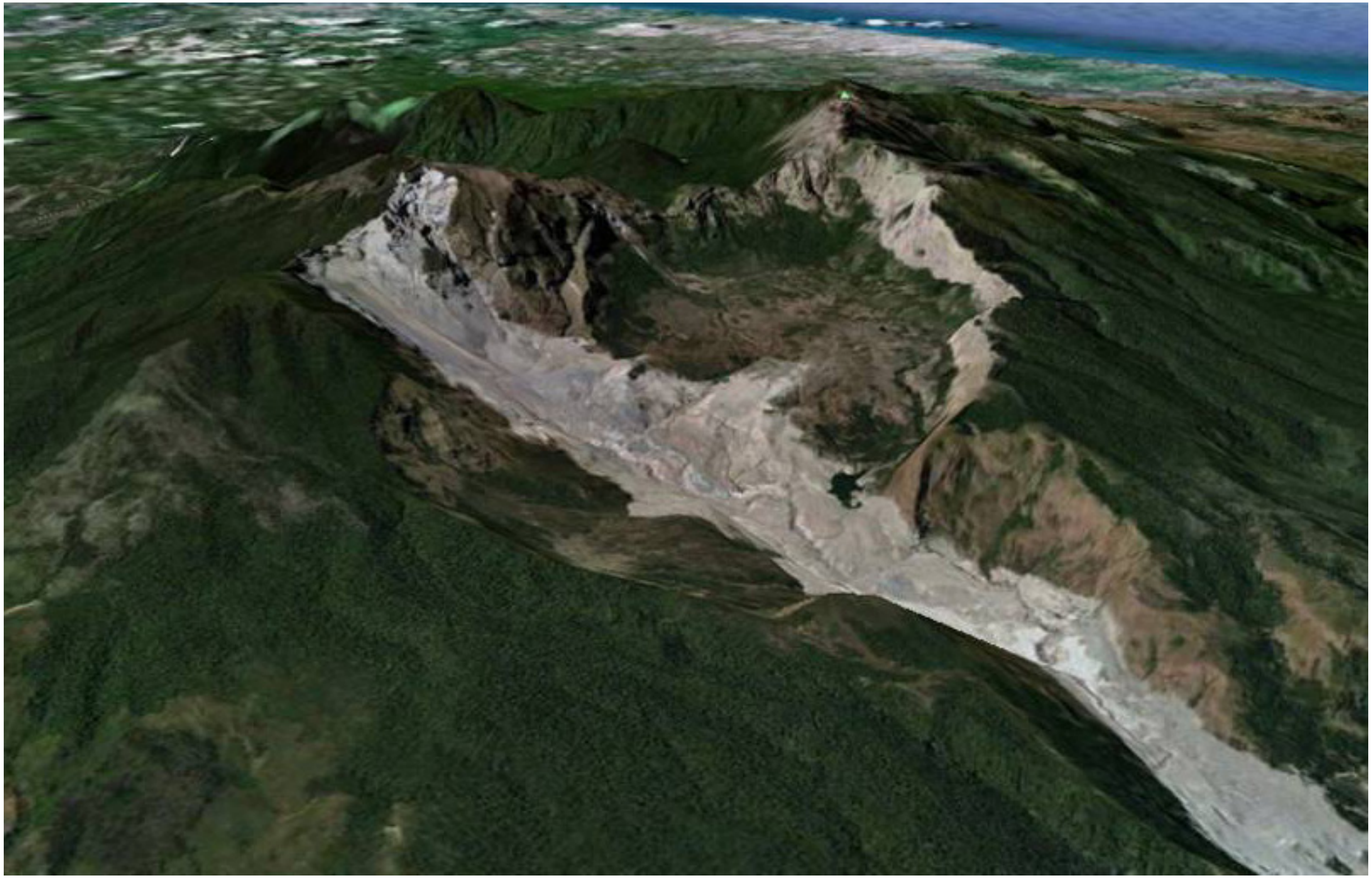

Appendix 2 Condition of upstream area of Jeneberang river

Appendix 3 Sediment deposited along the river and unstable slope

Appendix 4 Landslide susceptibility map generated by 11 causative factors using certainty factor

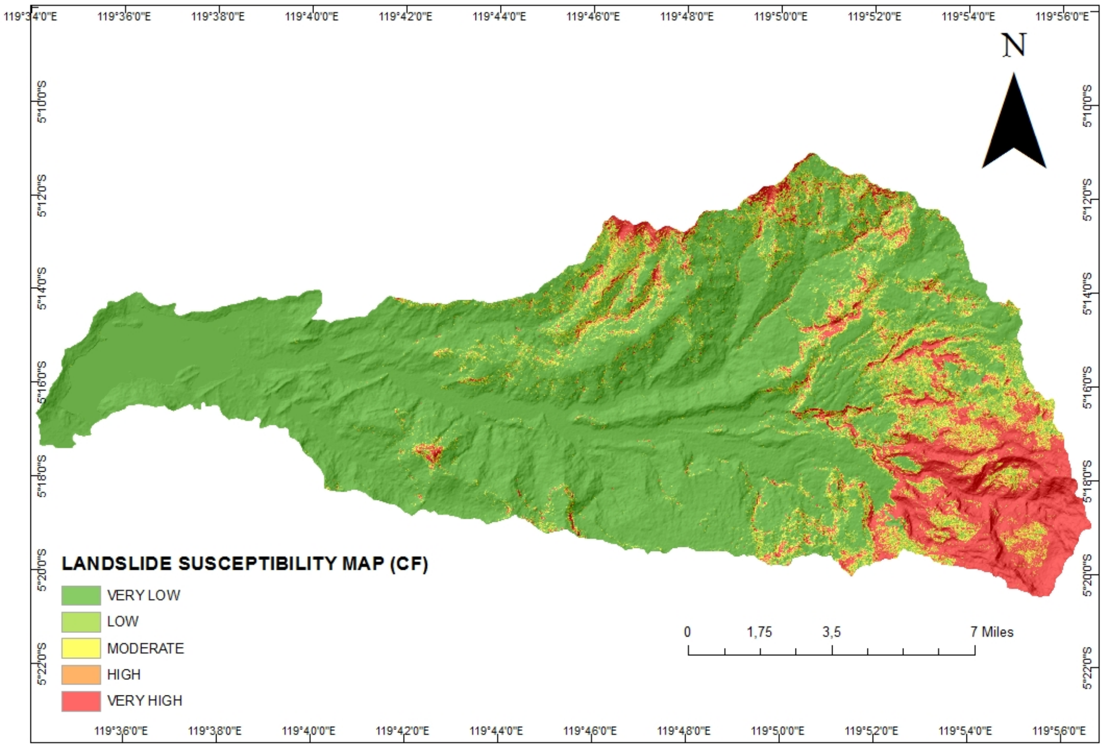

and ROC curves

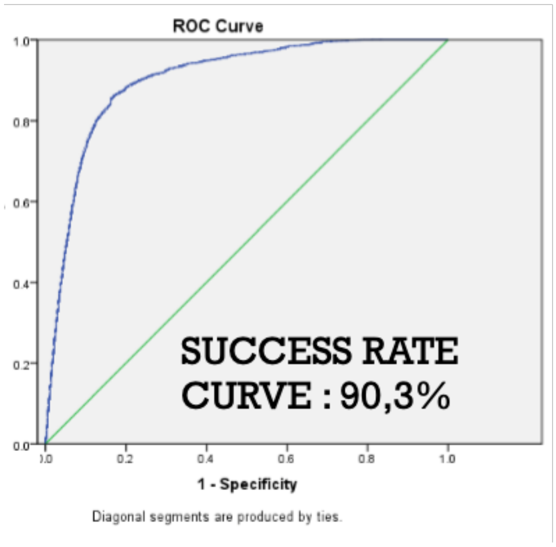

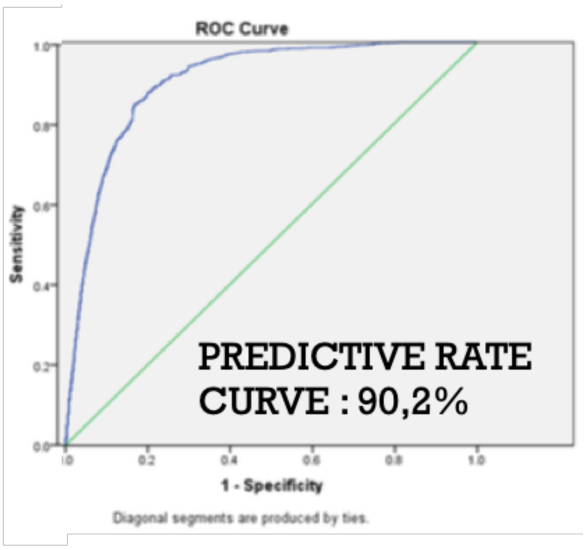

Appendix 5 Landslide susceptibility map generated by 10 variable and ROC curves

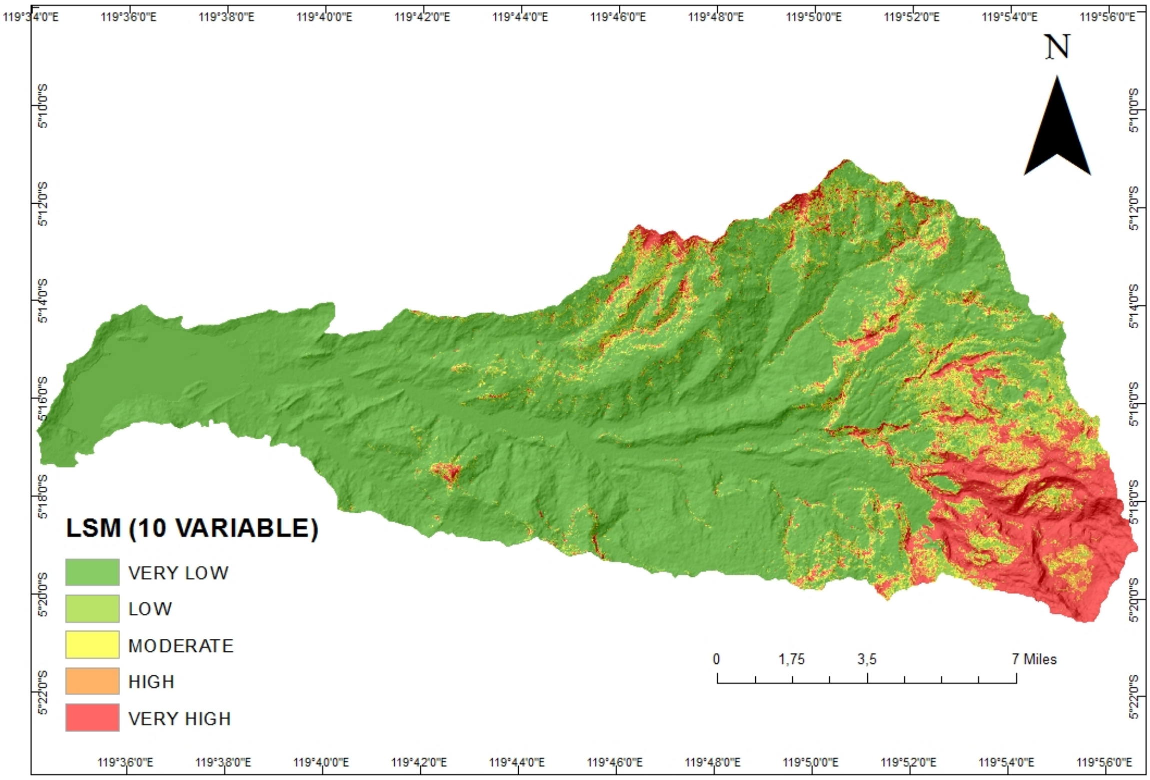

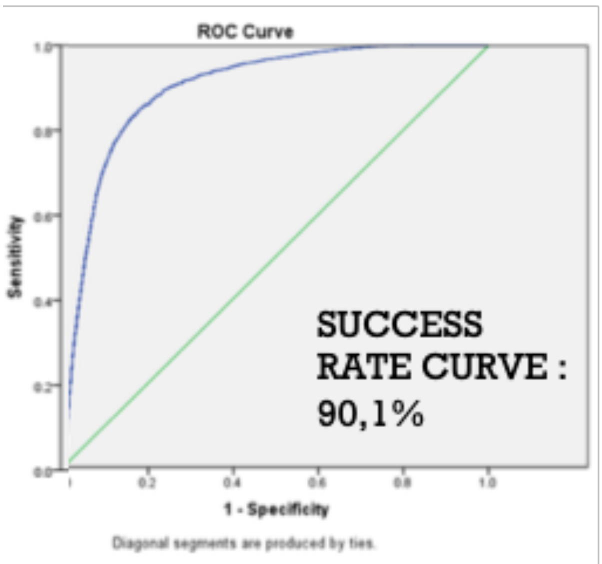

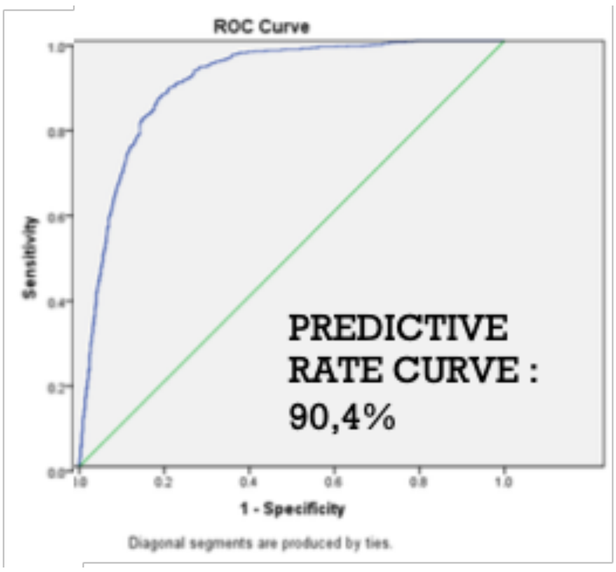

Appendix 6 Landslide susceptibility map generated by 12 variable using certainty factors and ROC curves

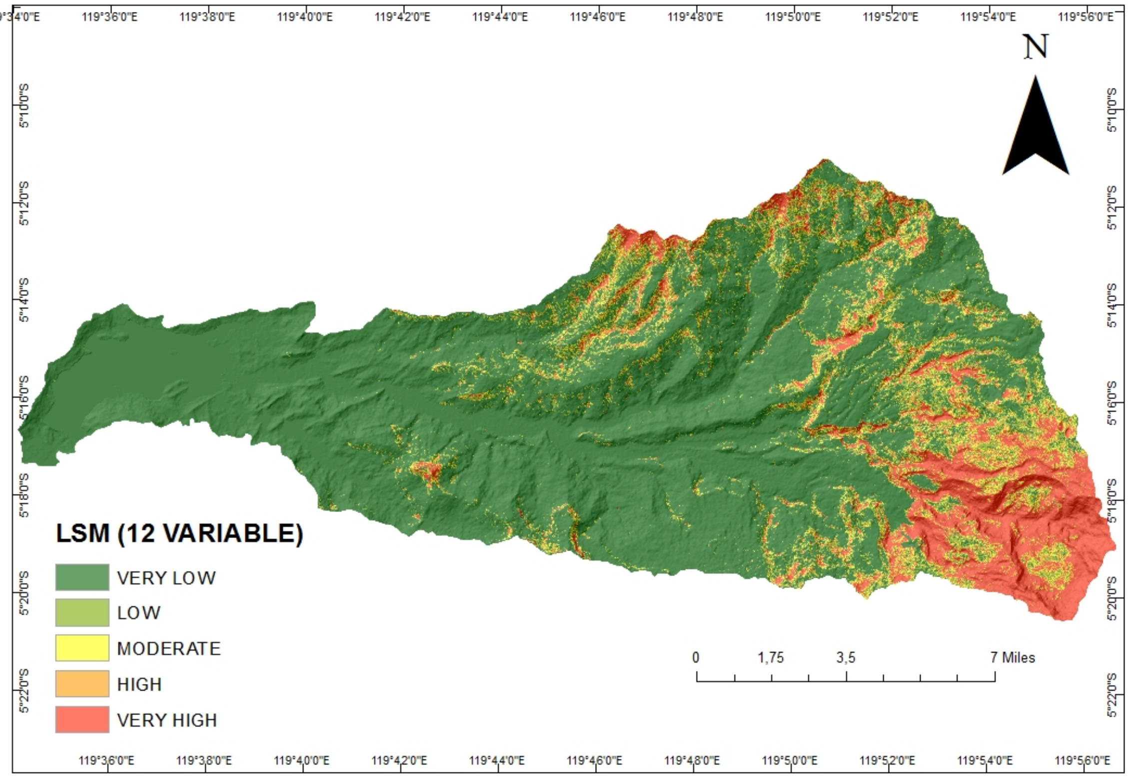

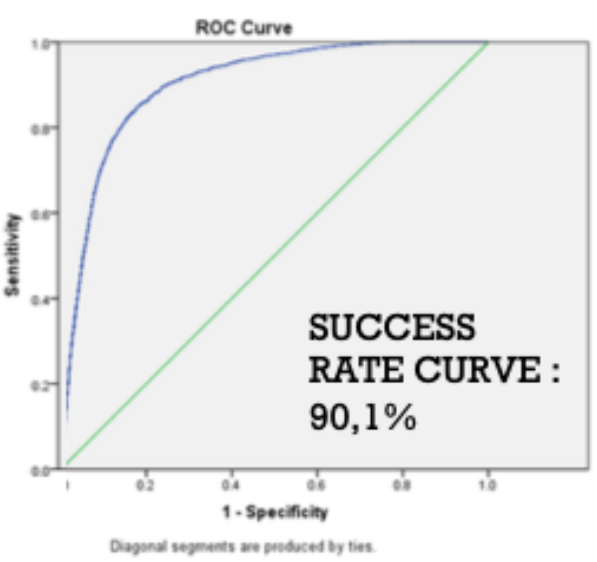

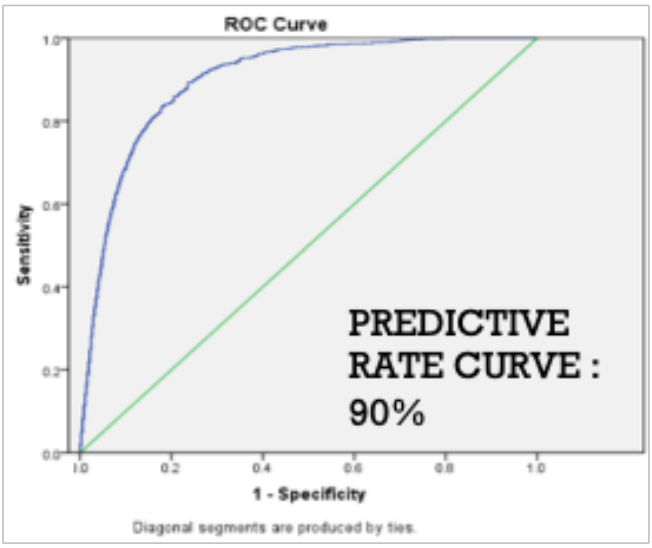

Appendix 7 Landslide susceptibility map by Weight of evidence and ROC curves

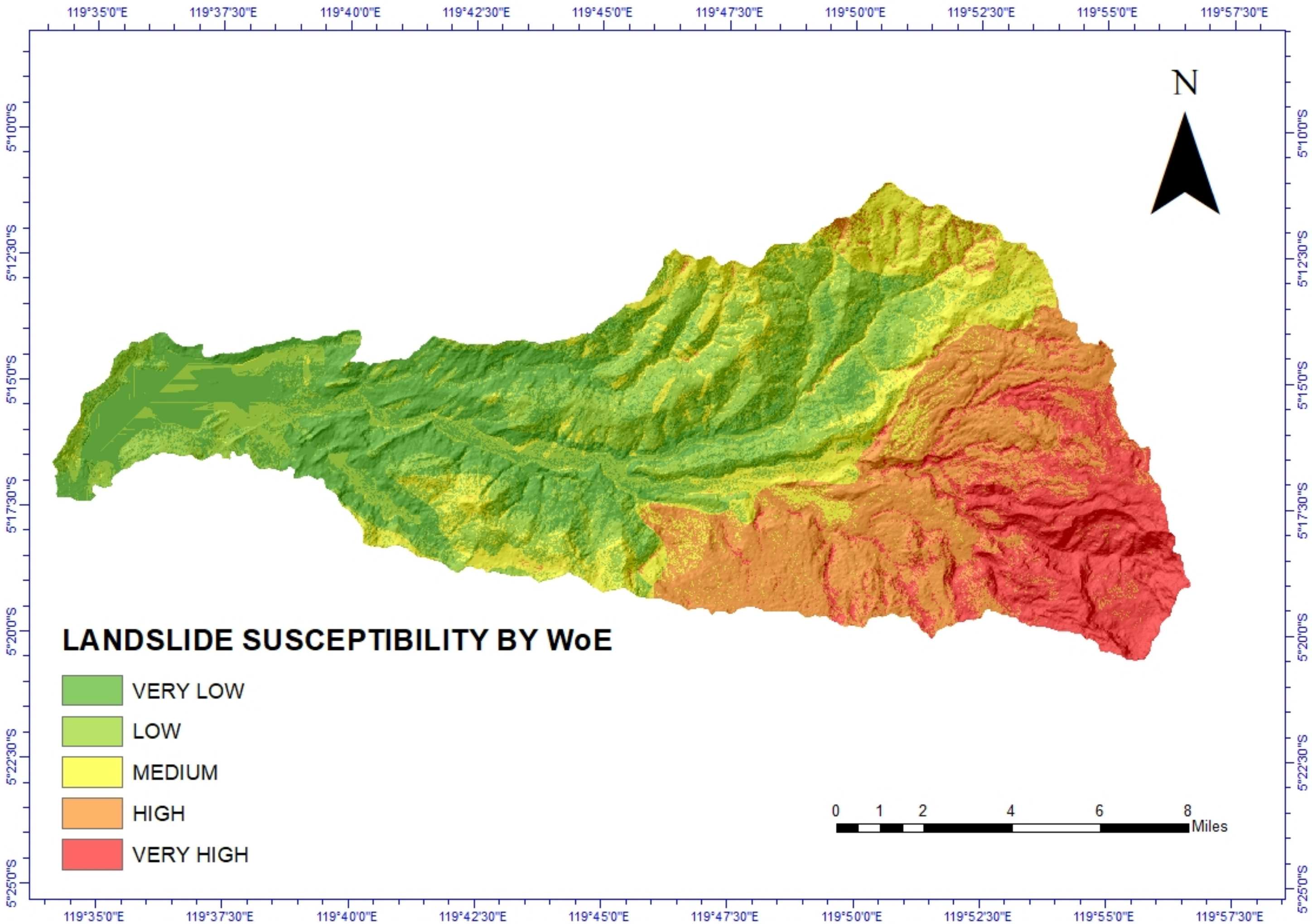

Appendix 8 Validation result for 16 combination of causative factor by Weight of Evidence

SCENARIO	FACTORS	AUC	PREDICTION ACCURACY (%)
1	ELEVATION,ASPECT,PROF CURVATURE,SPI,TPI	0.86	0.856
2	SLOPE,LUSE,SOIL	0.897	0.885
3	ELEVATION,ASPECT,PROF CURVATURE,PLAN CURVATURE,FAULT	0.825	0.798
4	CURVATURE,LITHO,LUSE,DISRIV,FAULT,SOIL,TPI	0.894	0.897
5	ELEVATION,ASPECT,PROF CURVATURE,LUSE,DISRIV,FAULT,RAIN	0.882	0.874
6	**ASPECT,PLAN CURVATURE,LITHO,LUSE,DISRIV,SOIL,SPI,TPI**	**0.901**	**0.903**
7	CURVATURE,PLAN CURVATURE,LITHO,SPI	0.87	0.866
8	PROF CURVATURE,RAIN	0	0
9	SLOPE,CURVATURE,PROF CURVATURE,PLAN CURVATURE,LUSE,TWI	0.808	0.787
10	DRAINDEN,TWI	0	0
11	CURVATURE,PROF CURVATURE,PLAN CURVATURE,DISRIV,SPI,TPI,TWI	0.835	0.881
12	ASPECT,CURVATURE,PROF CURVATURE,FAULT,TPI,TWI	0.794	0.797
13	SLOPE,CURVATURE,PLAN CURVATURE,SOIL,SPI	0.894	0.855
14	**ELEVATION,PLAN CURVATURE,LITHO,DISRIV,SOIL,SPI,TPI**	**0.901**	**0.899**
15	ELEVATION,CURVATURE,PLAN CURVATURE,DISRIV,FAULT,SPI,TPI	0.877	0.887
16	LUSE,DRAINDEN,DISRIV,FAULT,TWI	0.803	0.794

Appendix 9 Critical land map

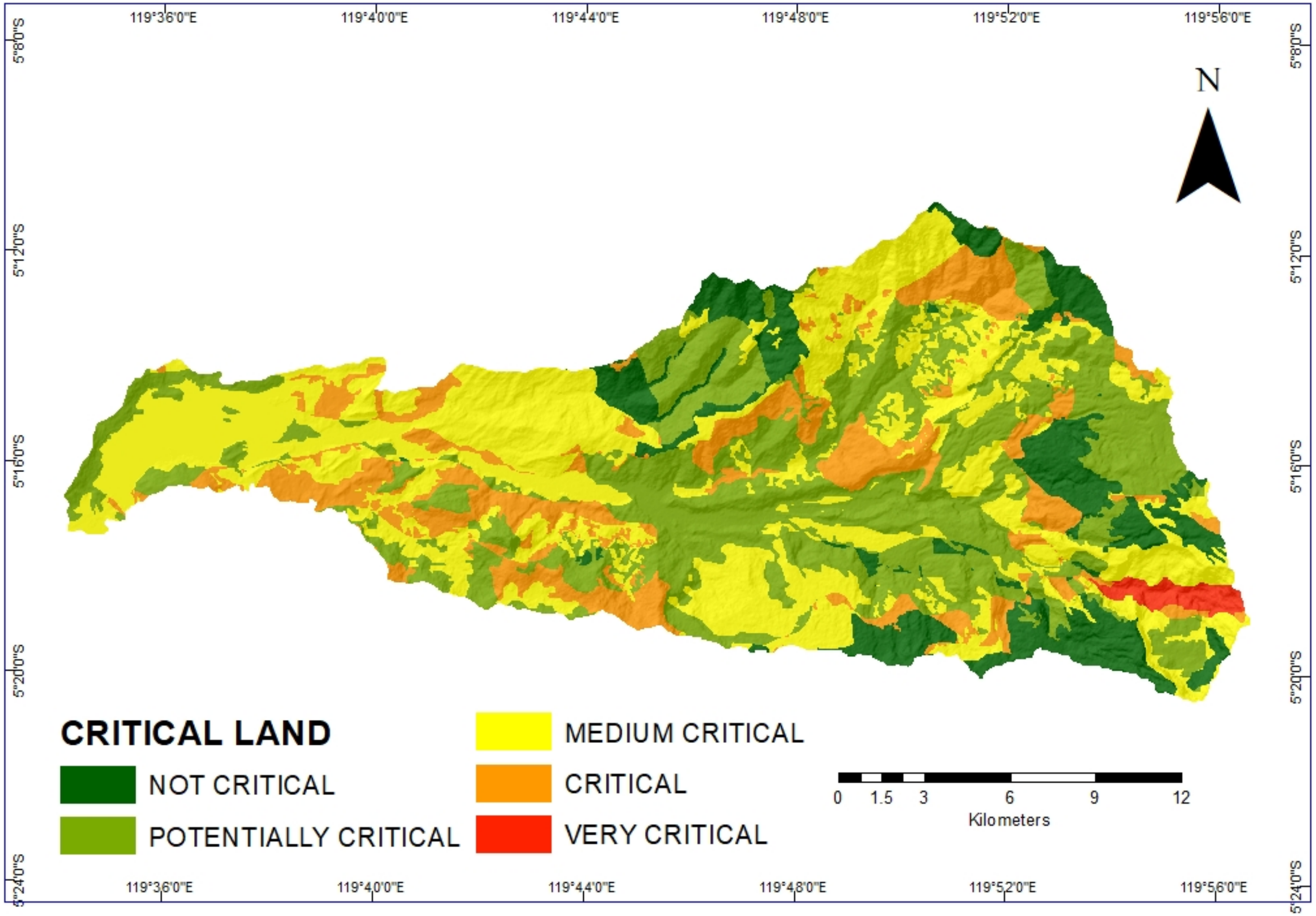

Appendix 10 Revegetation priority map

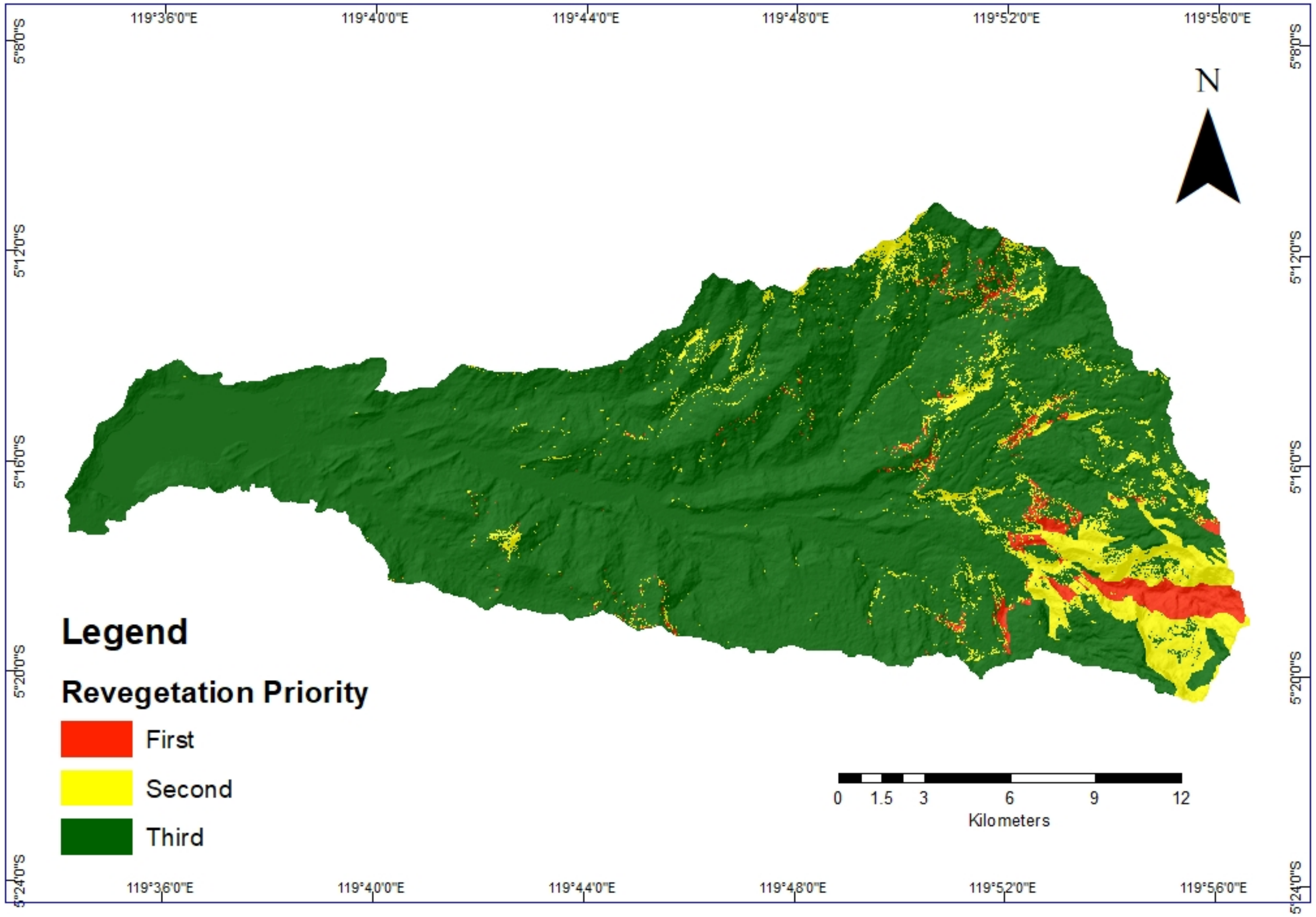

Appendix 11

Table 13 Initial Cost for Dredging work

No	Work Item	Unit	Vol. 82.000 m3		Vol. 246000 m3	
			Quantity	Cost	Quantity	Cost
1	**Preparation Work**					
A	Mobilization and Demobilization	LS	1	120,000,000	1	120,000,000
B	Survey	Month	9	380,160,000	9	380,160,000
C	Security , Safety and H ealth Control	Month	9	277,740,000	9	277,740,000
D	Test Quality Control	Month	9	432,540,000	9	432,540,000
E	Contractor's Facilities	LS	1	248,120,000	1	248,120,000
F	Progress Report,Progress Photos/Movies	Month	9	161,021,250	9	161,021,250
G	Temporary Plant	LS	1	459,866,387	1	459,866,387
H	Land Clearing with Bushes and Stripping	M2	10,000	135,260,000	10,000	135,260,000
I	Training for Dredging in reservoir	Month	1	21,090,000	1	21,090,000
J	insurance (in japanese yen)					
Sub Total of No. Item 1			**IDR**	**2,235,797,637**	**IDR**	**2,235,797,637**
			¥	**17,198,443**	**¥**	**17,198,443**
2	**Procurement of Equipment**					
A	Sand Pump with whisker	Unit	1	223,250,000	3	669,750,000
B	Relay station Sand pump	Unit	2	199,500,000	6	598,500,000
C	Bandless Discharge hose with abrasion	Unit	5	42,750,000	15	128,250,000
D	Starter Device(DP-150B-A)	Unit	1	33,250,000	3	99,750,000
E	Starter Device(HSP-75B)	Unit	2	47,500,000	6	142,500,000
F	Generator(600KVA)	Unit	1	66,500,000	3	199,500,000
G	Generator(150KVA)	Unit	1	350,000,000	3	1,050,000,000
H	Winch	LS	1	380,000,000	3	1,140,000,000
Sub Total of No. Item 2			**IDR**	**1,342,750,000**	**IDR**	**4,028,250,000**
			¥	**10,328,846**	**¥**	**30,986,538**
3	**Civil Works**					
A	Common Excavation	m3	6,226	278,198,116	15,565	695,495,290
B	Compaction Embankment	m3	172	9,023,203	430	22,558,008
C	CSG Placement	m3	1,488	1,005,197,249	3,720	2,512,993,123
D	Concrete(21N) Placement	m3	67	77,975,907	168	194,939,768
E	Form work	m2	238	102,983,808	595	257,459,520
F	Re-Bar	kg	3,219	51,735,768	8,048	129,339,420
G	Steel work	kg	3,820	84,534,387	9,550	211,335,968
H	Dredging in reservoir	Month	3	1,198,401,429	9	2,996,003,573
I	Road construction	LS	1	860,808,788	3	2,152,021,970
J	Installation for the discharge Pipe	m	1,150	2,384,809,050	2,875	5,962,022,625
K	Misselaneous	LS	1	227,894,012	1	227,894,012
Sub Total of No. Item 3			**IDR**	**6,281,561,717**	**IDR**	**15,362,063,275**
			¥	**48,319,706**	**¥**	**118,169,717**
4	**Mechanical & Dreging Works**					
A	Flat barge building	kg	150,000	4,983,750,000	375,000	12,459,375,000
B	Tug boat building	LS	1	965,077,413	3	2,412,693,533
C	Installation for Sand Pump and Relay station pump with electric system	LS	1	1,326,143,900	3	3,315,359,750
D	Installation for the discharge Pipe	m	460	3,186,918,180	1,150	7,967,295,450
E	Installation for the Crane and Wimch in Flat barge	set	6	1,926,238,398	15	4,815,595,995
F	Installation for Operation room and system in Flat barge	set	1	850,308,563	3	2,125,771,408
Sub Total of No. Item 4			**IDR**	**13,238,436,454**	**IDR**	**33,096,091,135**
			¥	**101,834,127**	**¥**	**254,585,316**
Total in Rupiahs			**IDR**	**23,098,545,808**	**IDR**	**54,722,202,047**
Total in Japanese Yen			**¥**	**177,681,121.60**	**¥**	**420,940,016**

Table 14 Initial Cost for Dredging work

IN SEDIMENTATION POND				
EXCAVATOR/BACKHOE	**EXISTING**	**SCENARIO 2**		
TOTAL EXCAVATION VOLUME	82,000	246,000	m^3	
DAILY WORKABILITY	300	300	m^3	
WORKABLE DAYS	125	125	DAYS	
UNIT NUMBER OF EXCAVATION	**2**	**7**	**UNIT**	
DUMP TRUCK CAPACITY (100 m3 X 1.5/0.8)				
DAILY HAULING VOLUME (SWELL FACTOR 1.20)				
TOTAL HAULING VOLUME	102,500	307,500	m^3	
WORKABLE DAYS	125	125	DAYS	
DAILY HAULING VOLUME	820	2,460	m^3/day	
DAILY HAULING VOLUME/UNIT TRUCK				
CAPACITY DUMP TRUCK	150	150	m^3	
HAULING TIME	1	1	DAYS	
HAULING VOLUME/TRUCK	188	188	m^3/day	
UNIT NUMBER	4	13	**UNIT**	

Appendix 13

Table 15 Calculation of disposal area

DISPOSAL AREA			
	EXISTING	**SCENARIO 2**	
DUMP TRUCK CAPACITY (100 m3 X 1.5/0.8)			
DAILY HAULING VOLUME (SWELL FACTOR 1.25)			
TOTAL HAULING VOLUME	98,400	295,200	m^3
WORKABLE DAYS	125	125	DAYS
DAILY HAULING VOLUME	787	2,362	m^3/day
DAILY HAULING VOLUME/UNIT TRUCK			
CAPACITY DUMP TRUCK	150	150	m^3
HAULING TIME	0.8	0.8	DAYS
HAULING VOLUME/TRUCK	188	188	m^3
UNIT NUMBER	**4**	**13**	**UNIT**
EXCAVATOR/BACKHOE	**EXISTING**	**SCENARIO 2**	
TOTAL EXCAVATION VOLUME	98,400	295,200	m^3
DAILY WORKABILITY	300	300	DAYS
WORKABLE DAYS	125	125	m^3/day
UNIT NUMBER OF EXCAVATION	**3**	**8**	**UNIT**
BULLDOZER	**EXISTING**	**SCENARIO 2**	
TOTAL SPREADING VOLUME	200,900	602,700	m^3
WORKABLE DAYS	125	125	DAYS
WORKABILITY	540	540	m^3
UNIT NUMBER	**3**	**9**	**UNIT**

Appendix 14

Table 16 Calculation of required heavy equipment

REQUIRED HEAVY EQUIPMENT EXISTING						
ITEM	SEDIMENTATION POND	DISPOSAL AREA	TOTAL			
BACKHOE	2	2	4			
DUMPTRUCK	6	4	11			
BULLDOZER	0	3	3			
	*ADDITIONAL 2 DUMPTRUCK REQUIRED TO SEQURE UNINTERUPTED LOADING WORKS					
Scenario 2						
ITEM	SEDIMENTATION POND	DISPOSAL AREA	TOTAL			
BACKHOE	7	7	14			
DUMPTRUCK	18	13	31			
BULLDOZER	0	9	9			

Appendix 15

Table 17 Calculation for dredging operational cost

No	Item	Calculation	SCENARIO 1 (Vol 82.000)		SCENARIO 2 (Vol. 246000)	
	CALCULATION FOR OPERATIONAL COST					
1	PREPARATORY WORK	10% of item 2,3,4		**639,182,074**		**1,923,196,222**
2	LABOR FOR DREDGER OPERATION			**80,820,000**		**242,460,000**
	FOREMAN	Rp 107,800 x 1 person x 150 days		16,170,000		48,510,000
	OPERATOR	Rp 89,800 x 2 person x 150 days		26,940,000		80,820,000
	ELECTRICIAN	Rp 89,800 x 1 person x 150 days		13,470,000		40,410,000
	ASSISTANT	Rp 80,800 x 2 person x 150 days		24,240,000		72,720,000
3	FUEL FOR DREDGER			**871,680,000**		**2,615,040,000**
	MAIN GENERATOR (600 kvA)	Rp 8000 x 71.3 L/hr x 8 hr/days x 150 days		684,480,000		2,053,440,000
	SUB GENERATOR (150 kVA)	Rp 8000 x 19.5 L/hr x 8 hr/days x 150 days		187,200,000		561,600,000
4	RENTAL FEE OF HEAVY EQUIPMENT			**5,439,320,741**		**16,374,462,222**
	BACKHOE	Rp 2,900,000 x units x 125 days		1,585,333,333		5,075,000,000
	DUMP TRUCK	Rp 2,100,000 x units x 125 days		2,775,080,000		8,062,740,000
	BULLDOZER	Rp 2,900,000 x units x 125 days		1,078,907,407		3,236,722,222.22
5	OVERHEAD & PROFIT	10 % of items 1,2,3,4		**703,100,281**		**2,115,515,844**
6	MAINTENANCE COST	10% of equipment cost (tabel 7.1)		**543,932,074**		**1,637,446,222**
	TOTAL in rupiahs		**IDR**	**8,278,035,170**	**IDR**	**24,908,120,511**
	TOTAL in Japanese Yen		**¥**	**63,677,194**	**¥**	**191,600,927**

Appendix 16

Table 18 Initial Cost for aerial seeding

NO	ITEMS	PRICE	QUANTITY	TOTAL
A. PRE SPREADING				
	RESEARCH AND GROUND CHECK	100,000,000	1	100,000,000
1	SEED			-
	SUKSESI (kg)	100,000	4,322	432,207,421
	TREMBESI (kg)	300,000	4,322	1,296,622,262
				-
2	TRANSPORTATION FOR DELIVERY	1,800,000	4	7,200,000
3	clay	125,000	1000	125,000,000
4	fertilizer (3.5 kg)	25,500	1000	25,500,000
5	machine	100,000,000	2	200,000,000
6	MAPPING			-
	CITRA ALOS	5,000,000	10	50,000,000
7	GPS	3,000,000	48	144,000,000
8	CLIMATE DATA	5,000,000	5	25,000,000
B. SPREADING				-
1	TRAINING AND EDUCATION TO LOCAL PEOPLE	50,000,000	1	50,000,000
2	AIR SEEDING			-
3	HELICOPTER RENTAL FEE INCLUDE FUEL	30,000,000	14	420,000,000
	(8 times fly - 30 minutes/route)			-
4	RACK	1,000,000	10	10,000,000
5	STORAGE ROOM			-
6	EQUIPMENT	30,000,000	1	30,000,000
C. LABOR				-
1	SUPERVISOR	2,500,000	24	60,000,000
2	LABOR (15 ORANG)	1,000,000	360	360,000,000
D. OPERATIONAL AFTER SPREADING				-
	MONITORING FEE (LOCAL PEOPLE) 10 ORG	1,500,000	240	360,000,000
	TRANSPORTATION	500,000	50	25,000,000
	GROUND CHECK & EVALUATION	100,000,000	1	100,000,000
E.MISSELANEOUS		100,000,000	1	100,000,000
TOTAL				IDR 3,920,529,682
				¥ 30,157,921
MONTHLY OPERATIONAL (5%)				IDR 196,026,484
				¥ 1,507,896

Appendix 17

Table 19 Deflator

Benefit

Scenario	Service Lifetime	Expected Rate of Return						
		4	5	6	7	8	9	10
6	39	19.6468	17.0597	14.9783	13.2851	11.8925	10.7352	9.7637
5	37	19.1682	16.7292	14.7493	13.1258	11.7814	10.6574	9.7090
4	35	18.7039	16.4021	14.5182	12.9620	11.6648	10.5742	9.6495
3	34	18.4324	16.2082	14.3791	12.8620	11.5927	10.5220	9.6116
2	25	15.5642	14.0486	12.7477	11.6255	10.6526	9.8050	9.0631
1	22	14.3446	13.0771	11.9721	11.0049	10.1550	9.4052	8.7412

Cost

Scenario	Service Lifetime	Expected rate of return						
		4	5	6	7	8	9	10
6	39	4.67	6.80	9.87	14.28	20.58	29.56	42.32
5	37	4.2869	6.1147	8.6925	12.3165	17.3947	24.4887	34.37
4	35	3.9707	5.5589	7.7574	10.7918	14.9669	20.6949	28.53
3	34	3.8066	5.2745	7.2859	10.0338	13.7771	18.8617	25.75
2	25	2.6495	3.3605	4.2528	5.3701	6.7663	8.5073	10.67
1	22	2.3462	2.8889	3.5502	4.3543	5.3305	6.5133	7.94

Appendix 18 Scenario 1

Table 20 Calculation of scenario 1 with interest rate 5.75%

Interest rate 5.75%							
Item	Value	Interest rate 5.75%		Total		B/C	B-C
		Convertion	PV				
Cost:							
Initial Investment	23,098,545,808	2.346238174	54,194,689,930.91		**IDR 76,637,479,075**		
Operational (Dredging)	8,278,035,170	2.346238174	19,422,242,119.67	COST			
Spoil bank	1,287,400,000	2.346238174	3,020,547,024.78		¥ 589,519,070		
							IDR 995,936,321,237
Benefit :						13.9954	
Irrigation	36,838,000,000	14.34464528	528,428,042,793.52		**IDR 1,072,573,800,312**		
Hydropower generation	6,381,000,000	14.34464528	91,533,181,526.29				
Material Selling	30,000,000,000	14.34464528	430,339,358,374.65	BENEFIT			
Raw water purification	1,419,120,000	14.34464528	20,356,773,008.55		¥ 8,250,567,695		¥7,661,048,625
Paddy Field Protection	133,600,000	14.34464528	1,916,444,609.30				

Table 21 Calculation of scenario 1 with interest rate 7%

Interest rate 7%							
Item	Value	Interest rate 7%		Total		B/C	B-C
		Convertion	PV				
Cost:							
Initial Investment	23,098,545,808	2.888943728	66,730,399,032.93		**IDR 94,364,402,972**		
Operational (Dredging)	8,278,035,170	2.888943728	23,914,777,783.81	COST			
Spoil bank	1,287,400,000	2.888943728	3,719,226,155.15		¥ 725,880,023		
							IDR 883,429,454,009
Benefit :						10.3619	
Irrigation	36,838,000,000	13.07705449	481,732,533,416.08		**IDR 977,793,856,981**		
Hydropower generation	6,381,000,000	13.07705449	83,444,684,720.34				
Material Selling	30,000,000,000	13.07705449	392,311,634,792.40	BENEFIT			
Raw water purification	1,419,120,000	13.07705449	18,557,909,572.22		¥ 7,521,491,208		¥ 6,795,611,185
Paddy Field Protection	133,600,000	13.07705449	1,747,094,480.28				

Table 22 Calculation of scenario 1 with interest rate 8%

Interest rate 8%							
Item	Value	Interest rate 8%		Total		B/C	B-C
		Convertion	PV				
Cost:				COST	**IDR 115,962,777,940**	7.71947	**IDR 779,208,706,305**
Initial Investment	23,098,545,808	3.550172835	82,003,829,846.54				
Operational (Dredging)	8,278,035,170	3.550172835	29,388,455,585.79				
Spoil bank	1,287,400,000	3.550172835	4,570,492,507.28		¥ 892,021,369		
Benefit :				BENEFIT	**IDR 895,171,484,245**		
Irrigation	36,838,000,000	11.97205955	441,026,729,579.28				
Hydropower generation	6,381,000,000	11.97205955	76,393,711,967.14				
Material Selling	30,000,000,000	11.97205955	359,161,786,399.33				
Raw water purification	1,419,120,000	11.97205955	16,989,789,143.83		¥ 6,885,934,494		¥ 5,993,913,125
Paddy Field Protection	133,600,000	11.97205955	1,599,467,155.43				

Table 23 Calculation of scenario 1 with interest rate 9%

Interest rate 9%							
Item	Value	Interest rate 9%		Total		B/C	B-C
		Convertion	PV				
Cost:				COST	**IDR 142,229,125,158**	5.78542	**IDR 680,625,674,725**
Initial Investment	23,098,545,808	4.3543108	100,578,247,484.86				
Operational (Dredging)	8,278,035,170	4.3543108	36,045,137,948.28				
Spoil bank	1,287,400,000	4.3543108	5,605,739,724.41		¥ 1,094,070,194		
Benefit :				BENEFIT	**IDR 822,854,799,882**		
Irrigation	36,838,000,000	11.00489329	405,398,259,101.96				
Hydropower generation	6,381,000,000	11.00489329	70,222,224,098.20				
Material Selling	30,000,000,000	11.00489329	330,146,798,769.18				
Raw water purification	1,419,120,000	11.00489329	15,617,264,168.98		¥ 6,329,652,307		¥ 5,235,582,113
Paddy Field Protection	133,600,000	11.00489329	1,470,253,743.85				

Table 24 Calculation of scenario 1 with interest rate 10%

Interest rate 10%							
Item	Value	Interest rate 10%		Total		B/C	B-C
		Convertion	PV				
Cost:							
Initial Investment	23,098,545,808	5.330457738	123,125,822,236.95		**IDR 174,113,970,157**		
Operational (Dredging)	8,278,035,170	5.330457738	44,125,716,628.67	COST			
Spoil bank	1,287,400,000	5.330457738	6,862,431,291.80		¥ 1,339,338,232		
							IDR 585,191,771,890
Benefit :						4.36097	
Irrigation	36,838,000,000	10.15498563	374,089,360,597.16		**IDR 759,305,742,048**		
Hydropower generation	6,381,000,000	10.15498563	64,798,963,297.97				
Material Selling	30,000,000,000	10.15498563	304,649,568,866.79	BENEFIT			
Raw water purification and material	1,419,120,000	10.15498563	14,411,143,205.67		¥ 5,840,813,400		¥ 4,501,475,168
Paddy Field Protection	133,600,000	10.15498563	1,356,706,080.02				

Table 25 Calculation of scenario 1 with interest rate 11%

Interest rate 11%							
Item	Value	Interest rate 11%		Total		B/C	B-C
		Convertion	PV				
Cost:					**IDR 212,749,748,110**		
Initial Investment	23,098,545,808	6.51328288	150,447,362,971.99	COST			
Operational (Dredging)	8,278,035,170	6.51328288	53,917,184,758.02				
Spoil bank	1,287,400,000	6.51328288	8,385,200,380.15		¥ 1,636,536,524		**IDR 490,492,894,456**
						3.30549	
Benefit :							
Irrigation	36,838,000,000	9.405195475	346,468,590,890.38		**IDR 703,242,642,566**		
Hydropower generation	6,381,000,000	9.405195475	60,014,552,322.91				
Material Selling	30,000,000,000	9.405195475	282,155,864,235.61	BENEFIT			
Raw water purification and material	1,419,120,000	9.405195475	13,347,101,001.80		¥ 5,409,558,789		¥ 3,773,022,265
Paddy Field Protection	133,600,000	9.405195475	1,256,534,115.40				

Table 26 Calculation of scenario 1 with interest rate 12%

Interest rate 12%							
Item	Value	Interest rate 11%		Total		B/C	B-C
		Convertion	PV				
Cost:				COST	**IDR 259,483,433,212**	2.51883	**IDR 394,110,530,882**
Initial Investment	23,098,545,808	7.944023522	183,495,391,220.75				
Operational (Dredging)	8,278,035,170	7.944023522	65,760,906,108.65				
Spoil bank	1,287,400,000	7.944023522	10,227,135,882.11		¥ 1,996,026,409		
Benefit :				BENEFIT	**IDR 653,593,964,093**		
Irrigation	36,838,000,000	8.741192046	322,008,032,572.69				
Hydropower generation	6,381,000,000	8.741192046	55,777,546,442.43				
Material Selling	30,000,000,000	8.741192046	262,235,761,365.45				
Raw water purification and material	1,419,120,000	8.741192046	12,404,800,455.63		¥ 5,027,645,878		¥ 3,031,619,468
Paddy Field Protection	133,600,000	8.741192046	1,167,823,257.28				

Appendix 19 Scenario 2

Table 27 Calculation of scenario 2 with interest rate 5.75%

Interest rate 5.75%							
Item	Value	Interest rate 5.75%		Total		B/C	B-C
		Convertion	PV				
Cost:							
Initial Investment	54,722,202,047	2.649485903	144,985,702,886.91		**IDR 221,212,261,497**		
Operational (Dredgin	24,908,120,511	2.649485903	65,993,714,156.94	COST			
Spoil bank	3,862,200,000	2.649485903	10,232,844,453.41		¥ 1,701,632,781		
							IDR 2,170,068,810,007
Benefit :						10.8099	
Irrigation	41,995,320,000	15.5642072	653,623,861,980.03				
Hydropower generati	7,274,340,000	15.5642072	113,219,335,015.33		**IDR 2,391,281,071,505**		
Material Selling	102,600,000,000	15.5642072	1,596,887,658,890.36	BENEFIT			
Raw water purificatio	1,617,796,800	15.5642072	25,179,724,605.38				
Paddy Field Protectio	152,304,000	15.5642072	2,370,491,013.64		¥ 18,394,469,781		¥ 16,692,837,000

Table 28 Calculation of scenario 2 with interest rate 7%

Interest rate 7%							
Item	Value	Interest rate 7%		Total		B/C	B-C
		Convertion	PV				
Cost:							
Initial Investment	54,722,202,047	3.360537134	183,895,992,010.81		**IDR 280,579,722,435**		
Operational (Dredgin	24,908,120,511	3.360537134	83,704,663,906.31	COST			
Spoil bank	3,862,200,000	3.360537134	12,979,066,517.47		¥ 2,158,305,557		
							IDR 1,877,839,281,127
Benefit :						7.69271	
Irrigation	41,995,320,000	14.04857045	589,974,211,601.64				
Hydropower generati	7,274,340,000	14.04857045	102,194,077,969.22		**IDR 2,158,419,003,561**		
Material Selling	102,600,000,000	14.04857045	1,441,383,328,197.71	BENEFIT			
Raw water purificatio	1,617,796,800	14.04857045	22,727,732,319.02				
Paddy Field Protectio	152,304,000	14.04857045	2,139,653,473.86		¥ 16,603,223,104		¥ 14,444,917,547

Table 29 Calculation of scenario 2 with interest rate 8%

Interest rate 8%							
Item	Value	Interest rate 8%		Total		B/C	B-C
		Convertion	PV				
Cost:				COST	**IDR 355,078,769,972**	5.51583	**IDR 1,603,474,731,298**
Initial Investment	54,722,202,047	4.2528212	232,723,740,972.59				
Operational (Dredging)	24,908,120,511	4.2528212	105,929,782,961.15				
Spoil bank	3,862,200,000	4.2528212	16,425,246,038.54		¥ 2,731,375,154		
Benefit :				BENEFIT	**IDR 1,958,553,501,270**		
Irrigation	41,995,320,000	12.7476995	535,343,719,585.96				
Hydropower generation	7,274,340,000	12.7476995	92,731,100,349.59				
Material Selling	102,600,000,000	12.7476995	1,307,913,968,259.32				
Raw water purification	1,617,796,800	12.7476995	20,623,187,451.51		¥ 15,065,796,164		¥ 12,334,421,010
Paddy Field Protection	152,304,000	12.7476995	1,941,525,623.99				

Table 30 Calculation of scenario 2 with interest rate 9%

Interest rate 9%							
Item	Value	Interest rate 9%		Total		B/C	B-C
		Convertion	PV				
Cost:				COST	**IDR 448,366,184,774**	3.98366	**IDR 1,337,772,788,517**
Initial Investment	54,722,202,047	5.370135804	293,865,656,497.63				
Operational (Dredging)	24,908,120,511	5.370135804	133,759,989,773.44				
Spoil bank	3,862,200,000	5.370135804	20,740,538,503.20		¥ 3,448,970,652		
Benefit :				BENEFIT	**IDR 1,786,138,973,291**		
Irrigation	41,995,320,000	11.62549957	488,216,574,650.12				
Hydropower generation	7,274,340,000	11.62549957	84,567,836,550.37				
Material Selling	102,600,000,000	11.62549957	1,192,776,255,999.52				
Raw water purification	1,617,796,800	11.62549957	18,807,696,004.60		¥ 13,739,530,564		¥ 10,290,559,912
Paddy Field Protection	152,304,000	11.62549957	1,770,610,086.68				

Table 31 Calculation of scenario 2 with interest rate 10%

Interest rate 10%							
Item	Year 0	Interest rate 10%		Total		B/C	B-C
		Convertion	PV				
Cost:							
Initial Investment	54,722,202,047	6.766296085	370,266,621,452.87		**IDR 564,935,128,482**		
Operational (Dredging)	24,908,120,511	6.766296085	168,535,718,291.33	COST			
Spoil bank	3,862,200,000	6.766296085	26,132,788,738.29		¥ 4,345,654,834		
							IDR 1,071,729,045,064
Benefit :						2.8970834	
Irrigation	41,995,320,000	10.65260819	447,359,689,593.01				
Hydropower generation	7,274,340,000	10.65260819	77,490,693,829.55		**IDR 1,636,664,173,547**		
Material Selling	102,600,000,000	10.65260819	1,092,957,599,852.63	BENEFIT			
Raw water purification	1,617,796,800	10.65260819	17,233,755,434.48		¥ 12,589,724,411.90		¥ 8,244,069,577
Paddy Field Protection	152,304,000	10.65260819	1,622,434,837.11				

Table 32 Calculation of scenario 2 with interest rate 11%

Interest rate 11%							
Item	Value	Interest rate 11%		Total		B/C	B-C
		Convertion	PV				
Cost:							
Initial Investment	54,722,202,047	8.507298758	465,538,121,509.76		**IDR 710,295,833,464**		
Operational (Dredging)	24,908,120,511	8.507298758	211,900,822,690.36	COST			
Spoil bank	3,862,200,000	8.507298758	32,856,889,263.47		¥ 5,463,814,104		
							IDR 796,148,636,874
Benefit :						2.1208691	
Irrigation	41,995,320,000	9.80504306	411,765,920,908.99				
Hydropower generation	7,274,340,000	9.80504306	71,325,216,931.44		**IDR 1,506,444,470,337**		
Material Selling	102,600,000,000	9.80504306	1,005,997,417,932.83	BENEFIT			
Raw water purification	1,617,796,800	9.80504306	15,862,567,285.96		¥ 11,588,034,387		¥ 6,124,220,284
Paddy Field Protection	152,304,000	9.80504306	1,493,347,278.18				

Table 33 Calculation of scenario 2 with interest rate 12%

Interest rate 12%							
Item	Value	Interest rate 11%		Total		B/C	B-C
		Convertion	PV				
Cost:				COST	**IDR 891,193,082,559**	1.5624653	**IDR 501,265,221,541**
Initial Investment	54,722,202,047	10.6739269	584,100,784,505.60				
Operational (Dredging)	24,908,120,511	10.6739269	265,867,457,576.68		¥ 6,855,331,404		
Spoil bank	3,862,200,000	10.6739269	41,224,840,477.01				
Benefit :				BENEFIT	**IDR 1,392,458,304,101**		
Irrigation	41,995,320,000	9.063137673	380,609,366,760.80				
Hydropower generation	7,274,340,000	9.063137673	65,928,344,896.59				
Material Selling	102,600,000,000	9.063137673	929,877,925,198.76				
Raw water purification	1,617,796,800	9.063137673	14,662,315,124.53		¥ 10,711,217,724		¥ 3,855,886,320
Paddy Field Protection	152,304,000	9.063137673	1,380,352,120.07				

Table 34 Calculation of scenario 3 with 5.75%

Interest rate 5.75%							
Item	Value	Interest rate 5.75%		Total		B/C	B-C
		Convertion	PV				
Cost:				COST	**IDR 140,008,180,434**	15.2007	**IDR 1,988,208,801,437**
Initial Investment	27,019,075,490	3.806583354	102,850,362,992.67				
Operational	8,474,061,654	3.806583354	32,257,222,031.76				
Spoil bank	1,287,400,000	3.806583354	4,900,595,409.48		¥ 1,076,986,003.34		
Benefit :				BENEFIT	**IDR 2,128,216,981,871**		
Irrigation	50,173,955,840	18.43243069	924,827,963,596.34				
Hydropower generation	22,311,188,735	18.43243069	411,249,440,025.83				
Material Selling	40,860,488,496	18.43243069	753,158,122,262.07				
Raw water purification	1,932,864,548	18.43243069	35,627,391,815.49		¥ 16,370,899,861		¥ 15,293,913,857
Paddy Field Protection	181,965,375	18.43243069	3,354,064,171.14				

Table 35 Calculation of scenario 3 with interest rate 7%

Interest rate 7%							
Item	Value	Interest rate 7%		Total		B/C	B-C
		Convertion	PV				
Cost:				COST	**IDR 193,998,365,306**	9.64648	**IDR 1,677,403,303,660**
Initial Investment	27,019,075,490	5.274484289	142,511,689,173.37				
Operational	8,474,061,654	5.274484289	44,696,305,059.36				
Spoil bank	1,287,400,000	5.274484289	6,790,371,073.47		¥ 1,492,295,118		
Benefit :				BENEFIT	**IDR 1,871,401,668,967**		
Irrigation	50,173,955,840	16.2081601	813,227,508,907.34				
Hydropower generation	22,311,188,735	16.2081601	361,623,318,948.13				
Material Selling	40,860,488,496	16.2081601	662,273,339,139.48				
Raw water purification	1,932,864,548	16.2081601	31,328,178,034.65		¥ 14,395,397,454		¥ 12,903,102,336
Paddy Field Protection	181,965,375	16.2081601	2,949,323,936.97				

Table 36 Calculation of scenario 3 with interest rate 8%

Interest rate 8%							
Item	Value	Interest rate 8%		Total		B/C	B-C
		Convertion	PV				
Cost:				COST	**IDR 267,978,594,988**	6.19535	**IDR 1,392,243,234,997**
Initial Investment	27,019,075,490	7.285880408	196,857,752,764.12				
Operational (Dredging)	8,474,061,654	7.285880408	61,740,999,786.62				
Spoil bank	1,287,400,000	7.285880408	9,379,842,437.56		¥ 2,061,373,808		
Benefit :				BENEFIT	**IDR 1,660,221,829,985**		
Irrigation	50,173,955,840	14.37913713	721,458,191,163.13				
Hydropower generation	22,311,188,735	14.37913713	320,815,642,256.45				
Material Selling	40,860,488,496	14.37913713	587,538,567,101.74				
Raw water purification	1,932,864,548	14.37913713	27,792,924,378.18		¥ 12,770,937,154		¥ 10,709,563,346
Paddy Field Protection	181,965,375	14.37913713	2,616,505,085.49				

Table 37 Calculation of scenario 3 with interest rate 9%

Interest rate 9%							
Item	Value	Interest rate 9%		Total		B/C	B-C
		Convertion	PV				
Cost:				COST	**IDR 369,049,593,821**	4.02398	**IDR 1,115,998,167,664**
Initial Investment	27,019,075,490	10.03382828	271,104,763,801.42				
Operational (Dredging)	8,474,061,654	10.03382828	85,027,279,489.84				
Spoil bank	1,287,400,000	10.03382828	12,917,550,529.88		¥ 2,838,843,029		
Benefit :				BENEFIT	**IDR 1,485,047,761,485**		
Irrigation	50,173,955,840	12.86195918	645,335,371,720.66				
Hydropower generation	22,311,188,735	12.86195918	286,965,598,679.52				
Material Selling	40,860,488,496	12.86195918	525,545,934,948.15				
Raw water purification	1,932,864,548	12.86195918	24,860,424,906.79		¥ 11,423,444,319		¥ 8,584,601,290
Paddy Field Protection	181,965,375	12.86195918	2,340,431,230.30				

Table 38 Calculation of scenario 3 with interest rate 10%

Interest rate 10%							
Item	Value	Interest rate 10%		Total		B/C	B-C
		Convertion	PV				
Cost:				COST	**IDR 506,729,815,589**	2.64144	**IDR 831,768,522,282**
Initial Investment	27,019,075,490	13.77711841	372,245,002,477.87				
Operational	8,474,061,654	13.77711841	116,748,150,864.53				
Spoil bank	1,287,400,000	13.77711841	17,736,662,246.65		¥ 3,897,921,658		
Benefit :				BENEFIT	**IDR 1,338,498,337,871**		
Irrigation	50,173,955,840	11.59269851	581,651,543,350.49				
Hydropower generation	22,311,188,735	11.59269851	258,646,884,511.22				
Material Selling	40,860,488,496	11.59269851	473,683,324,298.68				
Raw water purification	1,932,864,548	11.59269851	22,407,115,972.62		¥ 10,296,141,061		¥ 6,398,219,402
Paddy Field Protection	181,965,375	11.59269851	2,109,469,737.54				

Table 39 Calculation of scenario 3 with interest rate 11%

Interest rate 11%							
Item	Value	Interest rate 11%		Total		B/C	B-C
		Convertion	PV				
Cost:				COST	**IDR 693,743,807,083**	1.75119	**IDR 521,134,438,286**
Initial Investment	27,019,075,490	18.86170951	509,625,953,006.79				
Operational	8,474,061,654	18.86170951	159,835,289,258.60				
Spoil bank	1,287,400,000	18.86170951	24,282,564,817.37		¥ 5,336,490,824		
Benefit :				BENEFIT	**IDR 1,214,878,245,369**		
Irrigation	50,173,955,840	10.52202818	527,931,777,282.68				
Hydropower generation	22,311,188,735	10.52202818	234,758,956,611.86				
Material Selling	40,860,488,496	10.52202818	429,935,211,425.17				
Raw water purification	1,932,864,548	10.52202818	20,337,655,241.26		¥ 9,345,217,272		¥ 4,008,726,448
Paddy Field Protection	181,965,375	10.52202818	1,914,644,808.21				

Table 40 Calculation of scenario 3 with interest rate 12%

Interest rate 12%							
Item	Value	Interest rate 11%		Total		B/C	B-C
		Convertion	PV				
Cost:							
Initial Investment	27,019,075,490	25.74884934	695,710,104,088.79		**IDR 947,056,509,561**		
Operational	8,474,061,654	25.74884934	218,197,336,833.19	COST			
Spoil bank	1,287,400,000	25.74884934	33,149,068,639.38		¥ 7,285,050,074		
							IDR 162,707,101,872
Benefit :						1.1718	
Irrigation	50,173,955,840	9.611633131	482,253,656,266.35		**IDR 1,109,763,611,433**		
Hydropower generation	22,311,188,735	9.611633131	214,446,960,836.61	BENEFIT			
Material Selling	40,860,488,496	9.611633131	392,736,024,973.95				
Raw water purification	1,932,864,548	9.611633131	18,577,984,925.37		¥ 8,536,643,165		¥ 1,251,593,091
Paddy Field Protection	181,965,375	9.611633131	1,748,984,431.22				

ACKNOWLEDGEMENT

الحمد لله ربّ العالمين

First and foremost, praises and thanks to Allah Almighty.

It is a genuine pleasure to express my deep sense of thanks to my parents.

I would like to express the deepest appreciation to **Professor Tetsuya Kubota**, for his expertise, assistance, guidance and support throughout my study. I came to Kyushu University with zero knowledge and he teach me with patience.

Immeasureable appreciation and deepest gratitude for the help and support are extended to the following persons who in one way or another have contribute in making this study possible,

Dr. Hideaki Mizuno and Dr. Yoshinori Shinohara, thank you very much for your assistance and support during my study.

SABO Lab member, for the support they've lent me over all these years

Dr. Hasnawir for constant encouragement throughout my research period.

Dr. Aril Aditian for his untiring support and patience in answering all my "Why" question.

Dr. Andang Soma for providing necessary information regarding this research and sharing his knowledge.

I am extremely thankful to my husband **Meyrza and my lovely son Takeshi**, for everything.